



Universidad de Concepción  
Facultad de Ciencias Químicas



Université de Grenoble

**Thèse en Co-Tutelle**

*présentée par*

**Julio A. Sánchez Poblete**

*Pour obtenir le grade de*

**Docteur de l'Université de Grenoble**

**et de l'Université de Concepción**

**POLYELECTROLYTES CATIONIQUES  
SYNTHESE, CARACTERISATION ET APPLICATION EN  
ANALYSE ET ELIMINATION DE L'ARSENIC**

*Soutenue le 1<sup>er</sup> juin 2010*

**Jury**

***Rapporteurs :***

**Pr. Maria Angelica Del Valle  
Dr Alain Favre-Reguillon**

**Université Pontificale, Santiago du Chili  
Université Claude Bernard, Lyon**

***Examineurs :***

**Pr. Mario Suwalsky  
Dr. Redouane Borsali  
Dr. Liliane Guérente**

**Université de Concepción  
Université Joseph Fourier, Grenoble  
Université Joseph Fourier, Grenoble**

***Directeurs de Thèse :***

**Pr. Jean-Claude Moutet  
Pr. Bernabé L. Rivas Quiroz  
Pr. Amalia Pooley Topali**

**Université Joseph Fourier, Grenoble  
Université de Concepción  
Université de Concepción**

***Invité :***

**Dr. Luis Basaez**

**Université de Concepción**



# Contents

1. INTRODUCTION .....	7
1.1 Background .....	7
1.2 General aspects on arsenic as pollutant.....	9
1.2.1 Arsenic in water .....	9
1.2.2 Arsenic round the world.....	11
1.2.3 Arsenic in Chile .....	14
1.3 Chemistry of arsenic .....	14
1.3.1 Toxicity of arsenic.....	17
1.3.2 Health effects of arsenic.....	18
1.4 Removal of arsenic.....	18
1.4.1 Polymers with ability to remove arsenic.....	22
1.4.2 Overview of liquid-phase polymer-based retention technique (LPR).....	23
1.5 Analysis of arsenic .....	26
1.6 Brief overview of the electrocatalytic oxidation (EO) of arsenite .....	30
1.7 Properties of noble metal-polymer nanocomposites .....	31
1.7.1 Nanomaterials Fundamentals.....	31
1.7.2 Electrodes coated with polymeric films with incorporated metal-catalyst particles.....	34
1.8 Objectives of the study.....	37
1.8.1 Hypothesis.....	37
1.8.2 General objectives.....	38
1.9. References .....	40
2. EXPERIMENTAL PART.....	49
2.1 Synthesis of water-soluble polyelectrolytes.....	49
2.2 Characterization of water-soluble polyelectrolytes.....	51

2.2.1	Characterization of polymers by FT- IR spectroscopy .....	52
2.2.2	Characterization of polymers by <sup>1</sup> H-NMR spectroscopy.....	54
2.2.3	Thermogravimetry and differential scanning calorimetry (TG - DSC) .....	60
2.2.4	Conductivity measurements .....	62
2.3	LPR- Procedure.....	64
2.4	Preparation of noble metal nanoparticles-polymer modified electrodes.....	66
2.4.1	Synthesis of alkylammonium and ferrocenylalkylammonium N-substituted polypyrrole films (C poly1, C poly2).....	66
2.4.2	Electrochemical characterization .....	70
2.4.3	Elaboration of polymer-metal composites with Pt, Pd (C polymer - metal) .....	72
2.4.4	Synthesis of alkylammonium substituted polypyrrole films (C poly1) nanoparticles modified electrodes at preparative scale.....	73
2.4.5	Characterization of the nanocomposites by transmission electron microscopy.....	74
2.5	Conclusions.....	76
2.6	References .....	78
3.	RESULTS AND DISCUSSION .....	79
3.1	Removal of arsenic by LPR technique.....	79
3.1.1	Removal of arsenate by polymer containing ammonium groups through the LPR-washing method.....	81
3.1.2	Maximum retention capacity of arsenate through the enrichment method .....	90
3.1.3	Desorbing of arsenate: the charge-discharge process.....	94
3.1.4	Conclusions .....	97
3.2	Electrocatalytic oxidation (EO) of arsenite at analytical and preparative scales .....	99
3.2.1	Oxidation of arsenite using massive platinum electrodes .....	100
3.2.2	Electrocatalytic oxidation of As(III) to As(V) with different metal-polymer film modified electrodes .....	101
3.2.3	Electrocatalytic oxidation of arsenite to arsenate at the preparative scale using C poly1- Pt <sup>0</sup> under different conditions .....	113
3.2.4	Conclusions .....	118

3.3 Off-line coupled (EO - LPR) techniques to remove arsenic from aqueous solutions .....	120
3.3.1 Conclusions .....	129
3.4 Final remarks.....	130
3.5 References.....	133
ABBREVIATIONS AND SYMBOLS .....	136



# 1. INTRODUCTION

## *1.1 Background*

Arsenic is a highly toxic element at low levels of concentration thus creating potentially serious environmental concerns worldwide. This urges the scientific community to improve the methods for determining the level of arsenic in water and food as well as to develop appropriate technologies to remove traces of arsenic from drinking water, wastewaters and industrial effluents in order to reach acceptable levels.

The main arsenic species present in natural waters are arsenate (oxidation state V) and arsenite ions (oxidation state III) related to the arsenic acid ( $\text{H}_3\text{AsO}_4$ ) and arsenous acid ( $\text{H}_3\text{AsO}_3$ ) respectively. However, the forms, concentrations, and relative ratios of both As(V) and As(III) in water vary significantly depending on changes in input sources, such as the pH and oxidation potential.

Several methods are used to remove traces of arsenic from water including ion exchange resins, adsorption using especially modified chelating compounds, chemical precipitation, coagulation, and membrane processes used in reverse osmosis. However, as mentioned above, the redox- and pH-controlled diversity of arsenic species in water results in complex selectivity issues which have yet to be fully addressed.

This thesis research work has been carried out in the framework of a project, developed in collaboration between the Department of Polymers at the University of Concepción, and the Department of Molecular Chemistry at the University Joseph Fourier, France, related to the development of a remediation strategy to remove arsenic from contaminated water by combining complexation-ultrafiltration on membrane, with the electrocatalytic oxidation of

As(III) species into more easily extractable As(V) forms. The main obstacle in the As(III) to As(V) conversion lies in the high irreversibility of the electrochemical oxidation of As(III) into As(V). This obstacle is the technological key which remains to be solved. In particular, in aqueous media, and in the entire pH range, the anodic oxidation of As(III) is hindered by the oxidation of solvent resulting in a very low As(V) yield. This problem could be solved by using catalytically active electrode materials that can promote the oxidation of As(III) into As(V) in the solvent stability domain, which is thermodynamically possible.

The first step in this project is the oxidation of As(III) that can be quantitatively applied in the treatment of polluted water, by using catalysts or electrode materials possessing appropriate catalytic properties.

The second step is to study the efficiency of the extraction of As(V) species produced previously by electrocatalytic oxidation (EO) of As(III) solutions, using the same polyelectrolyte as the supporting electrolyte in the electrochemical cell and as extracting of arsenic species in ultrafiltration. The association of arsenic specific extracting water-soluble polymeric reagents, with  $(R)_4N^+X^-$  groups, and ultra-filtration membranes is the way to explore in order to achieve a selective separation of arsenic species from other charged or neutral substrates in water. This technique, called *liquid-phase polymer-based retention technique* (LPR) is based on the separation of arsenic bound to the soluble extracting polymers from other free ionic arsenic species taking advantage of their size differences.

The third step concerns the *in-situ* control of the advancement of the electrocatalytic process, i.e. to be able to follow the conversion of As(III) to As(V) into the electrochemical cell. This part of the project is close to the first two aims: if it is catalytically and efficiently possible to perform the exhaustive oxidation of As(III) solution, at the preparative scale, then it is obviously possible to follow the concentration in As(III) into the electrochemical cell by using

an analytical electrode based on the same catalytically active nanocomposite material. Thus, the third objective is to build an amperometric sensor for As(III) determination, based on the relationship between the concentration and the catalytic current recorded at the nanocomposite film modified electrode.

## ***1.2 General aspects on arsenic as pollutant***

Arsenic is an ubiquitous element that ranks 20<sup>th</sup> in abundance in the crust of earth, 14<sup>th</sup> in the seawater, and 12<sup>th</sup> in the human body [1]. Arsenic has been used in medicine, agriculture, livestock, electronics, industry and metallurgy [2, 3]. It is now well recognized that consumption of arsenic, even at low levels, is highly toxic [4].

The terrestrial abundance of arsenic is around  $1.5 \times 10^{-3}$  mg kg<sup>-1</sup>. The source of arsenic in the environment can be natural or anthropogenic. The natural sources, long before activities of man had any effect on the balance of nature; arsenic is distributed ubiquitously throughout earth crusts, soil, sediments, water, air and living organisms. Anthropogenic sources of arsenic exceed natural sources in the environment by 3:1 [5], and it may accumulate in soil through the use of arsenical pesticides, the application of fertilizers, from the dust, from the burning of fossil fuels and from the disposal of industrial and animal wastes [6, 7].

### **1.2.1 Arsenic in water**

Due to large environmental problems in Asia and in other parts of the world and the diseases caused by the contamination of drinking water there are now strict norms on arsenic in water. The maximum permissible concentration in Europe and accepted by the World Health Organization (WHO) for arsenic in drinking water is 10 µg L<sup>-1</sup>. On the other hand, developing

countries are struggling to find and implement systems to reach the standard of  $50 \mu\text{g L}^{-1}$  in areas affected by the presence of arsenic [8, 9].

The seawater ordinarily contains  $0.001\text{--}0.008 \text{ mg L}^{-1}$  of arsenic. The major chemical form in which arsenic appears to be thermodynamically stable in water is the arsenate ion [10].

Due to the discovery of high levels of arsenic in groundwater resources it is possible to say that the global cycle of arsenic has increased in both developed and developing countries because of the progressive industrialization and population growth. Amongst the 20 countries with severe groundwater arsenic contamination, the largest population at risk is in Bangladesh [11-14] and in West Bengal, India [12, 15-20]. In addition to these two geographical locations evidence of arsenic groundwater contamination has emerged in other Asian countries including Laos, Cambodia, Myanmar, Nepal and Vietnam. In these countries millions of people who consume untreated groundwater run a considerable risk of chronic arsenic poisoning [21].

This widespread human exposure comes in part from certain international organizations, such as the United Nations International Children's Emergency Fund (UNICEF), as these organizations have promoted the digging of wells, called "tube wells", because of their design that tap into the groundwater. In general, groundwater is free of the microbial contamination [13, 22], however, the digging of tube-wells for drinking water supply into aquifers with elevated arsenic levels has been described as the greatest mass poisoning in human history [13] with 36 million people exposed to arsenic via drinking water in Bangladesh and West Bengal, India alone [23]. Groundwater levels of arsenic in some areas of Bangladesh approach  $2 \text{ mg L}^{-1}$  (or 2 ppm), and it is predicted that 200 000 to 270 000 people will die of cancer from drinking arsenic-contaminated water in this country alone [24].

Arsenic poisoning episodes have been reported all over the world. Thousands and thousands of people are suffering from the toxic effects of arsenicals in many countries due to natural groundwater contamination as well as to industrial effluent and drainage problems [10].

Background concentrations of arsenic in groundwater are in most countries less than  $10 \mu\text{g L}^{-1}$  [25] and sometimes substantially lower. However, values quoted in the literature concerning the issue show a very large range from  $< 0.5$  to  $5000 \mu\text{g L}^{-1}$  (i.e. four orders of magnitude) and this range may occur under natural conditions. High concentrations of arsenic are found in groundwater in a variety of environments. This includes both oxidizing (under conditions of high pH) and reducing aquifers, and areas affected by geothermal, mining and industrial activity. However, most high-arsenic groundwater places are the result of natural occurrences of arsenic.

### **1.2.2 Arsenic round the world**

At the present, traces of arsenic in drinking water affect over 100 million people around the world, including countries like Bangladesh, India, China, Chile, Argentina, Mexico, Hungary, Taiwan, Vietnam, Japan, New Zealand, Germany, and United States among others (see figure 1) [10].

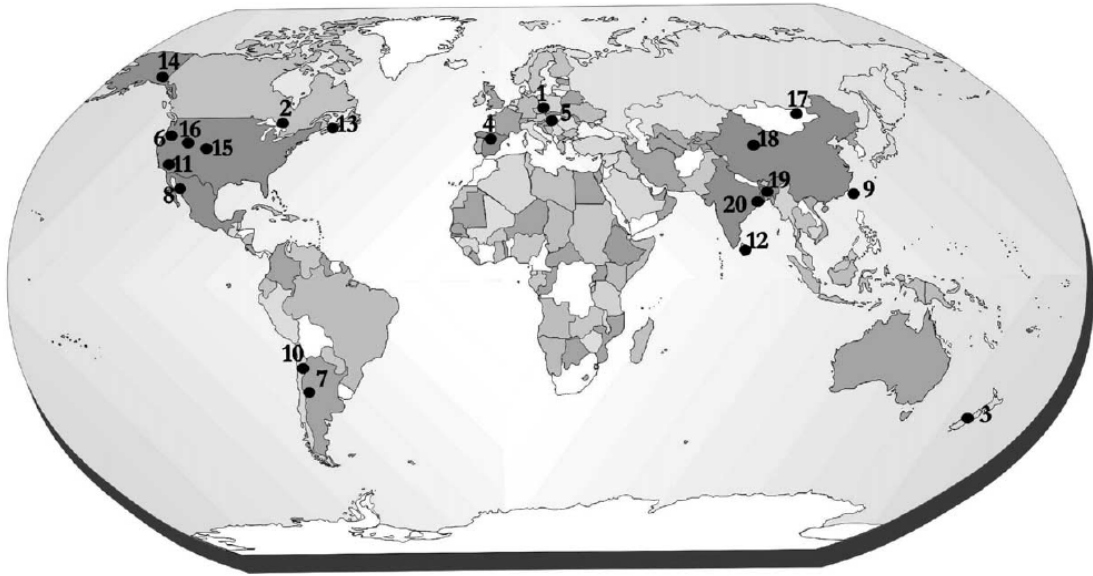


Figure 1. Documented groundwater As incidents round the world—(1) Poland; (2) Ontario, Canada; (3) New Zealand; (4) Spain; (5) Hungary; (6) western OR; (7) Cordoba, Argentina; (8) Lagunera, Mexico; (9) Taiwan; (10) Antofagasta, Chile; (11) Lassen County, CA; (12) Sri Lanka; (13) Nova Scotia, Canada; (14) Fairbanks, AK (15) Millard County, UT (16) Fallon, NV (17) inner Mongolia, China; (18) Xinjiang Utghur, China; (19) Bangladesh; (20) West Bengal, India [10].

The arsenic contents in groundwater of different countries are summarized in Table 1.

Table 1. Concentration of arsenic in groundwater of the arsenic-affected countries [10].

Location	Sampling period	Arsenic source	Concentration ( $\mu\text{g L}^{-1}$ ) *
Hungary	N.S.	Deep groundwater	68 ( 1 – 174)
South-west Finland	1993 – 1994	Well waters, natural origin	17 – 980 (range)
New Jersey, USA	1977 – 1979	Well waters	1 (median), 1160 maximum
Western, USA	N.S.	Geochemical environments	48000 (maximum)
South – west, USA	1970	Alluvial aquifers	16 – 62 (range)
Southern Iowa and western, Missouri, USA	N.S.	Natural origin	43 - 490 (range)
Northeastern Ohio, USA	N.S.	Natural origin	1 – 100 (range)
Lagunera region, northern Mexico	N.S.	Well waters	8 – 624 (range)
Chile	N.S.	Mining activity	470 – 770 (range)
Pampa, Cordoba, Argentina	N.S.	2- 15 m	100 – 3810 (range)
Kuitun-Usum, Xinjiang, PR China	1983	Well waters	0.05 – 850 (range)
Shanxi, PR China	1988	Well waters	0.03 –1.41 (range)
Hsinchu, Taiwan	N.S.	Well waters	< 0.7
West Bengal, India	1989 –1996	Arsenic-rich sediment	0.003 – 3700 (range)
Calcutta, India	1990 –1997	Near pesticide production plant	< 50 – 23080 (range)
Bangladesh	1996 –1997	Well waters	10 – 1000 (range)
Nakhon Si Thammarat Province, Thailand	1994	Shallow (alluvial) groundwater; mining activity	503.5 (1.25 – 5114)
Fukuoka, Japan	1994	Natural origin	0.001– 0.293 (range)
Hanoi, Vietnam	1999 –2000	Arsenic-rich sediment	159 (1 – 3050)

NS means not stated.

\* Mean and ranges of total arsenic unless stated otherwise.

### **1.2.3 Arsenic in Chile**

In northern Chile arsenic is the most harmful environmental pollutant in the area. The arsenic is of natural origin but is also released in the environment due to the exploitation of copper. The concentrations of arsenic in air, water and soils in the region, both in community and working settings, exceed in some cases both the nationally and internationally established permissible limits. This may have consequent impacts on the health of the population exposed to arsenic [26]. Some reports indicate that Antofagasta, the second region of Chile has high natural water pollution caused by arsenic, and thus life expectancy is lower than the national average [27, 28].

The Chilean norm 409 for water allows a maximum concentration of  $50 \mu\text{g L}^{-1}$  of arsenic in water until 2004. Currently, this rule has been modified and the goal is to achieve a concentration of  $30 \mu\text{g L}^{-1}$  in 2010 and  $10 \mu\text{g L}^{-1}$  in 2015 [29].

### ***1.3 Chemistry of arsenic***

Arsenic is very unique among the heavy metals and elements forming oxy-anions (Se, Sb, Mo, V, Cr, U, Re). It exists in four oxidation states: - 3, 0, + 3 and + 5 with oxidized As(III) and As(V) as the most widespread forms in nature. Carbon forms organoarsenicals with both the trivalent and pentavalent forms [30].

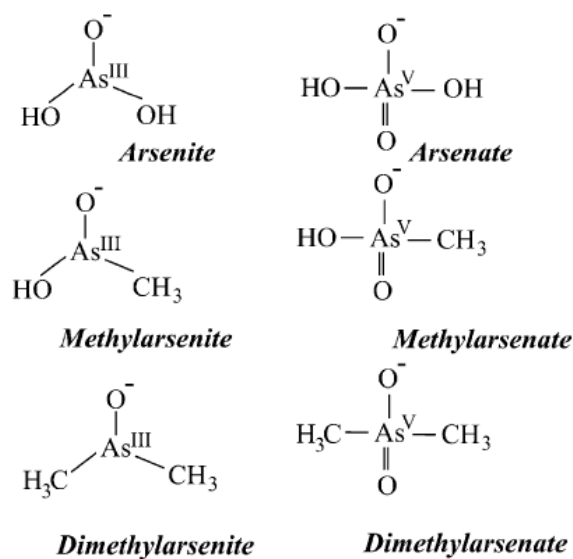


Figure 2. Arsenic species found in water [35].

The main arsenic species present in natural waters are arsenate (oxidation state V) and arsenite ions (oxidation state III) related to the arsenic acid ( $\text{H}_3\text{AsO}_4$ ) and arsenous acid ( $\text{H}_3\text{AsO}_3$ ) respectively (see table 2) [31 - 34].

Table 2. The equilibrium and dissociation constants of the arsenic species.

<b>Arsenite:</b>		<b>Arsenate:</b>	
$\text{H}_3\text{AsO}_3 \rightleftharpoons \text{H}^+ + \text{H}_2\text{AsO}_3^-$	pKa = 9.23	$\text{H}_3\text{AsO}_4 \rightleftharpoons \text{H}^+ + \text{H}_2\text{AsO}_4^-$	pKa = 2.22
$\text{H}_2\text{AsO}_3^- \rightleftharpoons \text{H}^+ + \text{HAsO}_3^{2-}$	pKa = 12.13	$\text{H}_2\text{AsO}_4^- \rightleftharpoons \text{H}^+ + \text{HAsO}_4^{2-}$	pKa = 7.08
$\text{HAsO}_3^{2-} \rightleftharpoons \text{H}^+ + \text{AsO}_3^{3-}$	pKa = 13.40	$\text{HAsO}_4^{2-} \rightleftharpoons \text{H}^+ + \text{AsO}_4^{3-}$	pKa = 11.53

However, the forms, concentrations, and relative proportions of As(V) and As(III) in water vary significantly according to changes in input sources such as pH (see Table 2) and oxidation potential (see the Pourbaix diagram on figure 3). At high redox potential arsenic is stabilized as series of pentavalent (arsenate) oxy-arsenic species:  $\text{H}_3\text{AsO}_4$ ,  $\text{H}_2\text{AsO}_4^-$ ,  $\text{HAsO}_4^{2-}$ , and  $\text{AsO}_4^{3-}$  whereas under most reducing (acid and mildly alkaline) conditions and low redox

potential, the trivalent arsenic species ( $\text{H}_3\text{AsO}_3$ ,  $\text{H}_2\text{AsO}_3^-$ ,  $\text{HAsO}_3^{2-}$  and  $\text{AsO}_3^{3-}$ ) become stable.

Both species are in equilibrium depending on pH (see figure 4).

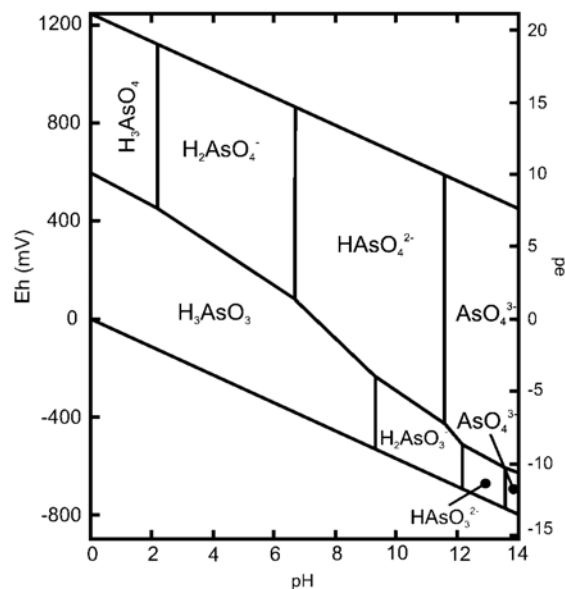


Figure 3. Diagram of E - pH of aqueous arsenic species [36].

Arsenate is less toxic than arsenite, but more abundant and more mobile in natural surface waters, whereas arsenite is found mostly in anaerobic environment such as groundwater [37].

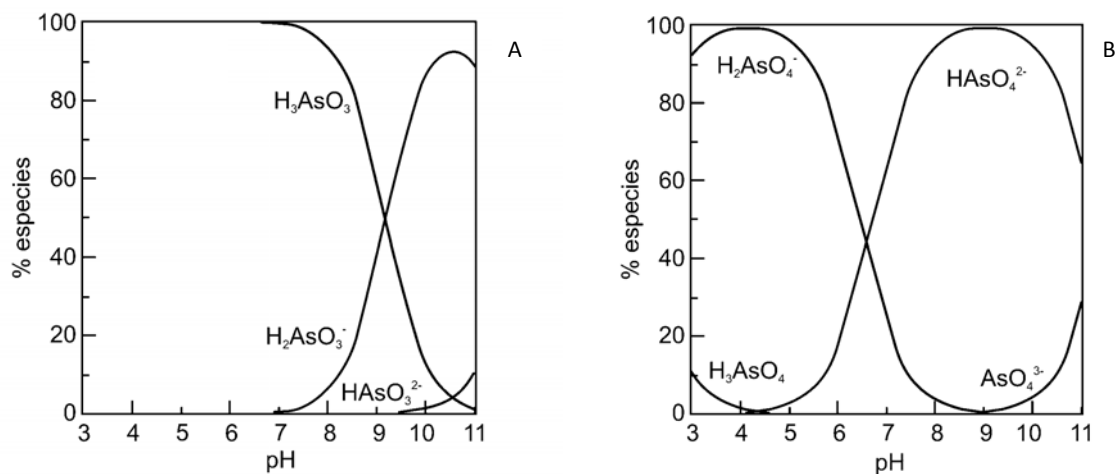


Figure 4. A) Arsenite species in function of pH. B) Arsenate species in function of pH.

### 1.3.1 Toxicity of arsenic

The chemical forms and oxidation states of arsenic are important concerning to the toxicity of it. The toxicity also depends on other factors such as physical state, gas, solution, or powder particle size, the absorption rate into cells, the elimination rate, the nature of chemical substituents in the toxic compound and, of course, the pre-existing state of the patient.

The toxicity of arsenicals decreases in the following order: inorganic As(III) > methylarsenite > dimethylarsenite > dimethylarsenate > methylarsenate > inorganic As(V) [38].

Some studies done in animals have demonstrated that the toxicity of arsenic is dependent on its form and its oxidation states. It is generally recognized that the soluble inorganic arsenicals are more toxic than the organic ones, and the As(III) are more toxic than As(V) [39, 40]. Maeda has reported that As(V) is less toxic than As(III) to both animals and humans but can be more toxic to plants [40].

The most common toxic mode of an element is the inactivation of enzyme systems, which serves as biological catalyst [41]. The As(V) does not react directly with the active sites of enzymes [42]. It first reduces to As(III) *in vivo* before exerting its toxic effect [43, 44].

Trivalent arsenic interferes with enzymes by bonding to -SH and -OH groups, especially when there are two adjacent SH-groups in the enzyme. The enzymes, which generated cellular energy in the citric acid cycle, are adversely affected. The inhibitory action is based on inactivation of pyruvate dehydrogenase by complexation with As(III), whereby the generation of adenosine-5-triphosphate (ATP) is prevented [31]. The strong bond between As(III) and sulfur may be the reason why arsenic accumulates in the keratin tissues of hair and nails. Peters has proposed that trivalent arsenic forms a stable ringed structure with vicinal dithiols of keratin in hair [45, 46].

### **1.3.2 Health effects of arsenic**

Chronic exposure to inorganic arsenic may produce several health effects. The earliest reports date back to the latter part of the 19<sup>th</sup> century when the onset of effects on skin (including pigmentation changes, hyperkeratosis and skin cancers) were linked to the consumption of arsenic in medicines and drinking water [8].

The health effects of arsenic exposure to various internal and external organs are summarized as: respiratory, pulmonary, cardiovascular, gastrointestinal, hematological, hepatic, renal, dermal, neurological, developmental, reproductive, immunologic, genotoxic, mutagenetic, carcinogenic, diabetes mellitus, and biochemical effects [10].

### ***1.4 Removal of arsenic***

In order to remove traces of arsenic from water various methods like ion-exchange, adsorption (especially with reagents impregnated resins and metal-loaded chelating resins), chemical precipitation-coagulation, membrane processes like reverse osmosis, and complexation have been used [47]. But the complete extraction of arsenic from drinking water, wastewaters, and industrial effluents in order to reach acceptable levels still represents a true challenge. The redox and pH controlled diversity of arsenic species in water bring about complex selectivity issues which have not fully been addressed yet.

Coagulation is the most common arsenic removal technology. As most the water in Bangladesh contains arsenite, oxidation with chlorine or permanganate is required first. Coagulation with ferric chloride works best at pH below 8. Alumina has a narrower effective range, from pH 6 - 8. Activated alumina, like ion exchange resins, is commercially available in coarse grains. Activated alumina beds usually have much longer run times than ion

exchange resins, typically several tens of thousands of beds can be treated before arsenic breakthrough. Activated alumina works best in slightly acidic waters (pH 5.5 – 6).

When arsenic-rich water also contains high levels of dissolved iron, iron removal will also remove much of the arsenic. Many new materials are being tested for arsenic removal, from low tech iron-coated sand and greensand to specially engineered synthetic resins.

Several technologies exist for arsenic removal using membrane or polymeric materials, including reverse osmosis, and nano / ultrafiltration. Compared with traditional adsorbents, the fibers have many advantages such as higher specific surface area, smaller diameter, and better elasticity and may occur in the form of filaments and other textile articles, and these materials can be regenerated and reused [48].

Currently available membranes are more expensive than other arsenic removal options but are more appropriate in municipal settings where very low arsenic levels are required.

Among the latest materials developed for the removal of arsenic are the cationic polyelectrolytes soluble in water, which are combined with filtration membranes to remove arsenic from aqueous solutions. Other techniques for arsenic removal are less well documented.

In all cases arsenic extraction efficiency strongly depends on the ability to convert As(III) species into the more easily extractable As(V) forms and these technologies should meet several basic technical criteria. The biggest challenges ahead lie however in applying the technologies described above in poor, rural settings, and in enabling these communities to choose safe sources of water for drinking and cooking.

Table 3 summarizes some of the key technologies for arsenic removal, with special reference to experiences gained from field application. Arsenic removal efficiency varies according to many site-specific chemical, geographic, and economic conditions and for this actual

applications may vary from the generalizations listed below. Because of the many factors that can affect arsenic removal efficiency (including arsenic concentration, speciation, pH and co-occurring solutes), any future technology should be tested using the real water to be treated, before implementation of arsenic removal systems at the field scale.

Table 3. Summary of technologies for arsenic removal [47].

Technology	Removal Efficiency		Institutional experience and issues
	As(III)	As(V)	
Coagulation with iron salts	++	+++	Well proven at central level, piloted at community and household levels. Phosphate and silicate may reduce arsenic removal rates. Generates arsenic -rich sludge. Relatively inexpensive.
Coagulation with alum	-	+++	Proven at central level, piloted at household levels. Phosphate and silicate may reduce arsenic removal rates. Optimal over a relatively narrow pH range. Generates arsenic -rich sludge. Relatively inexpensive
Lime softening	+	+++	Proven effective in laboratories and at pilot scale. Efficiency of this chemical process should be largely independent of scale. Chiefly seen in central systems in conjunction with water softening. Disadvantages include extreme pH and large volume of waste generated. Relatively inexpensive, but more expensive than coagulation with iron salts or alum because of larger doses required, and waste handling.
Ion Exchange resins	-	+++	Pilot scale in central and household systems, mostly in industrialized countries. Interference from sulfate and TDS. High adsorption capacity, but long-term performance of regenerated media needs documentation. Waters rich in iron and manganese may require pre-treatment to prevent media clogging. Moderately expensive. Regeneration produces arsenic -rich brine.
Activated alumina	+ / ++	+++	Shows effective in laboratory studies in industrialized countries. Research needed on removal of arsenite, and efficiency at high recovery rates, especially with low-pressure membranes. Pretreatment usually required. Relatively expensive, especially if operated at high pressures.
Fe-Mn oxidation	?	+ / ++ / +++	Small-scale application in central systems, limited studies in community and household levels. More research needed on which hydrochemical conditions are conducive for good arsenic removal. Inexpensive.
Porous media sorbents (iron oxide coated sand, greensand, etc.)	+ / ++	++ / +++	Shows effective in laboratory studies in industrialized and developing countries. Need to be evaluated under different environmental conditions, and in field settings. Simple media are inexpensive, advanced media can be relatively expensive.
Membrane methods	- / +++	+++	Shows effective in laboratory studies in industrialized countries. Research needed on removal of arsenite, and efficiency at high recovery rates, especially with low-pressure membranes. Pretreatment usually required. Relatively expensive, especially if operated at high pressures.
In-situ immobilization	++	+++	Very limited experience. Long-term sustainability and other effects of chemical injection not well documented. Major advantage is no arsenic -rich wastes are generated at the surface, major disadvantage is the possibility of aquifer clogging. Should be relatively inexpensive.

Key: +++ Consistently > 90% removal  
 ++ Generally 60 – 90% removal  
 + Generally 30 – 60% removal  
 - < 30% removal  
 ? Insufficient information

### 1.4.1 Polymers with ability to remove arsenic

The polyelectrolytes can be distinguished from chelating polymers (polychelatogens) because the former have charged functional groups, or are easily ionisable in aqueous solution, whereas polychelatogens have functional groups capable to form coordinating bonds with metal ions in solution. The most usual procedure to synthesize polymers is the free radical polymerization. With a suitable choice of monomers it is possible to provide the polymer with certain characteristics such as solubility in water, ability to bond ions and selectivity [49]. These macromolecules can be homo or copolymers, and possess one or more functional groups in the chain. Among them, polymers containing amino groups have been extensively studied by ultrafiltration, especially the functionalized polyethylenimines [50]. The most studied ligands in the case of polyelectrolyte are amines, carboxylic acids, sulfonic acids, amides, alcohols, amino acids, *etc* [51]. Polyelectrolytes have long-range electrostatic interactions, in which counterions tend not to specify their union polyelectrolyte and are able to move along the polymeric chain. In the short-range interactions, the counter ions bind to specific site of the polyelectrolytes associated with one or more charged group [52].

In some cases the inter / intra-chain interactions predominate which consider the existence of a dominant polymer with constant concentration of ligands and the distances between them are kept in a small range in the polymer chain [53, 54].

The cationic polyelectrolytes consisting of quaternary ammonium salts have high capacity to link to arsenate oxy-anions. This interaction occurs between the nitrogen of the ammonium group (positively charged) and the oxygen of the anion arsenate forming a dipole as seen in the figure 5.

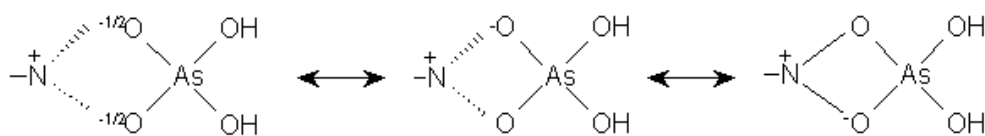


Figure 5. Electrostatic interaction of quaternary ammonium group of cationic polyelectrolyte with oxy-anion arsenate [55].

### 1.4.2 Overview of liquid-phase polymer-based retention technique (LPR)

A large number of water-soluble and functional hydrophilic polymers have a high capacity to separate ions in solution through a membrane. This method is known as liquid-phase polymer-based retention (LPR) [50, 56], and it involves the use of a ultrafiltration membrane that separates the ionic species interacting with the functional groups of water soluble polymers with high molecular weights thus preventing them from passing through the membrane (see figures 6 and 7).

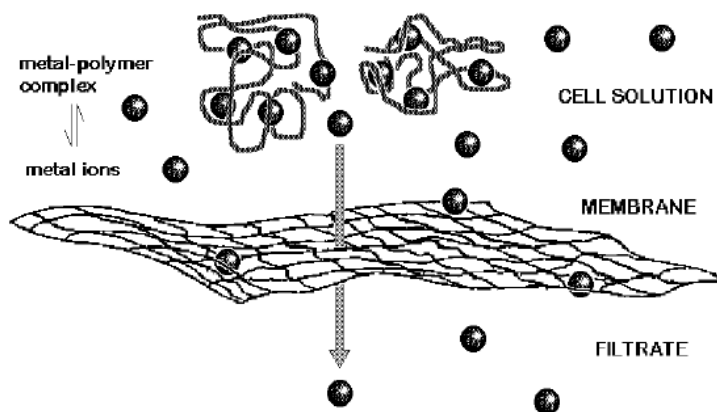


Figure 6. Principle of liquid phase polymer based retention technique (LPR) [50].

In the LPR experiments the fractions of high molecular weight polymers are used in combination with membranes with a lower exclusion limit to assure that the macromolecule remains in the feed phase.

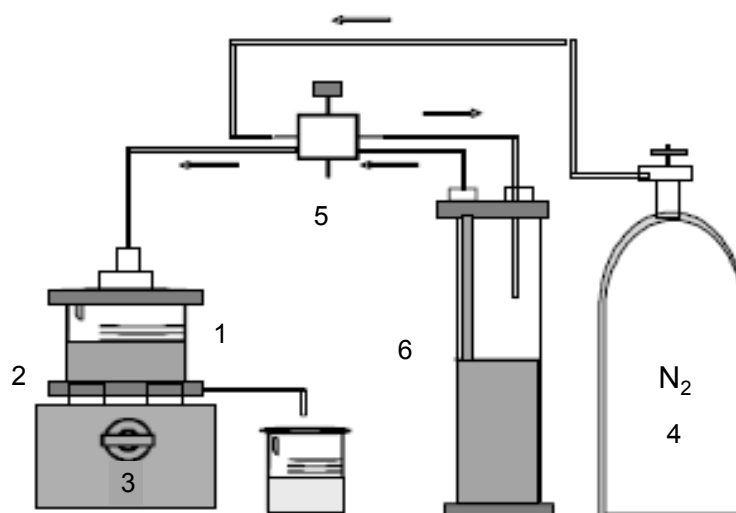


Figure 7. (1) Filtration cell with polymeric and / or metal ion solution; (2) membrane filtration; (3) magnetic stirrer; (4) pressure trap; (5) selector; (6) reservoir with water [50].

The most important physical properties of these membranes are interfacial tension and interfacial adsorption. In this context, the van der Waals interactions, hydrogen bonds, electrostatic effects, charge transfer interactions, and dipole moments play a critical role in membrane functioning. The membranes are usually made up of polycarbonate or cellulose esters, polyamides and polysulfones. The typical ultrafiltration system consists of an ultrafiltration cell, membrane, magnetic stirrer, flow switch, reservoir, and pressure source (see fig.7).

In order to systematize the study of polymer interactions with ions in solution using the ultrafiltration technique, two factors should be defined: 1) retention and 2) filtering factor. Retention ( $R_z$ ) is the fraction of ions remaining in the cell. According to the expression

$$R_z = M_z^c / M_z^{init} \quad (1)$$

where  $M_z^c$  is the absolute amount of ions that are in the feed phase and  $M_z^{init}$  is the absolute amount of ions at the start of the experiment. The subscript z refers to ion charge.

The filtration factor ( $Z$ ) is the ratios between the total volume of permeate and the volume of retentate:

$$Z = V_f / V_o \quad (2)$$

Depending on the experimental data, a graph in which  $R_z$  is represented as a function of  $Z$  can be drawn. This chart is called the retention profile.

Different separation types can be performed using the LPR technique. In the washing method, the solution containing the ionic species and the polymer is placed into the cell with an ion solution and is ultrafiltrated by eluting with pure solvent. This method is similar to diafiltration or the batch method. In the enrichment method, the polymer solution is placed inside the cell and ultrafiltrated, creating a flow through the cell of liquid with an ion [50].

During the last few years, the ability of some polymers based on ammonium salts for the removal of arsenic species in solution by the LPR technique has been studied [55, 57 - 61].

The great advantage of the LPR method is being carried out in homogeneous media. It thus largely avoids the phenomenon of mass transfer or diffusion that occurs in heterogeneous methods. The LPR experiments use fractions of polymer with high molecular weight (>100000 Da) to interact with the anions. Membranes of poly(ether sulfone) are used, which have an exclusion limit of 10000 Da, with molecular weight much lower than that of the polymer. The solution of polymer / arsenate is placed in the cell, which is washed with distilled water at constant volume and determined pH.

Water-soluble cationic polyelectrolytes containing different exchanger counterions have been synthesized and studied recently, and these show different retention capability. Polymeric structures with quaternary ammonium salts with different counterions groups, such as methyl sulphate, chloride, bromide, and hydroxide, showed different capacities to remove arsenate from aqueous solution, since the type of counter ion in quaternary ammonium group influences retention. However, all the polymers remove more efficiently arsenate ions to basic pH.

### ***1.5 Analysis of arsenic***

The importance of arsenic detection and monitoring is a well recognized fact that is emphasized by the extensive studies carried out in this area, as illustrated in a issue of *Talanta* (Vol. 58 (1), 2002) entirely dedicated to various aspects of arsenic exposure in the nature. Different determination methods of inorganic arsenic have been developed over the past 40 years providing timely and efficient risk assessments of inorganic arsenic contamination worldwide. The current literature on the issue gives an overview consisting of more than 100 papers, regarding existing methods for analysis of As(III) and As(V) in water, including various spectroscopic, inductively coupled plasma (ICP) and electrochemical techniques.

Recent analytical applications of field portable instruments are also reviewed and most of these obtain limits of detection below the WHO arsenic permissible limits. However, a vast number of existing methods are suitable only for laboratory conditions. In these cases analysis is time consuming and not suitable for routine monitoring of large numbers of samples [46].

Accurate measurement of arsenic in drinking water requires expensive and sophisticated instrumentation and facilities as well as trained staff. Among others, these techniques include; atomic absorption spectroscopy (AAS) and graphite furnace -AAS applications that provide

accurate and reproducible results, atomic fluorescence spectrometry, ICP/atomic emission spectroscopy (ICP-AES), ICP/mass spectrometry (ICP-MS). Such techniques provide limits of detection well below the WHO arsenic guideline but are lab-based instrumentation.

The development of new technologies such as atomic force microscopy (AFM) and surface enhanced raman spectroscopy (SERS) are still in their beginning. On the other hand, X-ray fluorescence can be used for measuring arsenic in biological materials and environmental samples. This method has the advantage that no sample digestion or separation steps are required. However, the sample must be pre-concentrated on a suitable solid substrate such as resin to give a detection limit of 20 – 50  $\mu\text{g L}^{-1}$  [46].

Hydride generation combined with atomic fluorescence spectroscopy is a relatively new technique that provides a sensitivity better than 20 parts per trillion and linearity up to 10 mg  $\text{L}^{-1}$ .

Colorimetric assays offer rapid results and are cost effective, but the reliability and sensitivity remains critical issues. However, research is still active in order to improve detection sensitivity.

Due to their versatility and miniaturization, electroanalytical techniques have been of great interest in monitoring arsenic contamination on site. To date, electrochemical techniques provide reliable results for fairly clean and well-defined samples in laboratory conditions. However, extensive field testing and a more rigorous analysis of applicability for environmental measurements remain to be accomplished. Another criticism of using electrochemical methods is electrode fragility. Rugged field instruments and remote long-term sensors need to be developed and microfabrication and wireless technology could fulfill this requirement.

Another important issue is the measurement of the amount of arsenic that can be absorbed by a living organism. Although bioavailability will play a strong role in future environmental regulation, the techniques for measuring bioavailable arsenic are varied and the subject of future research endeavor. The field measurements of organoarsenic compounds have not received any attention perhaps because these are less acutely toxic than inorganic arsenic. However, as an important fraction of the total environmental arsenic they should not be disregarded.

The advantage and disadvantage of such techniques are discussed in Table 4 with respect to their sensitivity, ability to detect the chemical states of arsenic, reliability, potential interferences, and ease of operation.

Table 4. Some key features of different analytical techniques for analysis of arsenic [30].

Method	Limit of Detection (LOD), $\mu\text{gL}^{-1}$	Comments
ICP-AES	0.7	High sensitivity, however equipment is expensive and requiring trained personnel.
ICP-MS	0.002 - 0.06	Higher precision and lower detection limits compared to ICP-AES.
Neutron Activation Analysis	0.001 - 0.02	High sensitivity, possible spectral interferences.
Capillary Electrophoresis	2 - 5	Good sensitivity but requires indirect measurement methods.
Surface Enhanced Raman (SERS)	Not determined	Selectivity and sensitivity have been shown for chromate, could be promising for arsenic.
Colorimetric Assays (Gutzeit)	1 - 30	Simple, but generates arsine gas and is prone to false positive and false negative readings.
Polarography	10	Poor detection limits, use of toxic mercury and better electrochemistry techniques now available.
Cathodic Stripping Voltammetry	0.5	Sensitive, however copper interference a problem and use of mercury a concern.
Anodic Stripping Voltammetry	0.05 - 0.5	Highly sensitive, however interference from other metals (copper) a major concern, analysis time can be lengthy. Reusability of electrodes and reproducibility of signal a concern.
Modified boron doped diamond (BDD) with Pt nanoparticles	0.5	Sensitive and elimination of interferences by copper and chloride. Reproducible signal and reusable electrode.
Arsenite oxidase based Biosensor	1.0	Sensitive and very selective to As(III). No interference from copper and fast analysis time (10 s)
Biosensor (AcP and PPO)	1.5	Sensitive and selective to As(V), however enzymes can be inhibited by other metals and chemicals

All the present technologies focus on the modern electrochemical methods of arsenic detection in drinking water. In particular, emphasis has been devoted to more recent topics including

modern stripping voltammetry, electrode modification, nanomaterials, and biosensors. The necessity for field instrumentation, detection and monitoring has also been addressed. Electrochemical techniques have proven to be able to give reliable results in laboratory conditions and as such have potential for further development into mobile, low cost analytical devices capable of fulfilling the requirements of a rapid and accurate sensor [46].

### ***1.6 Brief overview of the electrocatalytic oxidation (EO) of arsenite***

As already emphasized above in this chapter, in natural waters arsenic normally occurs in the oxidation states + 3 (arsenite) and + 5 (arsenate). The removal of As(III) is more difficult than the removal of As(V). Therefore, As(III) has to be oxidized to As(V) prior to its removal from waters using different techniques [62].

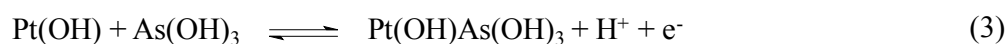
The oxidation in the presence of air or pure oxygen is slow. The oxidation rate can be increased by the use of ozone, chlorine, hypochlorite, chlorine dioxide, or H<sub>2</sub>O<sub>2</sub>. The oxidation of As(III) is also possible in the presence of manganese oxide coated sands or by advanced oxidation processes [62].

The electrochemical oxidation of arsenite combined with adsorption [63] or membrane ultrafiltration procedures [60, 61] have recently emerged as efficient strategies to remove arsenic from contaminated aqueous solutions.

The main unsolved obstacle to this conversion lies in the high irreversibility of the electrochemical oxidation of As(III) into As(V) at bare electrodes [46]. In particular, in aqueous media and for the entire pH range, the anodic oxidation of As(III) is hindered by the oxidation of the solvent, resulting in a very low As(V) yield. Present research is focused on developing catalytic systems able to promote the oxidation of As(III) into As(V) in the solvent's stability domain, which is thermodynamically possible. The oxidation of As(III)

could be quantitatively applied for the treatment of polluted water by using catalysts or electrode materials possessing appropriate catalytic properties.

The electrocatalytic oxidation and detection of As(III) has already been largely investigated at different platinum electrodes, including platinum wire [64, 65, 66] or disc [67] electrodes. More recently it has been especially shown that the use of platinum nanoparticles modified carbon electrodes results in better sensitivity than platinum macroelectrodes for arsenic sensing [68]. The As(III) to As(V) conversion is likely electrocatalyzed by the formation of platinum hydroxide on the electrode surface [66, 67]:



Thus there is a clear need for stable electrode materials affording better sensitivity and selectivity. Noble metals and metal oxides can be used for this purpose especially in the form of particles of nanometer size, particularly as electrode materials formed from the dispersion of nanoparticles in functionalized polymer matrices.

## ***1.7 Properties of noble metal-polymer nanocomposites***

### **1.7.1 Nanomaterials Fundamentals**

The scientific community has showed special interest and investment in the field of nanoscience and nanotechnology over the last few years. The ability to directly work and control systems at the same scale as nature can potentially provide a very efficient approach to the production of chemicals, energy and materials. The nanomaterials have therefore been regarded as a major step forward to miniaturisation and nanoscaling within various subfields that have been developed to study such materials.

The nanotechnology field is highly multidisciplinary; inputs from physicists, biologists, chemists and engineers are required for the advancement of the understanding in the preparation, application and impact of new nanotechnologies [69]. A nanomaterial can be defined as a material that has a structure in which at least one of its phases has one or more dimensions in the nanometer size range (1 – 100 nm). Such materials can be with nanometer-sizes, materials with surface spatially separated by distances on the order of nanometers, porous materials with particle sizes in the nanometer range or nanometer-sized metallic clusters dispersed within a porous matrix (supported metal nanoparticles).

In reality, nanoparticles are not cubes but often irregularly shaped objects, and hence there are additional defect sites. A general survey on the influence of particle morphology on the number and type of different surface sites has been emphasized in leading reviews [70, 71].

Among them, metal nanoparticles have attracted much attention over the last decade owing to their relatively high chemical activity and specificity of interaction. Furthermore, the properties of metal nanoparticles are very different to those of their bulk equivalents, such as a large surface-to volume ratio. Nanoparticles typically provide highly active centers but they are very small and not in a thermodynamically stable state. Structures at this size regime are indeed unstable as a result of their high surface energies and large surfaces [72, 73].

The versatility of physical and chemical properties afforded by metal nanoparticles makes them promising as devices with practical application in many fields, especially in catalysis [74]. In many instances, the ability to exploit catalytic properties of nanoparticles will require the morphologically controlled formation and/or highly ordered arrays of nanoparticles [75].

The control of size, shape and dispersity of nanoparticles is the key to selective and enhanced activity. A mechanism to achieve this control is to utilize another nanotechnology that of

(nanoporous) supports. These materials can be grouped as the so-called “supported metal nanoparticles”.

The unique properties of supported metal nanoparticles are directly related to the specific particle morphology (size and shape), metal dispersion, concentration and the electronic properties of the metal within their host environment [70, 76].

The potential for increased efficiency from nanoparticle catalysts, in combination with the advantages of such heterogeneous supports, increases the higher selectivity, conversion, yield and catalyst recovery. This provides the opportunity to develop specific devices for specific applications in various areas including medicine, sensors and in many industrial processes [77-79].

Polymer-nanoparticle assembly provides an effective method for the controlled creation of nanocomposites. In addition to their role in assembling nanoparticles, functionalized polymers can be used to control structural parameters such as particle size and distribution (see figure 8) [80]. The surface of nanoparticles plays an important role in catalysis being responsible for their selectivity and activity. Therefore, the characteristics of the stabilizing polymer (its functionalities and nanostructuring properties) are of great importance because they principally determine the state of the surface of nanoparticles [79]. It is obvious that future applications will require improved two- and three-dimensional manipulation of materials formed from the dispersion of nanoparticles in functionalized polymer matrices.

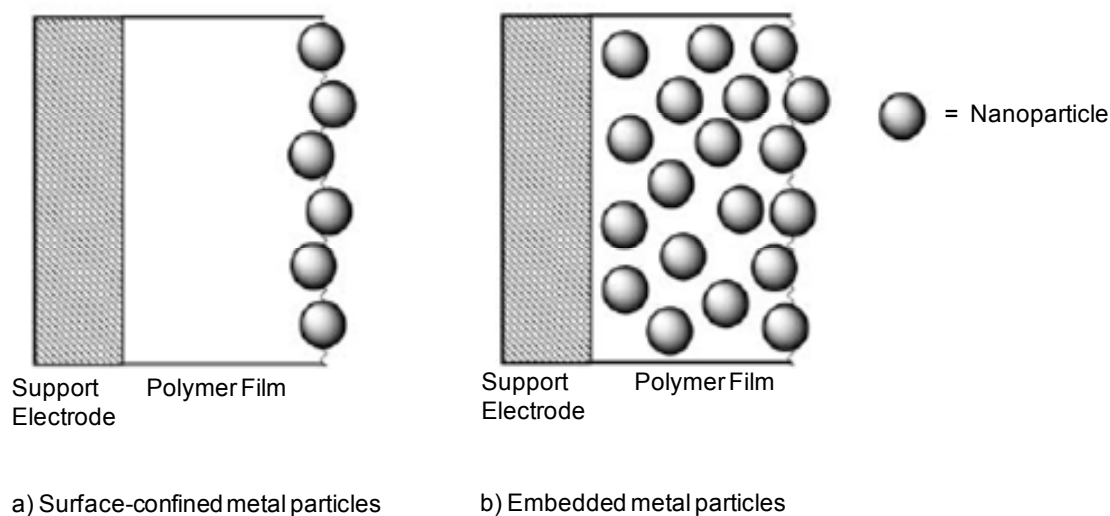


Figure 8. Schematic diagram of conducting polymer where the metal nanoparticles are (a) surface-confined and (b) distributed throughout the polymer matrix [80].

### 1.7.2 Electrodes coated with polymeric films with incorporated metal-catalyst particles

Electrochemical synthesis is a well-established technique used for the preparation of polymer films via oxidative coupling of monomers, although less diffuse than chemical routes, it has proved to be a powerful and versatile means of preparing nanoparticles for a wide range of noble and transition metals [81, 82]. The technique is very versatile and polymers with functional side groups can be synthesized by modifying the monomer prior to electro-oxidation. A wide variety of anions can also be incorporated as counterions. In recent years, electrochemical methods have also proved to be effective in incorporating metal nanoparticles in either pre-deposited polymers or in growing polymer films. Depending on the metal, the desired metal nanoparticles size and the type of polymer different techniques have been

developed [83, 84]. This is especially true in the case of electron-conducting polymers modified by noble metal nanoparticles synthesized for electrocatalytic applications [85].

Polymers used in electrochemical systems may be divided into two groups: ion-exchange (without electron conduction) and electron-conducting polymers. The first group, polymeric films with solely ionic conduction applied onto conductive supports should be, as a rule, functionalised by redox groups to find electrocatalytic applications. The latter act as mediators, so that the polymer-support system can accelerate certain electrode processes [86].

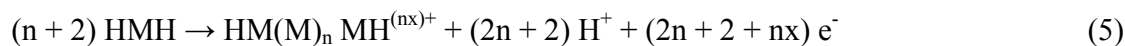
The second group with structures of electron-conducting organic polymers are characterised by the presence of conjugated bonds between electroactive groups in the chains, which is the reason for their high electron conductance in a certain potential range.

The development of such systems increases substantially the number of electrode processes where the use of polymers can be very effective. Particularly, this will allow the use of metal - polymer - support systems in redox activations such as electro-oxidation of hydrogen and simple organic compounds, or electroreduction of water or oxygen [84, 85, 87].

Various chemical and electrochemical methods for synthesizing conducting polymeric films on the surfaces of solid supports have been developed. As a rule, films of ion-exchange polymers are attached to the surface by chemical bonding or through adsorption interaction [88]. Solubility of the polymer is the important factor determining the adhesion of the film.

Synthesis of polymeric films by electrochemical polymerization shows a number of advantages over the method of chemical polymerization. First, the films are formed directly on the electrode surface, and the reaction produces an electroactive film that exhibits a high conductivity. Second, the electrosynthesis provides a good current efficiency and a strict stoichiometry of the process; hence, films of desired masses and thicknesses can be obtained.

Taking the electrochemical stoichiometry into account, the complete reaction equation for the polymerization of species HMH is:



$(2n + 2)$  electrons are used for the electropolymerization reaction itself, while the additional charging of the polymer film requires  $nx$  electrons. In general  $x$  lies between 0.25 and 0.4; this means in every 3<sup>rd</sup> to 4<sup>th</sup> monomeric subunit the film is charged [88].

Third, the properties of the polymeric film can be controlled in the course of the synthesis. Possible electrochemical and chemical reactions occurring during the syntheses of polyaniline and polypyrrole were described in detail in the literature [88]. Electrochemical properties of the support-electron-conducting polymer system depend strongly on the conditions of the polymer synthesis.

From the foregoing it follows that modifying polymeric films play the role of charge carriers in electrocatalysis, their catalytic activities manifest themselves in the processes free from destruction of substrate molecules. Platinum-group metals are the best electrocatalysts for the processes which involve cleavage of interatomic bonds (e.g., oxidation of hydrogen, organic substances, etc.). It is possible to prepare highly dispersed deposits of these metals by incorporating them into polymeric matrices. A specific feature of the systems thus obtained is that the polymeric matrix determines the conditions for the metal phase development.

It was proposed in many studies to prepare deposits of platinum-group metals using electron-conducting polymers where the formation conditions and the behavior of metal particles can differ substantially from those in ion-exchange films. This can result in a three-dimensional structure representing a conducting matrix with sufficiently uniformly distributed catalyst

microparticles. The porous structure of such a matrix can make the metal-catalyst accessible for reactants and provide the exit of the products to solution.

Due to the high work function values for metals of the platinum group as compared with other materials, it could be expected that the electrons would be partially transferred from the matrix to the microdeposit and, as a consequence, the mean electron density in the deposit would increase.

Polymer-modified electrodes are largely aimed at the elucidation of interrelations between the properties of support materials, polymeric coatings and incorporated metal-catalyst particles and/or certain functional groups. In the future it is likely that electrochemistry will remain the method of choice for investigating the electronic properties of new materials. Great interest to the new type of electrode systems was associated, first of all, with the great diversity of their practical applications, namely, the modernisation of present-day electrolyzers and electrochemical generators and development of their new types, synthesis of effective anticorrosion coatings, the development of biosensors, the extension of the possibilities of electrocatalysis, applications in micro- and nanoelectronics, *etc.*

## ***1.8 Objectives of the study***

### **1.8.1 Hypothesis**

This research project is supported by the following hypothesis:

- The water-soluble polymeric structures containing quaternary ammonium salts with small and hydrophilic counterions could present better properties for arsenate removal in aqueous solution than polyelectrolytes with large and hydrophobic counterions.

- During the ultrafiltration pH, molar ratio polymer : arsenate and ionic strength of the solution are factors which can influence the removal capacity of the polyelectrolytes. This is so because pH changes cause different species of arsenate and increased ionic strength can increase the concentration of anions in the medium causing competition with arsenate by the polyelectrolytes.
- It is possible to build modified electrodes, at analytical and preparative scale, with noble metal particles that would have the ability to perform an electrocatalytic oxidation of As(III) to generate As(V). Also, it is possible to use the water-soluble polyelectrolyte as supporting electrolyte and as an extractant in the ultrafiltration cell without the use of external agents.

### 1.8.2 General objectives

- The first goal of this project is to study the performances of catalytic electrodes based on the dispersion of noble metal (i.e., Pt, Pd, Rh) dispersed into polymer film coated on carbon surfaces, towards the electrooxidation of As(III) to As(V) species.
- These electrocatalytic systems will be applied to the quantitative oxidation of As(III) species into As(V) species which are more easier to remove by interactions with water-soluble polymers. The association of As(V) with water-soluble polymeric and ultrafiltration membranes working in combination with electrocatalytic oxidation of As(III) to As(V) species is the way we propose to explore in order to achieve a selective separation of total arsenic species from water.

- Catalytically active electrodes will also be evaluated in order to develop amperometric sensory devices for arsenic analysis, especially for the *in situ* controlled conversion of As(III) into As(V).

Thus, it is postulated that these cationic polyelectrolytes can be used as extractants of arsenic species in ultrafiltration and as the supporting electrolyte in the electrochemical cell. The monitoring of the exhaustive electrocatalytic oxidation of As(III) to As(V) can be measured in-situ, and removal of total arsenic will increase using these coupled techniques.

## **1.9. References**

- 1) Braman, R.S. Arsenic in the environment. In: Woolson, E.A. editor. Arsenical pesticides, ACS Ser. 1975, 108-123.
- 2) Sullivan, R.J. Preliminary air pollution survey of arsenic and its compounds. A literature review. National Air Pollution Control Administration Publication No. APTD 69-26, Raleigh, NC, 1969. p. 1-60.
- 3) Nriagu, J.O. and Azcue, J.M. Arsenic historical perspectives. In: J.O. Nriagu editor. Arsenic in the Environment. Part 1: Cycling and Characterization. New York: John Wiley and Sons, Inc, 1990. p.1-15.
- 4) Nordstrom, D.K. Worldwide occurrences of arsenic in ground water. Science 2002;296: p.2143-2145.
- 5) Woolson, E.A. In: Lederer, W.H. and Fensterheim R.J. editors. Industrial, Biomedical and Environmental Perspective. New York: Van Nostrand Reinhold Company, 1983. p. 1-393.
- 6) Piver, W.T. Mobilization of arsenic by natural and industrial processes. Top. Environ. Health 1983;6:p.1-50.
- 7) Woolson, E.A. Emissions, cycling and effects of arsenic in soil ecosystems. Top. Environ. Health 1983;6:p.51-139.
- 8) WHO. Arsenic Compounds, Environmental Health Criteria 224, 2nd ed., Geneva: World Health Organization, 2001.
- 9) U.S. Environmental Protection Agency. Interim Primary Drinking Water Standards. Fed. Reg. 1975, 40, 11, 1-990.
- 10) Mandal, B.K. and Suzuki, K.T. Arsenic round the world: a review. Talanta 2002; 58:p.201-235.
- 11) Tondel, M.; Rahman, M.; Magnuson, A.; Chowdhury, I.A.; Faruquee, M.H. and Ahmad, S.A. The relationship of arsenic levels in drinking water and the prevalence rate of skin lesions in Bangladesh. Environmental Health Perspectives 1999;107:p.727-729.
- 12) Chowdhury, U.K.; Biswas, B.K.; Roy Chowdhury, T.; Samanta, G.; Mandal, B.K.; Basu, G. K.; Chanda, C.R.; Lodh, D.; Saha, K.C.; Mukherjee, S.C.; Roy, S.; Kabir, S.; Quamruzzaman, Q. and Chakraborti, D. Groundwater arsenic contamination in Bangladesh and West Bengal, India. Environmental Health Perspectives 2000;108:p.393-397.

- 13) Smith, A.H.; Lingas, E.O. and Rahman, M. Contamination of drinking water by arsenic in Bangladesh: a public health emergency. *Bulletin of the World Health Organization* 2000;78:p.1093-1103.
- 14) Ahsan, H.; Perrin, M.; Rahman, A.; Parvez, F.; Stute, M.; Zheng, Y.; Milton, A.H.; Brandt-Rauf, P.; Geen, A.V. and Graziano, J. Associations between water arsenic, urinary arsenic, and skin lesions in Bangladesh. *Journal of Occupational and Environmental Medicine* 2000;42:p.1195-1201.
- 15) Bagla, P. and Kaiser, J. India's spreading health crisis draws global arsenic experts. *Science* 1996;274:p.174-175.
- 16) Mandal, B.K.; Roy Chowdhury, T.; Samanta, G.; Mukherjee, D.P.; Chanda, C.R.; Saha, K.C. and Chakraborti, D. Impact of safe water for drinking and cooking on five arsenic affected families for two years in west Bengal, India. *Science of Total Environment* 1998;218:p.185-201.
- 17) Roy Chowdhury, T.; Basu, G.K.; Mandal, B.K.; Biswas, B.K.; Samanta, G.; Chowdhury, U.K.; Chanda, C.R.; Lodh, D.; Roy, S.L.; Saha, K.C.; Roy, S.; Kabir, S.; Quamruzzaman, Q. and Chakraborti, D. Arsenic poisoning in the Ganges delta. *Nature* 1999;401:p.545-546.
- 18) Chowdhury, U.K.; Rahman, M.M.; Mondal, B.K.; Paul, K.; Lodh, D.; Biswas, B.K.; Chanda, C.R.; Basu, G.K.; Saha, K.C.; Mukherjee, S.C.; Roy, S.; Das, R.; Kaies, I.; Barua, A.K.; Palit, S.K.; Quamruzzaman, Q. and Chakraborti, D. Ground water arsenic contamination and human suffering in West Bengal, India and Bangladesh. *Environ. Sci.* 2001;8:p.393-415.
- 19) Rahman, M.M.; Chowdhury, U.K.; Mukherjee, S.C.; Mondal, B.K.; Paul, K.; Lodh, D.; Biswas, B.K.; Chanda, C.R.; Basu, G.K.; Saha, K.C.; Roy, S.; Das, R.; Palit, S.K.; Quamruzzaman, Q. and Chakraborti, D. J. Chronic arsenic toxicity in Bangladesh and West Bengal, India: A review and commentary. *Toxicol Clin. Toxicol* 2001;39:p.683-700.
- 20) Chakraborti, D.; Rahman, M.M.; Chowdhury, U.K.; Paul, K.; Sengupta, M.K.; Lodh, D.; Chanda, C.R.; Saha, K.C. and Mukherjee, S.C. Arsenic calamity in the Indian sub-continent. What lessons have been learned? *Talanta* 2002;58:p.3-22.
- 21) Berg, M.; Tran, H.C.; Nguyen, T.C.; Pham, M.V.; Schertenleib, R. and Giger, W. Arsenic contamination of groundwater and drinking water in Vietnam: A human health threat. *Environmental Science and Technology* 2001;35:p.2621-2626.

- 22) Christen, K. In Vietnam and other developing countries, arsenic contamination of groundwater is becoming the key environmental health problem of the 21st century. *Environmental Science and Technology* 2001;35:p.2621-2626.
- 23) Nordstrom, D.K. Worldwide occurrences of arsenic in ground water. *Science* 2002;296:p.2143-2145.
- 24) Alam, M.B.; Sattar, M.A. Assessment of arsenic contamination in soils and waters in some areas of Bangladesh. *Water Sci Tech* 2000;42:p.185-193.
- 25) Chen, M.; Ma, L.Q.; Hoogeweg, C.G. and Harris, W.G. Arsenic background concentrations in Florida, U.S.A. surface soils: Determination and interpretation. *Environ. Forensics* 2001;2: p.117-126.
- 26) Sancha, A.M. Review of coagulation technology for removal of arsenic: Case of Chile, *J Health. Popul. Nutr.* 2006;24:p.267-272.
- 27) Ferreccio, C; González, C; Milosavljevic, V; Marshall, G; Sancha, A.M. and Smith, A.H. Lung cancer and arsenic concentrations in drinking water in Chile. *Epidemiology* 2000;11:p.673-679.
- 28) Smith, A.H., Arroyo, A.P., Mazumder G., D.N. and Kosnett, M.J. Arsenic-induced skin lesions among atacameño people in northern Chile despite good nutrition and centuries of exposure. *Environ. Health Perspect* 2000;108:p.617-620.
- 29) NCh 409/1.Of 2005 drinking water. Pt.1.Requirements. Santiago: Instituto Nacional de Normalización Chile, 2005:p.1-9.
- 30) Luong, J.H.T.; Majid, E. and Male, K.B. Analytical Tools for Monitoring Arsenic in the Environment. *The Open Analytical Chemistry Journal* 2007;1:p.7-14.
- 31) Fergusson, Gavis. A review of the arsenic cycle in nature waters. *J. Water Res.* 1972;6:p.1259-1274.
- 32) Cullen, R.W. and Reimer, K. Arsenic speciation in the environment. *J. Chem. Rev.* 1989;89:p.713-764.
- 33) Welch, A.H.; Westjohn, D.B.; Helsel, D.R. and Wanty, R.B. Arsenic in ground water of the United States: occurrence and geochemistry. *Ground Water* 2000;38:p.589-604.
- 34) Chen, H; Frey, M.M.; Clifford, D.; Mc Neil, L.S. and Edwards, M. Arsenic treatment considerations. *J. Am. Water Works Assoc* 1999;91:p.74-85.
- 35) Hung, D.Q.; Nekrassova, O. and Compton, R.G. Analytical methods for inorganic arsenic in water: a review. *Talanta* 2004;64:p.269-277.

- 36) Smedley, P.L. and Kinniburgh, D.G. A review of the source, behavior and distribution of arsenic in natural waters. *Applied Geochemistry* 2001;17:p.517-568.
- 37) Melamed, D. Monitoring arsenic in the environment: a review of science and technologies for field measurements and sensors. EPA 542/R-04/002, 2004:1-29
- 38) Vega, L.; Styblo, M.; Patterson, R.; Cullen, W.; Wang, C. and Germolec, D. Differential effects of trivalent and pentavalent arsenicals on cell proliferation and cytokine secretion in normal human epidermal keratinocytes. *Toxicol. Appl. Pharmacol.* 2001;172:p.225-232.
- 39) Smedley, P.L. and Kinniburgh, D.G. Source and behaviour of arsenic in natural waters. United Nations Synthesis Report on Arsenic in Drinking Water, 2001.
- 40) Maeda, S. Biotransformation of arsenic in the freshwater environment. In: Nriagu, J.O. editor. *Arsenic in the Environment. Part I, Cycling and Characterization.* New York: Wiley, 1994. p.155-187.
- 41) Dhar, R.K.; Biswas, B.K.; Samanta, G.; Mandal, B.K.; Chakraborti, D.; Roy, S.; Fafar, A.; Islam, A.; Ara, G.; Kabir, S.; Khan, A.W.; Ahmed, S.A. and Hadi, S.A. Groundwater arsenic calamity in Bangladesh. *Curr. Sci.* 1997;73:p48-59.
- 42) Johnstone, R.M. Sulfhydryl agents: arsenicals. In: Hochster, R.M. and Quastel, J.H. editors. *Metabolic Inhibitors: A Comprehensive Treatise*, vol. 2. New York: Academic Press, 1963. p.99-118.
- 43) Pauwels Borst, G.W.F.; Peter, J.K.; Jager, S. and Wijffels, C.C.B. A study of the arsenate uptake by yeast cells compared with phosphate uptake. *Biochim. Biophys. Acta* 1965;94:p.312-314.
- 44) Ginsburg, J.M. and Lotspeich, W.D. Interrelations of arsenate and phosphate transport in the dog kidney. *Am. J. Physiol.* 1963;205:p.707-714.
- 45) Peters, R.A. The study of enzymes in relation to selective toxicity in animal tissues. *Sym. Soc. Exp. Biol.* 1949;3:p.36-59.
- 46) Driscoll, J. N. Determination of ppb Levels of Metals in Water by XRF. *Am. Lab. News* 2002; 16-18.
- 47) Johnston, R. and Heijnen, H. Safe water technology for arsenic removal. In: Feroze Ahmed, M; Ashraf Ali, M; Zafar A. editors. *Technologies for arsenic removal from drinking water. Bangladesh*, 2001. p.1-22.
- 48) Zhang, X.; Jiang, K.; Tian, Z.; Huang, W. and Zhao, L. Removal of arsenic in water by an ion-exchange fiber with amino groups. *J. Appl. Polym. Sci* 2008;110:p.3934-3940.

- 49) Pizarro, G.C.; Marambio, O.G.; Jeria-Orell, M.; Huerta, M.R.; Sánchez, J. and Rivas, B.L. Preparation, characterization, and thermal properties of hydrophilic copolymers: *p*-chlorophenylmaleimides with hydroxylethyl methacrylate and  $\beta$ -methyl itaconate. *Polym. International* 2007;56:p.1166-1172.
- 50) Rivas, B.L.; Pereira, E.D. and Moreno-Villoslada, I. Water-soluble polymer–metal ion interactions. *Progr Polym Sci* 2003; 28:p.173-208.
- 51) Geckeler, K.E. Polymer-metal complexes for environmental protection. Chemoremediation in the aqueous homogeneous phase. *Pure Appl. Chem.* 2001; 73:p.129-136.
- 52) Manning, G.S. Limiting laws and counterion condensation in polyelectrolyte solutions. VIII. Mixtures of counterions, species selectivity, and valence selectivity. *J. Phys. Chem.* 1984; 88:p.6654-6661.
- 53) Tsuchida, E. and Abe, K. Interactions between macromolecules in solution and intermacromolecular complexes. *Adv. Polym. Sci* 1982;45:p.1-91.
- 54) Geckeler, K.E.; Lange, G., Eberhardt, H. and Bayer, E. Preparation and application of water-soluble polymer-metal complexes. *Pure Appl. Chem* 1980;52:p.1883-1905.
- 55) Rivas, B.L., Aguirre, M.C. and Pereira, E. Retention properties of arsenate anions of water-soluble polymers by a liquid-phase polymer-based retention technique. *J. Appl. Polym. Sci* 2006;102:p.2677-2684.
- 56) Spivakov, B.Y., Geckeler, K.E. and Bayer, E. Liquid-phase polymer-based retention - the separation of metals by ultrafiltration on polychelators. *Nature* 1985;315:p.313-315.
- 57) Rivas, B.L.; Aguirre, M.C. and Pereira, E. Cationic water-soluble polymers with the ability to remove arsenate through ultrafiltration technique. *J. Appl. Polym. Sci.* 2007;106:p.89-94.
- 58) Rivas, B.L.; Aguirre, M.C.; Pereira, E.; Moutet, J.-C. and Saint-Aman, E. Capability of cationic water-soluble polymers in conjunction with ultrafiltration membranes to remove arsenate ions. *Polym. Eng. Sci.* 2007;47:p.1256-1261.
- 59) Rivas, B.L. and Aguirre, M.C. Arsenite retention properties of water-soluble metal-polymers. *J. Appl. Polym. Sci* 2007;106:p.1889-1894.
- 60) Rivas, B.L.; Aguirre, M.C.; Pereira, E.; Bucher, C.; Royal, G.; Limosin, D.; Saint-Aman, E. and Moutet, J.-C. Off-line coupled electrocatalytic oxidation and liquid phase polymer

based retention (EO-LPR) techniques to remove arsenic from aqueous solutions. *Water Res.* 2009;43:p.515-521.

- 61) Rivas, B.L.; Aguirre, M.C.; Pereira, E.; Bucher, C.; Moutet, J.-C.; Royal, G.; Saint-Aman, E. Efficient polymers in conjunction with membranes to remove As(V) generated *in situ* by electrocatalytic oxidation, *Polym. Adv. Technol.* In press.
- 62) Arienzo, M.; Chiarenzelli, J. And Scrutato, R. Removal of arsenic in aqueous solution by electrochemical peroxidation. *Fresenius Environ. Bull.* 2001;10:p.701-705.
- 63) Bissen, M. and Frimmel, F.H. Arsenic – A review. Part II: Oxidation of arsenic and its removal in water treatment. *Acta Hydrochim. Hydrobiol.* 2003;31:p.97-107.
- 64) Cox, J.A. and Kulesza, P.J.P. Electrocatalytic oxidation and determination of arsenic(III) on a glassy carbon electrode modified with a thin film of mixed-valent ruthenium(III, II) cyanide. *Anal. Chem.* 1984;56:p.1021-1025.
- 65) Forsberg, G.; O’Laughlin, J.W.; Megargle, R.G. and Koirtiyohann, S.R. Determination of arsenic by anodic stripping voltammetry and differential pulse anodic stripping voltammetry. *Anal Chem.* 1975;47:p.1586-1592.
- 66) Cabelka, T.D.; Austin, D.S. and Johnson, D.C. Electrocatalytic oxidation of As(III). Part I. Voltammetric studies at Pt electrodes in 0.5 M HClO<sub>4</sub>. *J. Electrochem. Soc.* 1984;131:p.1595-1602.
- 67) Williams, D.G. and Johnson, D.C. Pulsed voltammetric detection of arsenic(III) at platinum electrodes in acidic media. *Anal Chem.* 1992;64:p.1785-1789.
- 68) Dai, X. and Compton, R.G. Detection of As(III) via oxidation to As(V) using platinum nanoparticle modified glassy carbon electrodes: arsenic detection without interference from copper. *Analyst.* 2006;131:p.516-521.
- 69) Campelo, J.M.; Luna, D.; Luque, R.; Marinas, J.M. and Romero, A.A. Sustainable Preparation of Supported Metal Nanoparticles and Their Applications in Catalysis. *ChemSusChem* 2009;2:p.18-45.
- 70) Henry, C.R. Surface studies of supported model catalysts. *Surf. Sci. Rep.* 1998;31:p.231-325.
- 71) Raimondi, F.; Scherer, G.G.; Kotz, R. and Wokaun, A. Nanoparticles in Energy Technology: Examples from Electrochemistry and Catalysis *Angew. Chem. Int. Ed.* 2005;44:p.2190-2209.

- 72) Schmid, G.; Maihack, V.; Lantermann, F. and Peschel, S. Ligand-stabilized metal clusters and colloids: Properties and applications. *J. Chem. Soc. Dalton Trans.* 1996;5:p.589-595
- 73) Doyle, A.; Shaikhutdinov, S.K.; Jackson, S.D. and Freund, H.J. Hydrogenation on metal surfaces: Why are nanoparticles more active than single crystals? *Angew. Chem. Int. Ed.* 2003;42:p.5240-5243.
- 74) Bonnemann, H. and Ryan, R.M. Nanoscopic metal particles-synthetic methods and potential applications. *Eur.J. Inorg. Chem.* 2001;10:p.2455-2480.
- 75) Sergeev, G.B. and Petrukhina, M.A. Encapsulation of small metal particles in solid organic matrices. *Prog. Solid St. Chem.* 1996;24:p.183-211.
- 76) White, R.J.; Luque, R.; Budarin, V.; Clark, J.H. and Macquarrie, D.J. Supported metal nanoparticles on porous materials. Methods and applications. *Chem. Soc. Rev.* 2009;38:p.481-494.
- 77) Cai, D.; Mataraza, J.M.; Qin, Z.H.; Huang, Z.; Huang, J.; Chiles, T.C.; Carnahan, D.; Kempa, K. and Ren, Z. Highly efficient molecular delivery into mammalian cells using carbon nanotube spearing. *Nature Methods* 2005;2:p.449-454.
- 78) Doering, W.E.; Piotti, M.; Natan, R.J. and Freeman, R.G. SERS as a foundation for nanoscale, optically detected biological labels. *Adv. Mater.* 2007;19:p.3100-3108.
- 79) Fendler, J.H. and Tian, Y. Nanoparticles and nanostructured films: preparation, characterisation and applications. Ed. J. H. Fendler, Wiley-VCH, Weinheim, 1998. T. A. Skotheim, R. L. Elsenbaumer and J. R. Reynolds, *Handbook of Conducting Polymers*, Marcel Dekker, New York, N.Y., 1998.
- 80) Sih, B.C. and Wolf, M.O. Metal nanoparticle – conjugated polymer nanocomposites, *Chem. Commun.* 2005;p.3375-3384.
- 81) Reetz, M.T. and Helbig, W. Size-selective synthesis of nanostructured transition metal clusters. *J. Am. Chem. Soc.* 1994;116:p.7401-7402.
- 82) Riley, D.J. Electrochemistry in nanoparticle science. *Current Opinion in Colloid & Interface Science.* 2002;7,186-192.
- 83) Gangopadhyay, R. and De, A. Conducting polymer nanocomposites: a brief overview. *Chem. Mater.* 2000;12:p.608-622.
- 84) Hepel, M. The Electrocatalytic oxidation of methanol at finely dispersed platinum nanoparticles in polypyrrole films. *J. Electrochem. Soc.* 1998; 145:p.124-134.

- 85) Lamy, C. and Leger, J.-M. Catalysis and electrocatalysis at nanoparticles surfaces. In: Wieckowski, A.; Savinova, E.R. and Vayenas, C.G. editors. New York: Marcel Dekker, 2003.
- 86) Podlovchenko, B.I. and Andreev, V.N. Electrocatalysis on polymer-modified electrodes. Russ. Chem. Rev. 2002;71:p.837-851.
- 87) Malinauskas, A. Electrocatalysis at conducting polymers. Synth. Met 1999; 107:p.75-83.
- 88) Heinze, J. Electrochemistry IV. In: Steckhan, E. editor. Topics in current chemistry. Berlin: Springer-Verlag, vol 152, p.1-38.



## 2. EXPERIMENTAL PART

This section summarizes the synthesis and the characterization of all water-soluble polymers, metal-polymer nanocomposites and polymers films modified electrodes used in this research.

### *2.1 Synthesis of water-soluble polyelectrolytes*

Free-radical polymerization the most widespread method used in industry to produce polymeric materials, including plastics rubbers and fibers. It is relatively tolerant to functional groups on the monomers as ionic moieties, ligands, nucleophilic and electrophilic sites, acids and bases, and can be carried out in a wide variety of solvents. Many impurities including water are not a real problem. Complicated procedures and sophisticated equipments are not necessary in order to work under strict humidity free conditions. On the contrary, polymerizations can even be done directly in water (water working as a solution, suspension or emulsion) provided that oxygen is excluded. Depending on the monomer-initiator couple, polymerization can be done in a wide temperature range.

In this research all the water-soluble polyelectrolytes with different counter ions were prepared in the same conditions by free radical polymerization. The following monomers were used for the free-radical polymerization: [3-(methacryloylamino)-propyl]trimethylammonium chloride solution (CIAPTA) (75 wt-% in water; Aldrich, St. Louis, MO), [2-(acryloyloxy)ethyl]trimethylammonium chloride solution (CIAETA) (80 wt-% in water; Aldrich), (ar-vinylbenzyl)trimethylammonium chloride (CIVBTA) (99%-wt % in water; Aldrich) and [2-(acryloyloxy)ethyl]trimethylammonium methyl sulfate (SAETA) (80 wt-% in water; Aldrich).

Commercial water-soluble polymers were also used in this thesis. These include poly(4-vinyl-1-methyl pyridinium)bromide [P(BrVMP) (20 wt-% solution in water, Polysciences, Inc.), Warrington, PA] and poly(diallyl dimethyl ammonium) chloride, P(CIDDA), (20 wt-% solution in water; Aldrich).

The structures of the different polymers used in this study are summarized in figure 9.

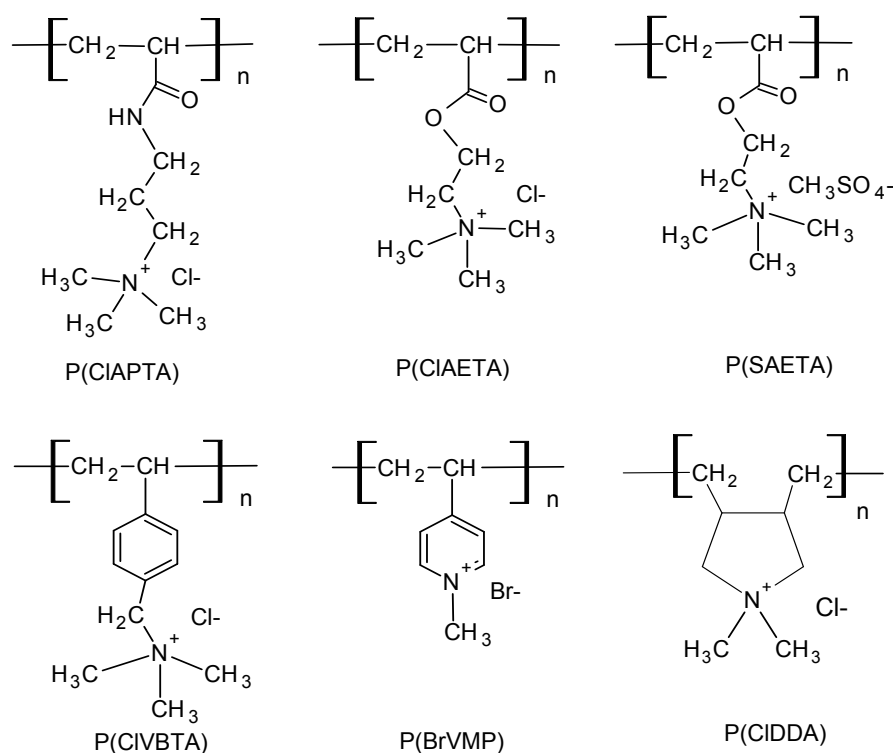


Figure 9. Structures of the water-soluble polyelectrolytes: poly[3-(acryloylamino) propyl] trimethylammonium chloride, P(CIAPTA), poly[2-(acryloyloxy) ethyl] trimethylammonium chloride, P(CIAETA), poly[2-(acryloyloxy) ethyl] trimethylammonium methyl sulfate, P(SAETA), poly(*ar*-vinyl benzyl) trimethylammonium chloride, P(CIVBTA). The commercial polymers were: poly(4-vinyl-1-methyl-pyridinium)bromide, P(BrVMP) and poly(diallyl dimethyl ammonium) chloride, P(CIDDA).

The experimental procedure for the synthesis of P(CIVBTA), P(CIAPTA), P(SAETA), and P(CIAETA) by free radical polymerization was as follows. Approximately five grams of each monomer and 1 mol-% ammonium persulfate (AP; Aldrich), used as an initiator, were

dissolved in 40 mL of water under an inert atmosphere. The reaction mixture was kept at 70 °C under N<sub>2</sub> for 24 hours.

The products were dissolved in water, purified with ultrafiltration membranes, and fractionated by ultrafiltration membranes with different molar mass cut-offs (MMCO) range (10000, 30000, 50000, and 100000 Da). Finally, the products were lyophilized and characterized. The polymerization yields in mass at these conditions are summarized in the table 5:

Table 5. Polymerization yield in mass over a fraction above than 100000 g mol<sup>-1</sup>.

Polymer	Amount of initiator AP	Amount of monomer	Polymerization yield (mass %)
P(CIVBTA)	54 mg ( $2.40 \times 10^{-4}$ mol)	5.05g ( $2.40 \times 10^{-2}$ mol)	90%
P(CIAPTA)	70 mg ( $3.20 \times 10^{-4}$ mol)	5.01g ( $3.20 \times 10^{-2}$ mol)	99%
P(SAETA)	50 mg ( $2.32 \times 10^{-4}$ mol)	5.02g ( $2.30 \times 10^{-2}$ mol)	77%
P(CIAETA)	60 mg ( $2.58 \times 10^{-4}$ mol)	5.00g ( $2.50 \times 10^{-2}$ mol)	95%

## 2.2 Characterization of water-soluble polyelectrolytes

The main fractions of each polymer (above 100000 g mol<sup>-1</sup>) were characterized by Fourier transform-infrared spectroscopy (FT-IR), proton nuclear magnetic resonance (<sup>1</sup>H-NMR), thermal analysis as termogravimetry, differential scanning calorimetry (TG–DSC) and conductivities measurements.

In order to determine the molecular weight, the characterization of this kind of polyelectrolytes is much more difficult than for neutral polymers since the interactions between the polymer charges and the counterions largely affect the dimensions of the chain. Thus, the size of the polymer and the elution volume change with the ionic strength of the

medium. Furthermore, the charged polymer may interact with the packing of the chromatographic column, thus modifying the exclusion mechanism in chromatography [1].

### 2.2.1 Characterization of polymers by FT- IR spectroscopy

Fourier transformed-infrared spectroscopy was performed with a Magna Nicolet 550 and Nexus Nicolet spectrometers. For quantitative analysis, 1 mg of the sample per 100 mg of KBr was employed.

The FT-IR studies were performed in the range of 400 – 4000  $\text{cm}^{-1}$  for all cases (see fig. 10). The spectra showed the following main characteristic absorption bands (in  $\text{cm}^{-1}$ ): around of 3400  $\text{cm}^{-1}$  (N-H stretching), around 3000  $\text{cm}^{-1}$  (C-H stretching) and of 1735  $\text{cm}^{-1}$  (C=O stretching of the ester bond). The bending band of the quaternary ammonium groups, (-N+(CH<sub>3</sub>)) is seen round 1480  $\text{cm}^{-1}$ . In the case of P(CIVBTA), a typical band is seen between 1641 – 1408  $\text{cm}^{-1}$ , corresponding to (C=C) of the aromatic ring.

In comparison with P(CIAETA), P(SAETA) shows the distinctive asymmetric stretching (1253–1219  $\text{cm}^{-1}$ ) and symmetric stretching (1061–1018  $\text{cm}^{-1}$ ) (S=O) bands of the tetrahedral  $\text{SO}_4^{2-}$  group. The characteristic absorption bands are summarized in table 6.

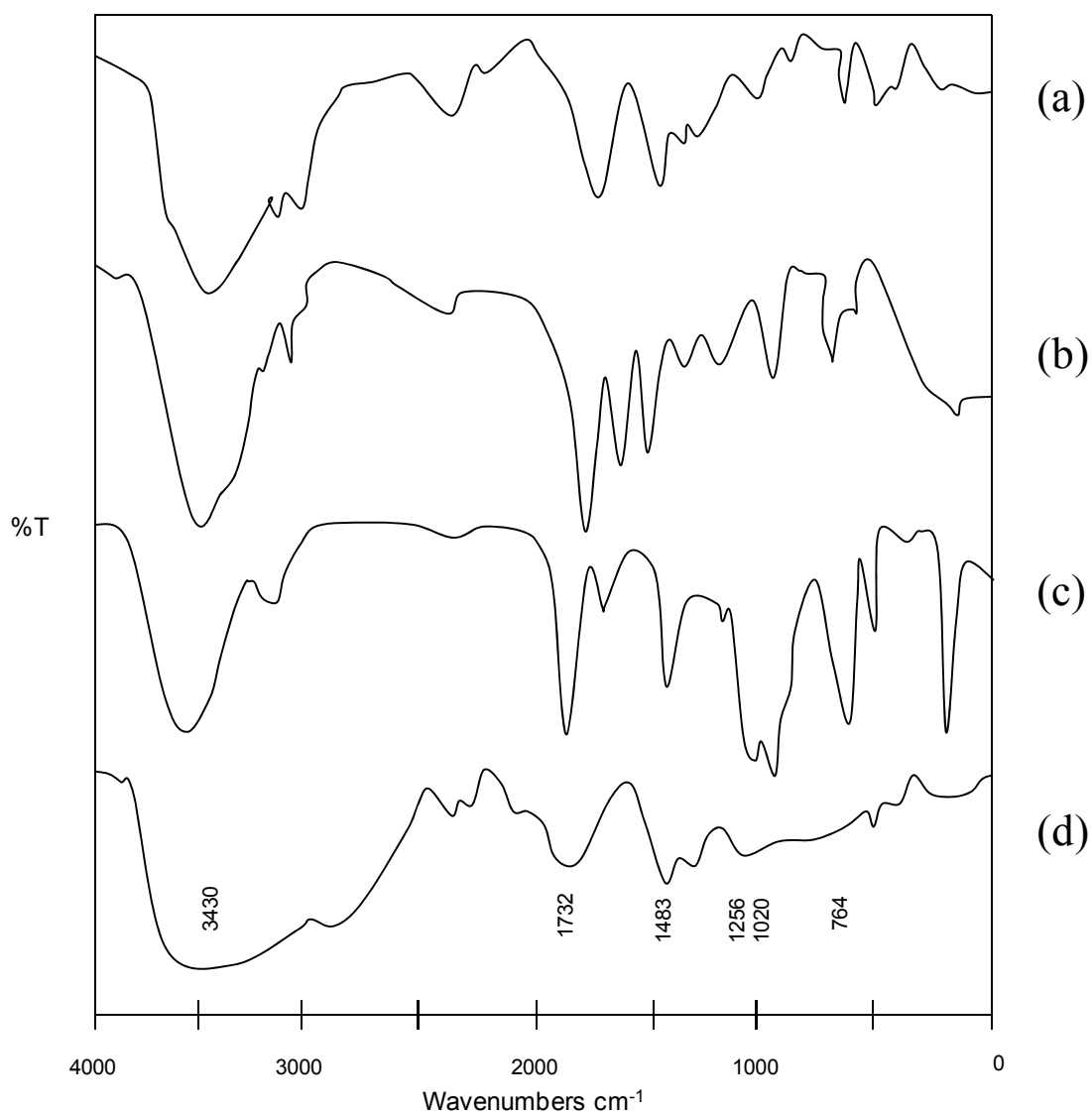


Figure 10. Fourier transformed-infrared spectroscopy in KBr pellet of: (a) P(CIVBTA), (b) P(CIAPTA), (c) P(SAETA) and (d) P(CIAETA).

Table 6. Characteristic absorption bands ( $\text{cm}^{-1}$ ) of the different polyelectrolytes.

Functional Group	P(CIVBTA)	P(CIAPTA)	P(SAETA)	P(CIAETA)
$\nu(\text{N-H})$ o $\nu(\text{OH})$	3435	3426	3434	3430
$\nu(\text{C-H})$	3025-2928	2948	3020	3010
$\nu(\text{C=O})$	----	1649 (amide)	1732	1732
$\nu_{\text{asymm}}(\text{COO}^-)$	----	----	1639	1635
$\nu(\text{C=C})$ aromatic ring	1641-1483	----	----	----
$\delta(\text{N-H})$	----	1552	----	----
$\delta(\text{N-H})$ of $\text{RN}^+(\text{CH}_3)_3$	1417	1482	1482	1483
$\nu_{\text{asymm}}\text{SO}_2$	----	----	1256-1217	----
$\nu_{\text{symm}}\text{SO}_2$	----	----	1061-1020	----
$\delta(\text{C-H})$	981-716	----	----	----
$\nu(\text{S-N})$	----	----	764	----

### 2.2.2 Characterization of polymers by $^1\text{H-NMR}$ spectroscopy

The NMR spectra were recorded with a multinuclear Bruker AC 250 spectrometer at 250 MHz at room temperature using  $\text{D}_2\text{O}$  as the solvent.

The  $^1\text{H-NMR}$  spectra of the monomers and homopolymers were analyzed comparatively, and the absence of the signals at 5,44 and 5,68 ppm, corresponding to protons of the vinylic bond, indicated that the polymerization was done. The  $^1\text{H-NMR}$  assignments of the homopolymers were as follows:

**P(CIVBTA):** Protons of the main chain:  $\delta = 1.5$  ppm (2H) (a) and  $\delta = 2.0$  ppm (1H) (b).  
 Protons of the side groups:  $\delta = 4.24$  ppm (2H) (e) and  $\delta = 7.03$  ppm (2H) (d) and  $\delta = 6.54$  ppm (2H) (c) for the aromatic ring and  $\delta = 2.79$  ppm (9H) (f) for the methyl protons of quaternary ammonium group.

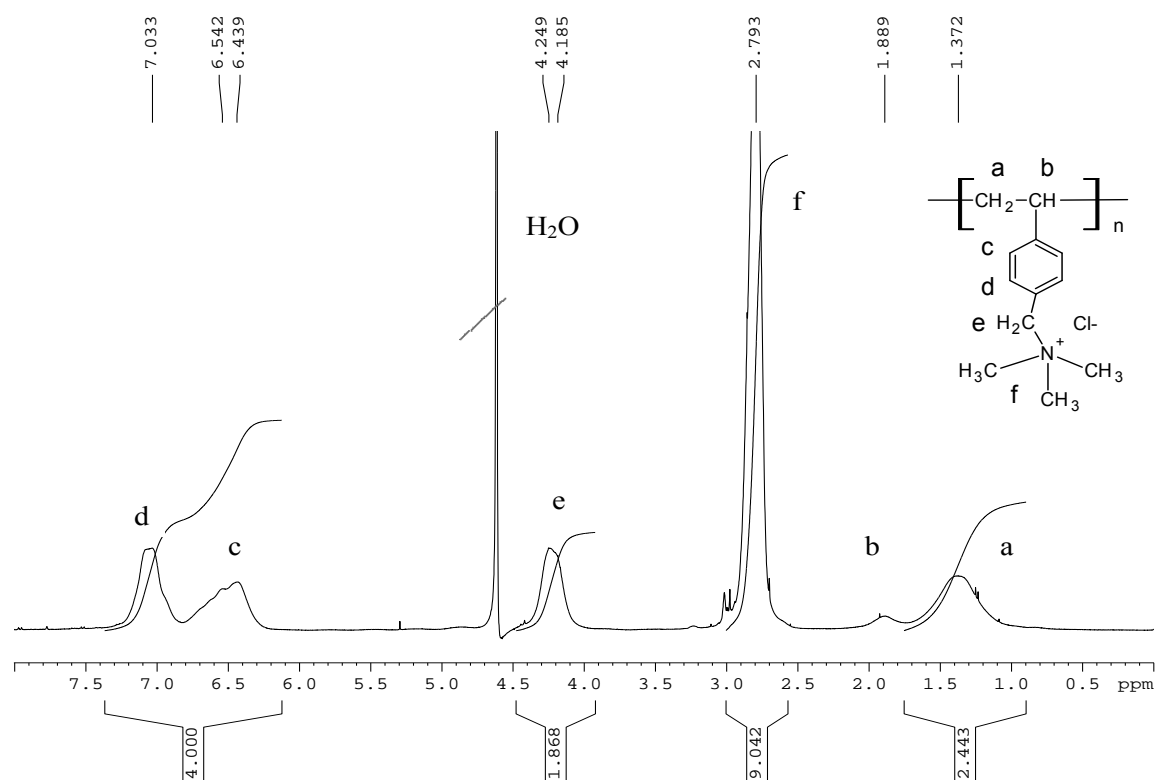


Figure 11.  $^1\text{H-NMR}$  (250 MHz,  $\text{D}_2\text{O}$ ) at room temperature for P(CIVBTA).

**P(CIAPTA)**: Protons of the main chain:  $\delta = 1.5$  ppm (1H) (b),  $\delta = 1.7$  ppm (2H) (a), Protons of side groups:  $\delta = 2$  ppm (2H) (d),  $\delta = 3.17$  ppm (2H) (e),  $\delta = 3.3$  ppm (2H) (c) and  $\delta = 3.1$  ppm (9H) (f) for the quaternary ammonium group.

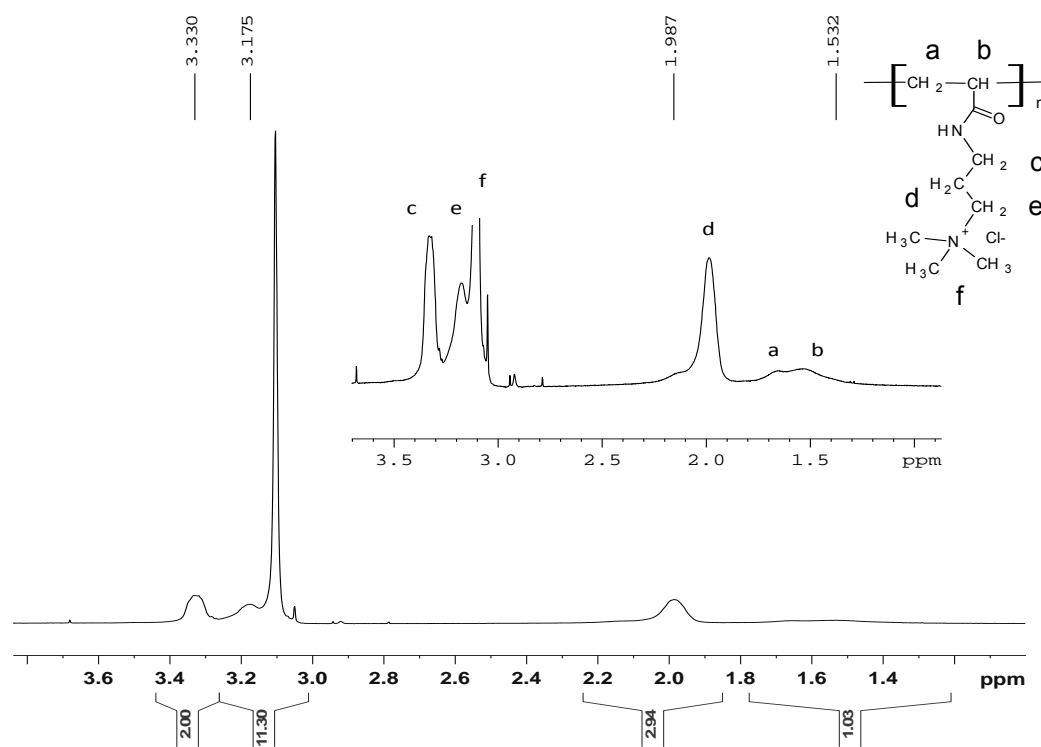


Figure 12. <sup>1</sup>H-NMR (250 MHz, D<sub>2</sub>O) at room temperature for P(CIAPTA).

In order to distinguish the CH<sub>2</sub> of this structure, the technique called “*distorsionless enhancement by polarization transfer*” (DEPT-RMN) was used. This technique is useful to distinguish among signals due to CH<sub>3</sub>, CH<sub>2</sub>, CH and quaternary carbons. That is, the number of hydrogen attached to each carbon in a molecule can be determined. [2] A DEPT experiment was done in two stages. The first one was to run an ordinary <sup>13</sup>C-NMR spectrum to locate the

chemical shifts of all the carbons:  $\delta$  (ppm): 23.5 (-CH<sub>2</sub>)(d), 37.0(-CH<sub>2</sub>)(c), 43.1 (-CH), 54.0 (-CH<sub>3</sub>), 64.1(-CH<sub>2</sub>)(e) (see fig. 13 A). At The second stage a DEPT-135 was run, using conditions under which CH<sub>3</sub> and CH resonances appear as positive signals, CH<sub>2</sub> appears as negative signals, which are as a peak below the baseline (see fig. 13 B). The signal corresponding to CH (a) was difficult to determine probably because it is in the main chain.

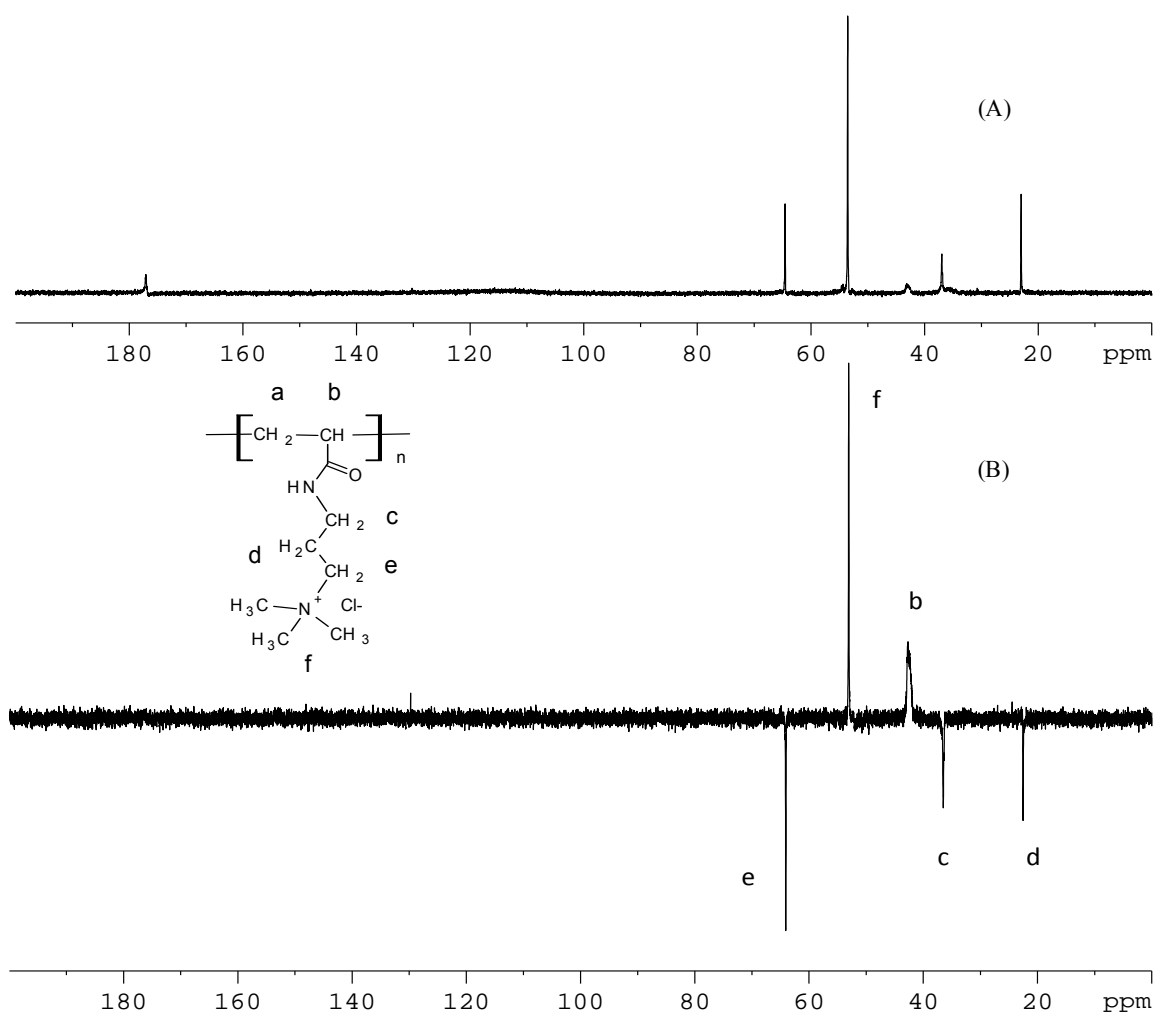


Figure 13. (A) spectrum <sup>13</sup>C-NMR and (B) DEPT-135 experiment of P(CIAPTA).

**P(CIAETA)**: Protons of the main chain:  $\delta = 1.8$  ppm (2H) (a) and  $\delta = 2.43$  ppm (1H) (b).  
 Protons of the side groups:  $\delta = 3.72$  ppm (2H) (c),  $\delta = 4.5$  ppm (2H) (d) and  $\delta = 3.20$  ppm (9H) (e) for the quaternary ammonium group.

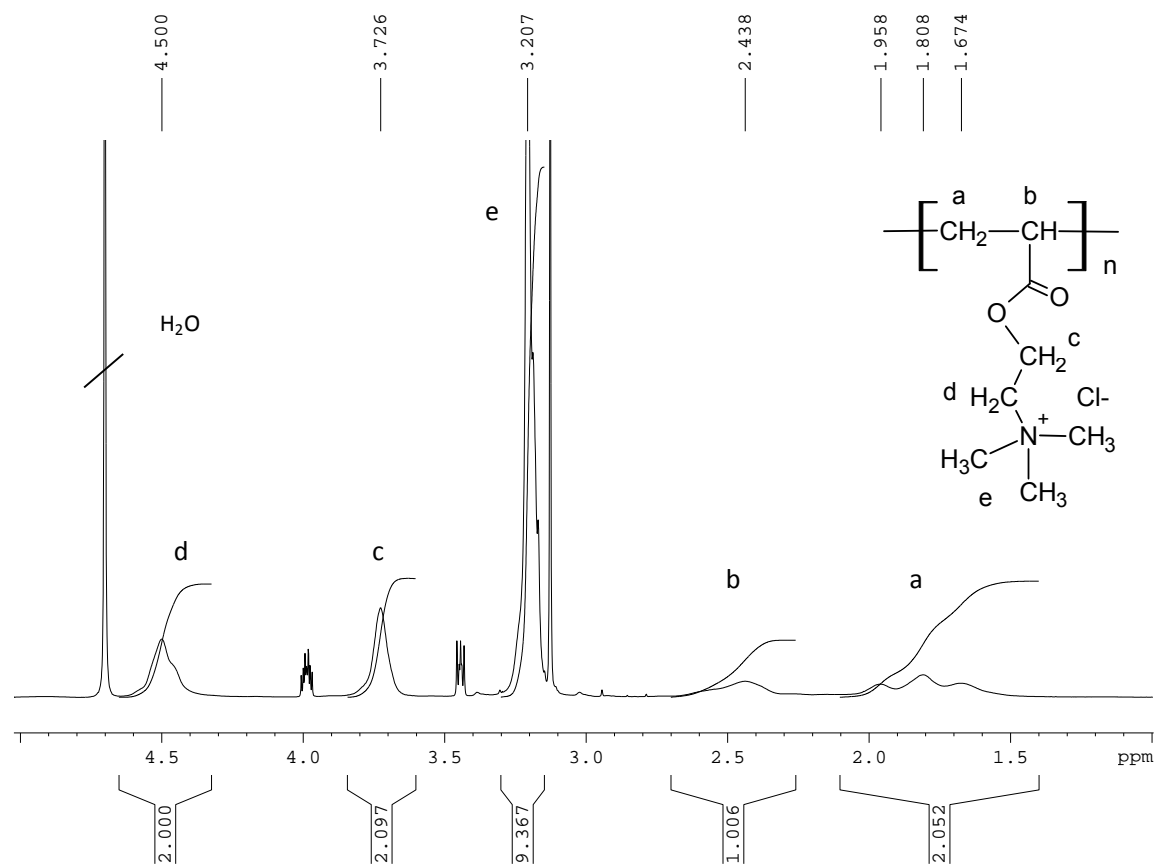


Figure14.  $^1\text{H-NMR}$  (250 MHz,  $\text{D}_2\text{O}$ ) at room temperature for P(CIAETA).

**P(SAETA)**: Protons of the main chain:  $\delta = 1.8$  ppm (2H) (a) and  $\delta = 2.43$  ppm (1H) (b). Protons of the side groups:  $\delta = 3.72$  ppm (2H) (c),  $\delta = 4.5$  ppm (2H) (d) and  $\delta = 3.20$  ppm (9H) (e) for the quaternary ammonium group. The difference between P(CIAETA) and P(SAETA) signals correspond to  $\delta = 3.69$  ppm (3H) for the  $\text{CH}_3\text{OSO}_3^-$  group (f) in the case of the last one (see fig. 15).

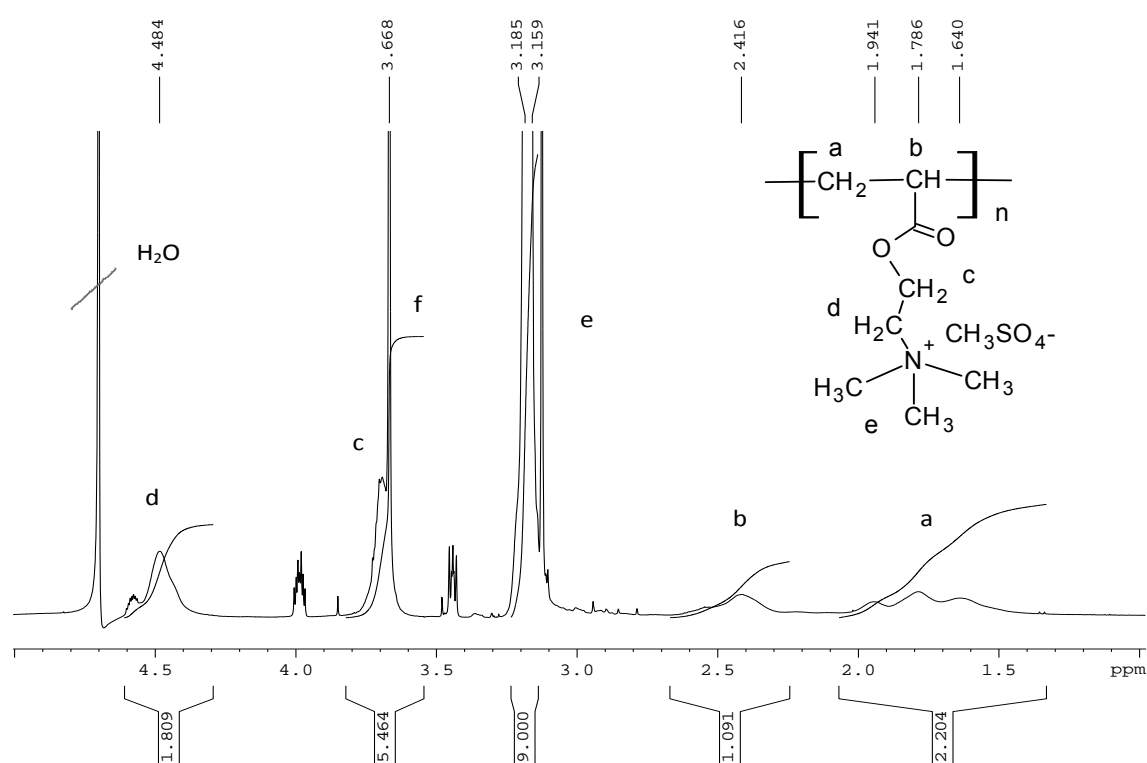


Figure 15.  $^1\text{H-NMR}$  (250 MHz,  $\text{D}_2\text{O}$ ) at room temperature for P(SAETA).

### 2.2.3 Thermogravimetry and differential scanning calorimetry (TG - DSC)

Thermal behavior was studied under N<sub>2</sub> by a thermogravimetric analyzer using a TGA 625 from Polymer Laboratories U.K. The heating rate was 10°C min<sup>-1</sup> in all the cases. The samples weighed 0.5 - 3 mg.

The table 7 shows the maximum decomposition temperature, weight-loss percentage, and enthalpy [decomposition heat (mcal/mg)] obtained by TG–DSC assays. The thermograms for all the polymers presented a typical sigmoid shape indicating that the polycationic structures degraded in several steps. In DSC the decomposition maximum temperature occurred in each step. For all the cases the total weight loss was above 85%.

The TG-DSC essays indicated a weight loss in two steps at different decomposition temperature maximum. For the two homopolymers, P(CIAETA) and P(SAETA) the weight loss was nearly 85%, which occurred at 265 and 330 °C for P(CIAETA) and P(SAETA) respectively (see fig. 16 d and 16 c). The melting temperature range was narrower for P(CIAETA) than for P(SAETA). This difference suggests a slightly better crystallinity in P(CIAETA). The last peak at 420 °C was attributed to exothermic reactions corresponding to ammonium salt decomposition.

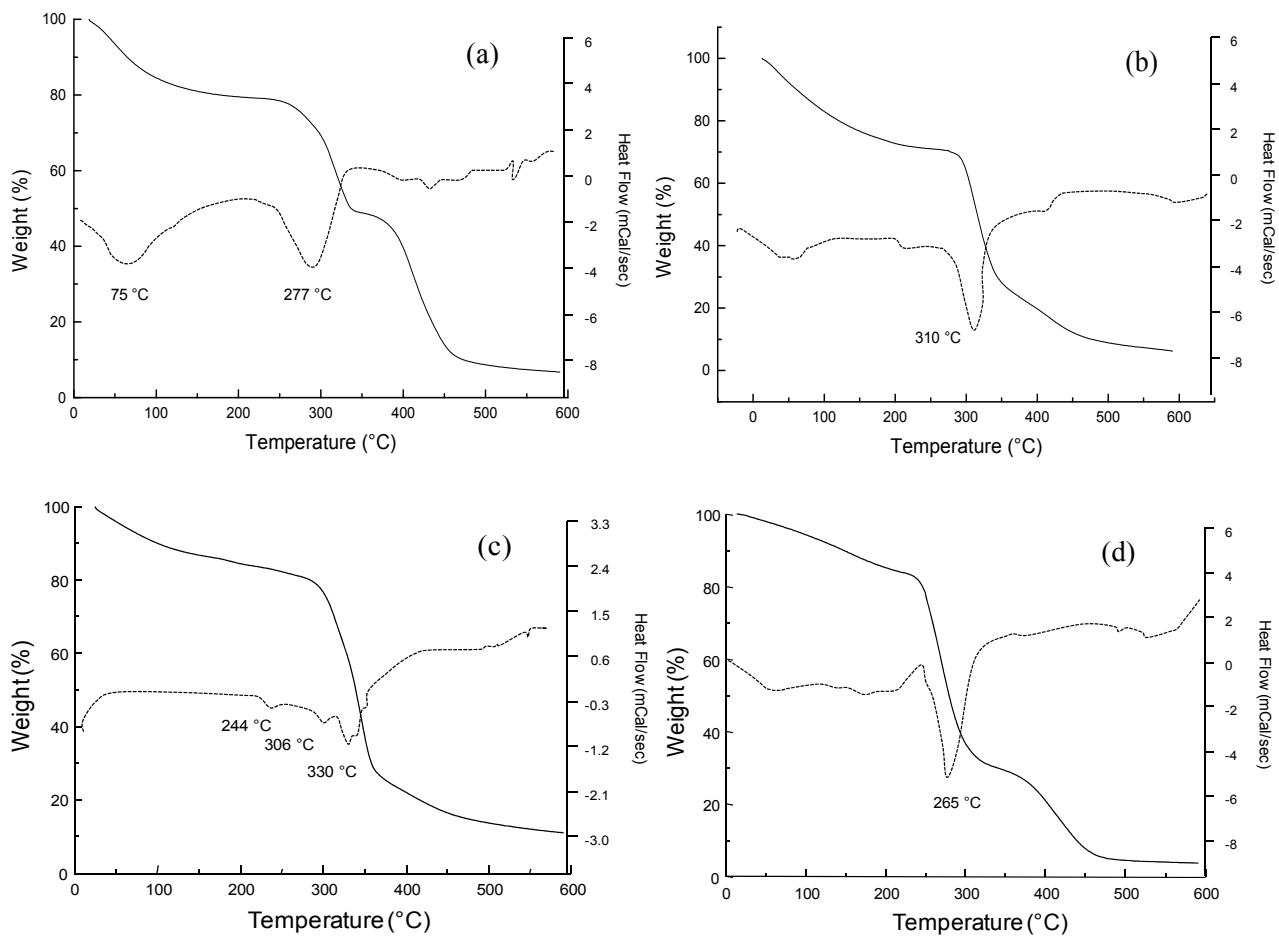


Figure 16. TGA/DSC of (a) P(CIVBTA), (b) P(CIAPTA), (c) P(SAETA) and (d) P(CIAETA). Heating rate 10°C min<sup>-1</sup> under nitrogen.

Table 7. Thermal properties of the water-soluble polyelectrolytes

Polymer	Maximum decomposition temperature (°C)	Descomposition heat (mcal / mg)	$\Delta m$ (wt %)	$\Delta T$ (°C)
P(CIVBTA)	75; 277	105	20; 70	100
P(CIAPTA)	310	106	67	113
P(SAETA)	244; 330	126	10; 58	42; 86
P(CIAETA)	265	88	52	60

### 2.2.4 Conductivity measurements

The solution behavior of the polymers can be further characterized by studying the dependence of the electrical conductivity of the polymer solution on concentration.

The theoretical values of the molar conductivity of polyelectrolyte can be expressed by the equation:

$$\Lambda = f(\lambda_c^\circ + \lambda_p) \quad (6)$$

where  $f$  is the fraction of the free counterions, i.e. the fraction of counterions that have not condensed on the polyion. The molar conductivity of the polyion residue  $\lambda_p$  depends on the nature of counterion through both its charge  $|z_c|$  and molar conductivity at infinite dilution,  $\lambda_c^\circ$ . [3]

The uncondensed counterions fraction  $f$ , according to theory of Manning [3, 4], depends on the inverse of charge density parameter  $\xi$

$$\xi = e^2 / \epsilon k T b \quad (7)$$

where  $e$  is the proton charge,  $\varepsilon$  the bulk dielectric constant of medium,  $k$  the Boltzmann constant,  $T$  the absolute temperature and  $b$  the average distance, taken along the chain, between the charged group, of the polyion.

Conductivity measurements were carried out in water solutions at 25 °C (thermostatic water bath) with a model 4310 conductivity meter. Calibration was made with a standard  $1 \times 10^{-2}$  M KCl solution, ( $\kappa = 1413 \mu\text{S}/\text{cm}$  at 25 °C).

Table 8. Conductivity ( $\kappa$ ) and equivalent molar conductivity ( $\Lambda$ ) measured for the solutions of polyelectrolytes at different concentrations

Polymer	Molecular weight (g mol <sup>-1</sup> )	Concentration (mol L <sup>-1</sup> )	$\kappa$ ( $\mu\text{S cm}^{-1}$ )	$\Lambda$ (S.cm <sup>2</sup> mol <sup>-1</sup> )
			25°C	25°C
P(CIAPTA)	>100000	0.01	649.0	65
P(CIAPTA)	>100000	0.05	2270.2	45
P(CIVBTA)	>100000	0.01	1040.0	104
P(BrVMP)	>50000	0.01	673.5	67
P(CIAETA)	>100000	0.01	729.6	73
P(SAETA)	>100000	0.01	850.5	85
P(CIDDA)	>100000	0.01	763.0	76

The possibility to use the water-soluble polyelectrolytes as supporting electrolytes was evaluated. At first, conductivity measurements were performed in aqueous solutions containing increasing concentrations of different polymers used in this study. The results are summarized in table 8. As expected, both the concentration and molecular weight of polymers significantly influence the conductivity of the solutions. Increasing polymer sizes and concentrations simultaneously diminish conductivity values but all the investigated polymers

can overall be regarded as efficient electrolytes whose conductivity values fall in the range of commonly used aqueous electrolytes.

### **2.3 LPR- Procedure**

The main features of an LPR system (by Amicon) are a filtration cell with a magnetic stirrer containing a membrane filter of poly(ethersulfone) with a known exclusion rating and reservoir and a pressure source, *e.g.* a nitrogen bottle (see fig. 7 chapter 1). In ideal cases this system may be considered a steady-state mixed flow reactor. Conventional stirred filtration cells or a specially designed tangential-flow cell equipped with a pump can be used. Essential parameters are the molar mass exclusion rate in a wide pH range (1 – 12), an appropriate permeate flow rate (0.5 – 12 mL min<sup>-1</sup>), retentate volume (2 – 50 mL) and gas pressure, where 3 bar is a suitable pressure in most cases. The most usual molar mass cut-offs (MMCO) range between 1000 and 300000 Daltons (Da). A nominal exclusion rate of 10000 Da proved to be convenient for polymers having a molecular mass between 30 and 50 kg mol<sup>-1</sup>.

Different modes of separations by LPR can be used for inorganic ions. The first one is the washing method. This is a batch-like method where a liquid sample containing the polymer and the ions to be separated is placed in the ultrafiltration cell at a given pH and ionic strength. This is then washed with a water solution contained in the reservoir that may reproduce the same pH and ionic strength values. The washing method can also be applied to purify a macromolecular compound by eliminating the microsolute. The second mode is the enrichment method, analogous to a column method. A solution containing the metal ions to be separated is passed from the reservoir through the ultrafiltration cell containing a polymer solution. Both cell and reservoir solutions may be adjusted to the same values of pH and ionic

strength. In both cases a blank experiment (in the absence of the water-soluble polymer) is needed in order to evaluate the interaction of the membrane with the metal ions.

Using the washing method, several experiments at different mole polymer : As(V) feed mol ratios were studied. The different mole of the polymer in the range above  $100000 \text{ g mol}^{-1}$  were dissolved in twice-distilled water and added together with the solution containing the minimum of  $1 \times 10^{-5} \text{ mol}$  of arsenate to the cell solution.

The solutions were brought to 20 mL of total volume, and the pH was adjusted by adding  $10^{-1} \text{ M}$  NaOH or  $\text{HNO}_3$  (by Merck) and the ionic strength was adjusted using different concentrations from  $1 \times 10^{-2}$  to  $1 \times 10^{-1} \text{ M}$  of NaCl and  $\text{Na}_2\text{SO}_4$  (by Sigma Aldrich). The washing water of the reservoir was at the same pH of the cell. The ultrafiltration experiments were performed under a total pressure of 3.5 bar at room temperature using a ultrafiltration membrane which have MMCO of 10000 Da. The total volume (20 mL) in the cell was kept constant. Fractions of 20 mL were collected by filtration, and the metal ion concentration was analyzed.

The enrichment method to determine the maximum capacity of polymer was used in aqueous solution, using  $4 \times 10^{-3} \text{ M}$  of As(V) solution and  $8 \times 10^{-4} \text{ mol}$  of water-soluble polymers at 300 mL of total filtrate volume. Arsenic concentration was measured in the filtrate by atomic absorption spectrometry (AAS) using a Perkin Elmer 3100 spectrometer; the quantity of arsenic species retained was determined from the difference with the initial concentration. The pH was controlled by a pH meter (H. Jürgen and Co).

## ***2.4 Preparation of noble metal nanoparticles-polymer modified electrodes***

In this paragraph we describe the synthesis of nanocomposites electrode materials, obtained by the dispersion of noble metal micro and nanoparticles into poly(pyrrole-alkylammonium) films coated onto carbon electrodes, which display strong electrocatalytic properties towards the oxidation of arsenite to arsenate. In addition, the nanocomposites were further characterized by transmission electron microscopy (TEM).

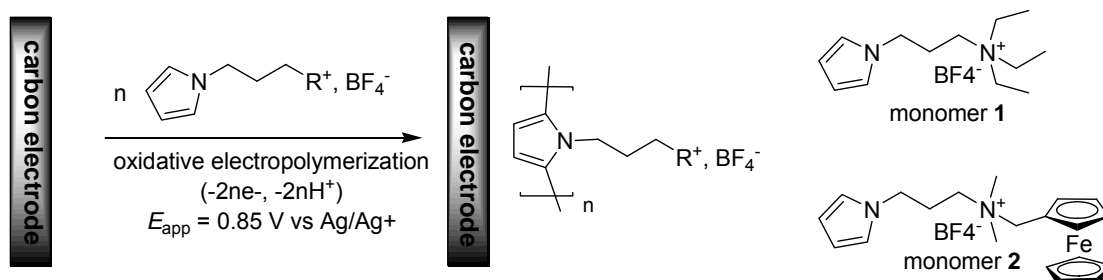
The procedure used for the electrosynthesis of the nanocomposite film modified electrodes is summarized on Scheme 17.

### **2.4.1 Synthesis of alkylammonium and ferrocenylalkylammonium N-substituted polypyrrole films (C|poly1, C|poly2)**

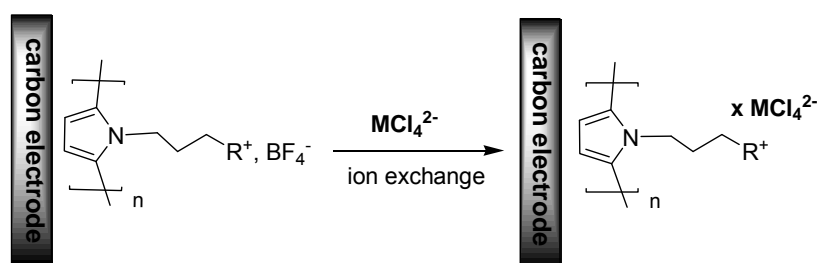
All electrochemical experiments were carried out using an EGG PAR model 273 potentiostat equipped with an *x-y* recorder. A standard three-electrode cell was used for analytical experiments. Potentials are referred to the Ag|AgCl in 3 M KCl reference electrode in aqueous electrolytes, and to the Ag|Ag<sup>+</sup> 10<sup>-2</sup> M in CH<sub>3</sub>CN + 10<sup>-1</sup> M TBAP. The glassy carbon disc electrodes (3 mm diameter) were polished with 1- $\mu$ m diamond paste. All experiments were run at room temperature under an argon atmosphere.

Potassium tetrachloroplatinate and palladate, sodium hexachlororhodate and acetonitrile (Rathburn HPLC grade S) was used as received. Tetra-*n*-butylammonium perchlorate (TBAP, Fluka puriss) was dried under vacuum at 80°C for 3 days. Distilled water was obtained from an Elgastat water purification system (5 M $\Omega$  cm).

### 1. Electropolymerization of pyrrole-alkylammonium monomer



### 2. Inclusion by ion exchange of a metal salt ( $M = \text{Pt, Pd}$ )



### 3. Electroreductive precipitation of $M(0)$ nanoparticles

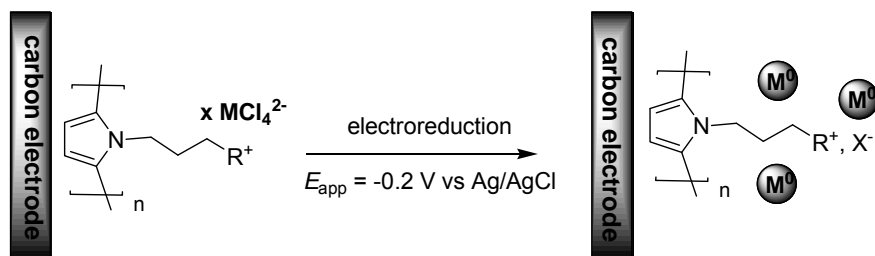


Figure 17. Scheme of electrochemical strategies for synthesis of catalytic nanocomposite electrode materials in three steps. 1) Oxidative electropolymerization at 0.85 V vs. Ag/Ag<sup>+</sup> of  $4 \times 10^{-3}$  M solutions of monomer 1 or 2 monomer in CH<sub>3</sub>CN containing 10<sup>-1</sup> M TBAP as supporting electrolyte. 2) C|Poly1 or C|Poly2 modified electrodes were immersed for 30 min into 10<sup>-3</sup> M of K<sub>2</sub>PtCl<sub>4</sub> or K<sub>2</sub>PdCl<sub>4</sub> aqueous solutions containing 10<sup>-1</sup> M Na<sub>2</sub>SO<sub>4</sub> to ensure a large incorporation by ion exchange of inorganic anions in the polymer film. 3) Electroreductive precipitation of M<sup>0</sup> nanoparticles by controlled potential at -0.2 V vs. Ag|AgCl in the same solution.

### Monomer 1

The (3-pyrrol-1-yl propyl)triethylammonium tetrafluoroborate (see fig.18.1), denoted monomer **1**, was prepared according to a previously reported procedure [5], by reacting triethylamine with N-(3-bromopropane-1-yl)pyrrole. The latter was obtained from 2,5-dimethoxytetrahydrofuran and 3-bromopropylamine following the procedure described for N-(2-chloroethane-1-yl)pyrrole, and purified by chromatography on a silica column eluted with  $\text{CH}_2\text{Cl}_2$  [6].

### Monomer 2

Monomer **2** (see fig. 18.2) was prepared according to a previously reported procedure [7]: equimolar mixtures of (dimethylamino)methylferrocene and iodopropylpyrrole were stirred for 2 hours at 60 °C. The yellow precipitates formed were collected by suction filtration and washed with acetone to give the iodide salt of structure **2** in 74% yield. The tetrafluoroborate salts of structure **2** were obtained by ion-exchange chromatography on Amberlite IRA 93 column in its  $\text{BF}_4^-$  form.

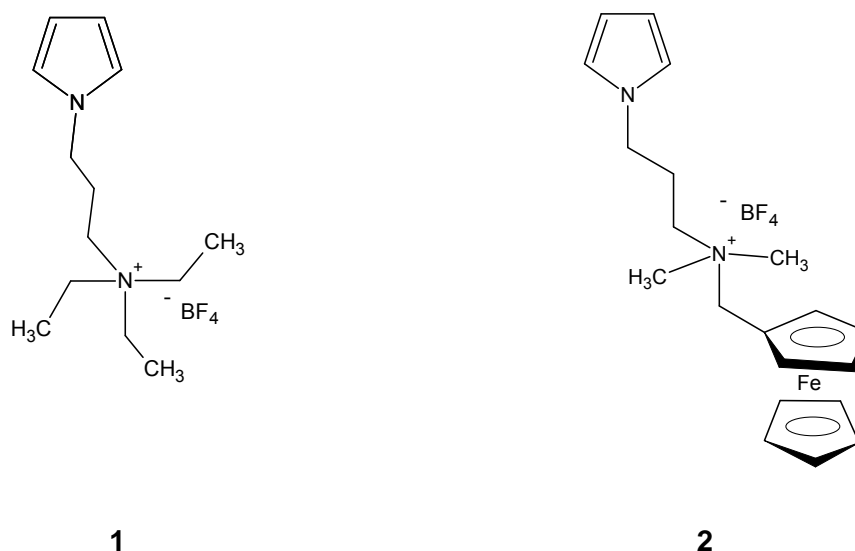


Figure 18. Structure of monomer **1** and monomer **2**.

The polymer films (denoted poly1 and poly2) can be grown by repeated cyclic voltammetry scans, from unstirred  $4 \times 10^{-3}$  M solutions of monomer **1** and **2** respectively, in  $\text{CH}_3\text{CN}$  containing  $10^{-1}$  M TBAP as supporting electrolyte. The increase in current with each cycle of a multisweep CV is a direct measure of the increase in the surface of the redoxactive polymer. A typical example is shown on figure 19.

Polymers were also by potentiostatic oxidative electropolymerization at + 0.85 V vs.  $\text{Ag}|\text{Ag}^+$   $10^{-2}$  M [5, 7]. Polymerization experiments were controlled through the anodic charge recorded during the electrolysis.

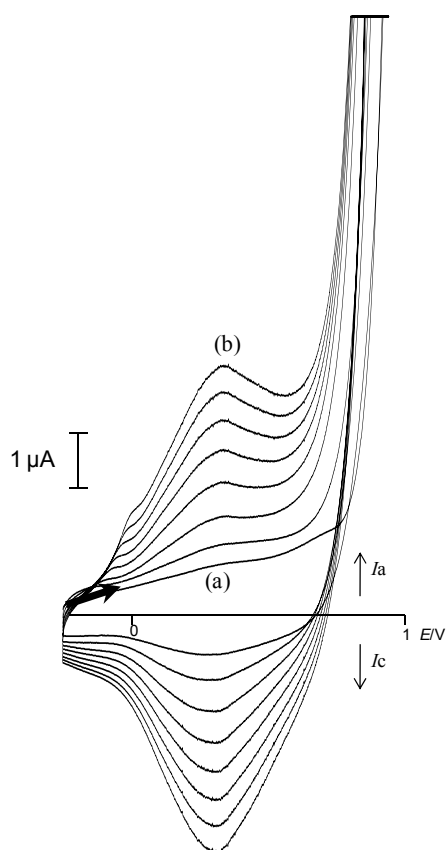


Figure 19. Successive cyclic voltammetry curves for  $4 \times 10^{-3}$  M of monomer **1**, in  $\text{CH}_3\text{CN}$  containing  $10^{-1}$  M TBAP as supporting electrolyte, between -0.2 to +1 V vs.  $\text{Ag}|\text{Ag}^+$   $10^{-2}$  M. Scan rate  $50\text{mVs}^{-1}$ , (a) 1<sup>st</sup> cycle and (b) 18<sup>th</sup> cycle.

## 2.4.2 Electrochemical characterization

The amount of pyrrole units in the films and thus, the apparent surface coverage in ammonium units  $\Gamma_{N^+}$  ( $\text{mol cm}^{-2}$ ) were determined after transfer of the modified electrodes to monomer-free  $\text{CH}_3\text{CN}$  electrolyte from the integration of the polypyrrole oxidation wave recorded at low scan rate ( $10 \text{ mV s}^{-1}$ ), assuming that one in three pyrrole units is oxidized [8].

The intensity is a direct function with the moles numbers of pyrrole sites ( $N$ ) in the polymer. The integration of the quantity of current consumed for the polypyrrole oxidation ( $Q_a$ ) is possible to obtain the amount of moles numbers in the following relation,

$$N = |Q_a| / n F \quad (8)$$

where  $n$  is the number of electrons exchanged by pyrrole unit during the oxidation of polymer ( $n = 0.3$ ) and  $F$  is the faraday number ( $96500\text{C}$ ).

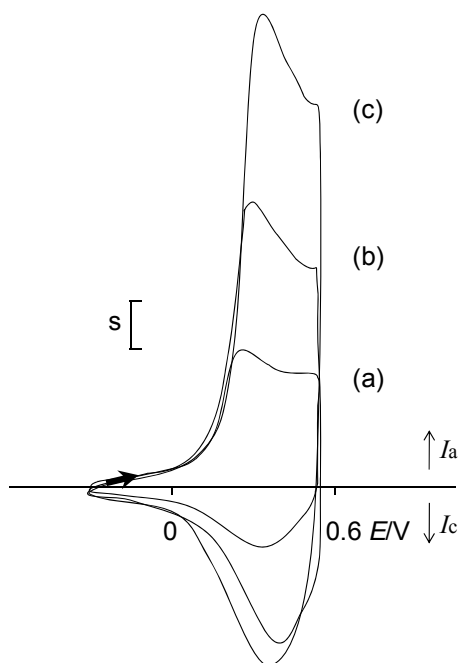


Figure 20. Cyclic voltammetry curves recorded ( $10\text{mVs}^{-1}$  in  $\text{CH}_3\text{CN}$  containing  $0.1 \text{ M}$  TBAP as supporting electrolyte) for C|poly1 modified electrodes synthesized using  $4 \times 10^{-3}\text{M}$  of monomer at  $+ 0.85 \text{ V}$  at different polymerization charges : (a) 1, (b) 2 and (c) 3 mC.  $S = 1 \mu\text{A}$ .

In the case of poly1 the signal obtained in CV between -0.2 and 0.5V prove the existence of polymer (see fig. 20). Typically films of poly1 showed  $\Gamma_{N^+}$  ranging from  $2.1 \times 10^{-8}$ ,  $3.7 \times 10^{-8}$  and  $4.8 \times 10^{-8} \text{ mol cm}^{-2}$  (see table 9) were coated onto the analytical (3 mm diameter) glassy carbon disc electrodes obtained using polymerization charges of 1, 2 and 3 mC, respectively.

In the case of poly2, the resulting modified display a stable electrochemical response (see fig. 21) for the ferrocene (Fc) center at  $E_{1/2} = + 0.26 \text{ V}$ .

The apparent surface concentration was determined by recording CV curve, between + 0.1 and + 0.4 V at  $10 \text{ mV s}^{-1}$  in  $\text{CH}_3\text{CN}$  electrolyte solution and measuring the charge under the anodic peak, but in this case taking account 1.3 exchange electrons per monomer – one for the ferrocene center and 0.3 for the polypyrrole center [7].

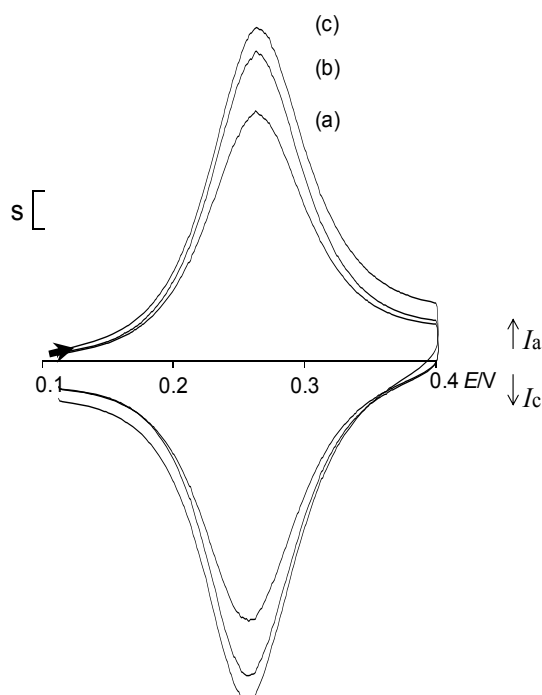


Figure 21. Cyclic voltammetry curves recorded ( $10 \text{ mV s}^{-1}$  in  $\text{CH}_3\text{CN}$  containing 0.1 M TBAP as supporting electrolyte) for C|poly2 modified electrodes synthesized using  $4 \times 10^{-3} \text{ M}$  of monomer at + 0.85 V at different polymerization charges : (a) 1, (b) 2 and (c) 3 mC.  $S = 0.25 \text{ } \mu\text{A}$ .

Table 9. Apparent surface coverage in function of polymerization charge applied.

Polymer Film	Polymerization Charge, $Q_p$ (mC)	Anodic Charge, $Q_a$ (C)	N	$\Gamma$ (mol $\text{cm}^{-2}$ )
C Poly1				
	1	$4.4 \times 10^{-5}$	$1.5 \times 10^{-9}$	$2.1 \times 10^{-8}$
	2	$7.7 \times 10^{-5}$	$2.6 \times 10^{-9}$	$3.7 \times 10^{-8}$
	3	$9.8 \times 10^{-5}$	$3.3 \times 10^{-9}$	$4.8 \times 10^{-8}$
C Poly2				
	1	$7.34 \times 10^{-6}$	$5.9 \times 10^{-11}$	$8.4 \times 10^{-10}$
	2	$8.12 \times 10^{-6}$	$6.5 \times 10^{-11}$	$9.2 \times 10^{-10}$
	3	$9.13 \times 10^{-6}$	$7.3 \times 10^{-11}$	$1.0 \times 10^{-9}$

### 2.4.3 Elaboration of polymer-metal composites with Pt, Pd (C|polymer - metal)

To fabricate polymer-metal composites with varying Pt and Pd dispersions on electrodes, C|Poly1 and C|Poly2 modified electrodes were immersed for 30 min into  $10^{-3}$  M of  $\text{K}_2\text{PtCl}_4$  or  $\text{K}_2\text{PdCl}_4$  aqueous solutions containing  $10^{-1}$  M  $\text{Na}_2\text{SO}_4$  to ensure a large incorporation by ion exchange of inorganic anions in the polymer film and then electroreduced by controlled potential at  $-0.2$  V vs. Ag|AgCl in the same solution. Prior to the incorporation of metal in poly1 films, the electroactivity of the polypyrrole matrice was destroyed [5] by repeated potential scans between  $-0.2$  and  $+1.5$  V in clean aqueous electrolyte. On the other hand, the electroactivity of poly2 was not destroyed prior to incorporation of metal due to use the Fc/Fc<sup>+</sup> couple for try to improve the arsenite analytical detection. This part will be discussed in the next chapter.

The metal loading was estimated from the cathodic charge passed. In the next chapter the influence and optimization of polymer thickness and metal loading in the arsenite oxidation will be discussed.

#### 2.4.4 Synthesis of alkylammonium substituted polypyrrole films (C|poly1) nanoparticles modified electrodes at preparative scale

For preparative-scale electro-oxidation of As(III) solutions polymer films were grown on carbon felt (RVC 2000,  $65 \text{ mg cm}^{-3}$ , from Le Carbone Lorraine) electrodes ( $20 \times 20 \times 4 \text{ mm}$ ) using a polymerization charge of 5 Coulomb (see fig. 22). This led to the deposition onto the carbon felt of a polymeric material containing about 8 - 9  $\mu\text{mol}$  of ammonium groups (polymerization yield 35 - 40%). The precipitation of platinum metal in the polymer was performed by electroreduction at  $-0.2 \text{ V}$  vs. Ag|AgCl in  $10^{-4} \text{ M K}_2\text{PtCl}_4$ ; a charge of 5 or 10 Coulomb was passed, which corresponds to the deposition of 5 or 10 mg of platinum, respectively.

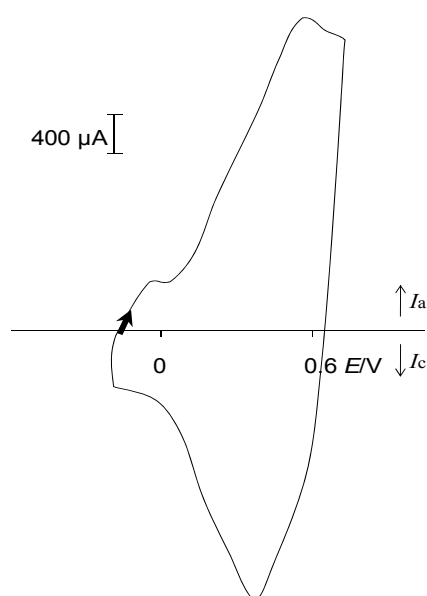


Figure 22. Cyclic voltammety curve recorded et  $10\text{mVs}^{-1}$  in  $\text{CH}_3\text{CN}$  containing  $10^{-1} \text{ M}$  TBAP as supporting electrolyte, for a carbon felt|poly1 modified macroelectrodes ( $20 \times 20 \times 4 \text{ mm}$ ) synthesized using  $4 \times 10^{-3} \text{ M}$  of monomer at  $+0.85 \text{ V}$  at polymerization charge of 5C.

#### 2.4.5 Characterization of the nanocomposites by transmission electron microscopy

For TEM experiments, Pt<sup>0</sup>-poly1 films were deposited onto ITO-coated on glass electrodes (1 cm<sup>2</sup>). Typically the poly1 films were deposited using a charge of 80 mC, and platinum was dispersed in the films by electroreduction using cathodic charges from 40 to 80 mC. The films of nanocomposites were peeled off, and a piece of film was deposited in flat mold filled with epoxy resin. The resin was cured at 60 °C for 72 hours. Cross-section through the thick of the nanocomposites was obtained with a diamond knife at a thickness of 70 nm using a Leica UC6 microtome. The thin sections were collected onto a formvar coated slotted patterns copper grid (type 75/300) and observed with a JEOL 3010 transmission electron microscope in the laboratory of the Science et Ingénierie des Matériaux et des Procédés (SIMAP, Grenoble).

Some information on the structure of the C|metal-poly1 modified electrodes prepared in the same way had already been obtained by scanning electron microscopy (SEM) and Auger electron spectroscopy (AES) [7]. Examination of noble metals-poly1 composites by SEM revealed that large metal particles, in the range 0.1 - 0.2 μm, were dispersed on the surface of the films. In addition, cross-sectional SEM views of metal-poly1 films showed a large accumulation of metal at the carbon substrate/polymer interface. AES depth profile analyses have confirmed the large accumulation of metal at the carbon substrate / polymer interface, also showing that some metal is dispersed throughout the polymer layers. However, no information could be obtained on the size of the metal particles in the bulk of the polymer. This information could be obtained in the course of the present thesis, using transmission electron microscopy (TEM) experiments carried out with Pt-containing composites. The TEM image showing the cross-sectional view of a Pt<sup>0</sup>-poly1 film (see fig. 23A) displays a dark band at the polymer / ITO interface, typical of the accumulation of metal in this area, confirming the previous results obtained from SEM experiments on similar materials. EDX analysis

demonstrated that the dark interfacial band (see fig.23 B) consisted of platinum, and that there is only a few amount of platinum in the polymer bulk. One can rationalize that the metal accumulates at the electrode / polymer interface, since this is the source of electron to reduce  $\text{PtCl}_4^-$  anions to  $\text{Pt}^0$ .

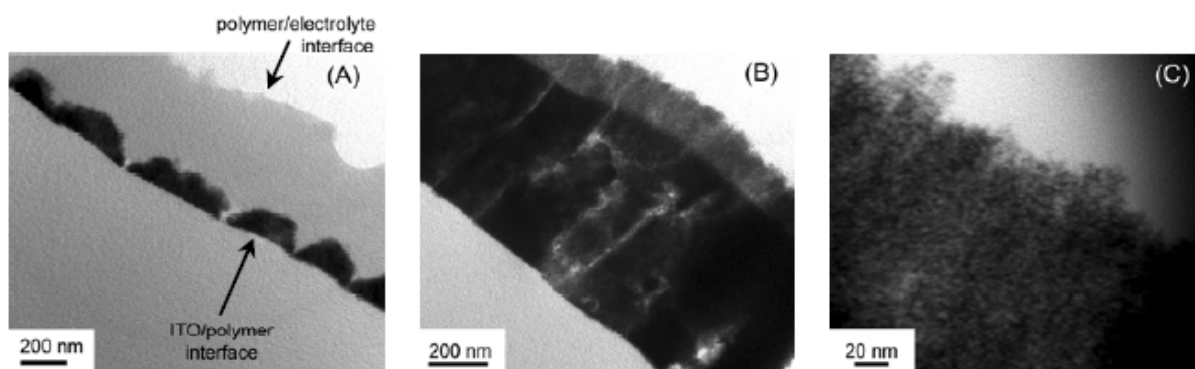


Figure 23. TEM images (cross-sectional views) a of poly1 film containing Pt particles.

The deposits of platinum were further analyzed by high resolution TEM. The microscopy indicates that, rather than being deposited as film or large particles, an aggregate of nanoparticles in the 3 - 5 nm size range is formed (see fig. 23C) [9]. One can also see that some nanoparticles coalesce.

## 2.5 Conclusions

The water-soluble cationic polymers synthesized by radical polymerization and having different groups as anion exchangers show polymerization yields in mass between 77% to 99%. Minimum yields in the case of P(SAETA) and maximum for P(CIAPTA).

The thermal analysis of all the water-soluble polymers indicated a weight loss in two steps at different decomposition temperature maximum. For the two similar homopolymers with different counterions, P(CIAETA) and P(SAETA), the weight loss was nearly 85%, which occurred at 265 and 330 °C for P(CIAETA) and P(SAETA), respectively. The melting temperature range was narrower for P(CIAETA) than for P(SAETA). This difference suggests a slightly better crystallinity in P(CIAETA). The last peak at 420 °C was attributed to exothermic reactions corresponding to ammonium salt decomposition in all the cases.

The possibility to use water-soluble polyelectrolytes as supporting electrolytes was evaluated. Increasing polymer sizes and concentrations simultaneously diminish the conductivity values but all the investigated polymers can be regarded as efficient electrolytes whose conductivity values, fall in the range of commonly used aqueous electrolytes.

The polymer films (denoted poly1 and poly2) were synthesized by repeated cyclic voltammetry scans and potentiostatic oxidative electropolymerization at + 0.85 V vs. Ag|Ag<sup>+</sup> 10<sup>-2</sup> M.

The amount of pyrrole units in the films were determined after transfer of the modified electrodes to monomer-free CH<sub>3</sub>CN electrolyte from the integration of the polypyrrole oxidation wave recorded at low scan rate. Typically films of poly1 showed  $\Gamma_{N^+}$  ranging from  $2.1 \times 10^{-8}$ ,  $3.7 \times 10^{-8}$  and  $4.7 \times 10^{-8}$  mol cm<sup>-2</sup> were obtained using polymerization charges of 1, 2 and 3 mC respectively. In the case of poly2, the resulting modified electrode display a stable

electrochemical response for the ferrocene (Fc) center at  $E_{1/2} = + 0.26$  V. Typically films of poly $2$  showed  $\Gamma_{N^+}$  ranging from  $8.4 \times 10^{-10}$ ,  $9.2 \times 10^{-10}$  and  $1.0 \times 10^{-9}$  mol  $\text{cm}^{-2}$ .

To prepare polymer-metal composites with varying Pt and Pd dispersions on electrodes C|Poly $1$  and C|Poly $2$  modified electrodes were immersed into  $\text{K}_2\text{PtCl}_4$  or  $\text{K}_2\text{PdCl}_4$  aqueous solutions to ensure a large incorporation by ion exchange of inorganic anions in the polymer film and then electroreduced by controlled potential. The metal loading was estimated from the cathodic charge passed.

Finally, the TEM image showing the cross-sectional view of a  $\text{Pt}^0$ -poly $1$  film displays a dark band at the polymer / ITO interface, typical of the accumulation of metal in this area, confirming the previous results obtained from SEM experiments on similar materials. EDX analysis demonstrated that the dark interfacial band consisted of platinum, and that there is only a small amount of platinum in the polymer bulk. One can rationalize that the metal accumulates at the electrode/polymer interface, since this is the source of electron to reduce  $\text{PtCl}_4^-$  anions to  $\text{Pt}^0$ .

The SEM indicated that, rather than being deposited as film or large particles, an aggregate of nanoparticles in the 3 - 5 nm size range was formed. One can also see that some nanoparticles coalesce. All these observations are in agreement with the formation of nanostructured platinum-polymer composite films, using this very simple all-electrochemical procedure.

## 2.6 References

- 1) Marcelo, G.; Tarazona, M.P. and Saiz, E. Solution properties of poly(diallyldimethylammonium chloride) (PDDA). *Polymer*. 2005;p.2584-2594.
- 2) J. Mc. Murry, in J. Huber editor. *Organic chemistry* 5<sup>th</sup> edition. Brooks/Cole Thompson Learning publishing C.A., 2000.
- 3) Manning, G.S. Limiting laws and counterion condensation in polyelectrolyte solution. IV. The approach to the limit and the extraordinary stability of the charge fraction. *Biophys.* 1977;7:95-102.
- 4) Manning, G.S. A limiting law for the conductance of the rod model of a salt-free polyelectrolyte *J. Phys. Chem.* 1975;79:p.262-265.
- 5) Cosnier, S.; Deronzier, A.; Moutet, J.-C. and Roland, J.F. Alkylammonium and pyridinium group-containing polypyrroles, a new class of electronically conducting anion-exchange polymers. *J. Electroanal. Chem.* 1989;271:p.69-81.
- 6) De Oliveira, I.M.F.; Moutet, J.-C. and Hamar-Thibault, S. Electrocatalytic hydrogenation activity of palladium and rhodium microparticles dispersed in alkylammonium- and pyridinium substituted polypyrrole films. *J. Mater. Chem.* 1992;2:p.167-173.
- 7) Reynes, O.; Royal, G.; Chaînet, E.; Moutet, J.-C. and Saint-Aman, E. Poly(ferrocenylalkylammonium): a molecular electrode material for dihydrogenphosphate sensing. *Electroanalysis* 2003;15:p. 65-69.
- 8) Deronzier, A. and Moutet, J.-C. Polypyrrole films containing metal complexes: syntheses and applications. *Coord. Chem. Rev.* 1996;147:p.339-371, and references therein.
- 9) Sánchez, J.; Rivas, B.L.; Pooley, A.; Basaez, L.; Pereira, E.; Pignot-Paintrand, I.; Bucher, C.; Royal, G.; Saint-Aman, E. and Moutet, J.-C. Electrocatalytic oxidation of As(III) to As(V) using noble metal-polymer nanocomposites. *Electrochim. Acta.* 2010, 55: p. 4876-4882.

### 3. RESULTS AND DISCUSSION

#### *3.1 Removal of arsenic by LPR technique*

Preliminary studies done in our research group proved the ability of some water-soluble polymers based on ammonium salts for the removal of arsenic species from aqueous solution using the LPR technique [1-5]. The main advantage of the LPR is that this technique is performed in homogeneous media and avoids the phenomena of mass transfer or diffusion that occur in heterogeneous methods. Other advantages are that it is also possible to obtain selectivity towards oxy-arsenic ions in solution, capacity of water-soluble polymer regeneration, and the technique has a low cost.

The first arsenic retention experiment was done in order to compare the removal capacity of As(V) and As(III) at pH 9 and polymer : arsenic (20:1) molar ratio using the LPR technique-washing method.

The results (see table 10) shows the high affinity of the polymer to interact and remove As(V) species and the non-retention of As(III) species. This can be explained by the speciation of As(III) in aqueous media. Different As(III) species are present in solution (see Chapter 1, table 2) according to the pH:  $\text{H}_2\text{AsO}_3^-$ ,  $\text{HAsO}_3^{2-}$  and  $\text{AsO}_3^{3-}$ , with  $\text{pK}_{a1} = 9.2$ ,  $\text{pK}_{a2} = 12.1$  and  $\text{pK}_{a3} = 13.4$ . Therefore, at pH 9 the As(III) species are in equilibrium between the non-dissociated salt and the mono arsenic oxy-anion. On the other hand, As(V) species coexist in an aqueous medium according to the pH:  $\text{H}_2\text{AsO}_4^-$ ,  $\text{HAsO}_4^{2-}$  and  $\text{AsO}_4^{3-}$ ;  $\text{pK}_{a1}: 2.2$ ;  $\text{pK}_{a2}: 7.0$  and  $\text{pK}_{a3}: 11.5$ .

The retention capacity of the polyelectrolyte is in direct relation with the anion exchange of the counterion corresponding to quaternary ammonium of polyelectrolyte because in these systems the electrostatic interactions are predominant. According to the literature it is

suggested that the anionic exchange prefers more divalent ions than monovalent ions at the same conditions [1]. This can be confirmed by the high retention capacity of As(V) species and the non-retention of As(III) species using the water-soluble polyelectrolyte at pH 9 with the LPR technique.

Table10. Removal of arsenic species from aqueous solution using different cationic polyelectrolytes with LPR technique-washing method at pH 9 and Z =10, with  $2 \times 10^{-4}$  mol absolute polymer and  $1 \times 10^{-5}$  mol absolute arsenic ion.

Polymer	R(%) of As(V)	R(%) of As(III)
P(CIVBTA)	95.1	0.0
P(CIAPTA)	94.4	0.0
P(SAETA)	67.7	0.0
P(CIAETA)	96.0	0.0
P(BrVMP)	54.3	0.0
P(CIDDA)	100	0.0

Lately the research of our group has been focused to develop systems to extract the most toxic arsenic species that is arsenite. A series of water-soluble polychelates have been prepared and used for retaining As(III) directly from the solution. The complex of poly(acrylic acid)-Sn, 10 and 20 percentage by weight of metal, introduced a high retention of As(III) species at pH 8, however the molar ratio of polychelate:As (III) was 400:1 [4].

### **3.1.1 Removal of arsenate by polymer containing ammonium groups through the LPR-washing method**

Polymers with high molecular weight (fractions above  $100000 \text{ g mol}^{-1}$ ) were used in LPR experiments to interact with the arsenate oxy-anions. Membranes of poly(ether sulfone) were used with molar mass cut-off (MMCO) of 10000 Da. This porous size in molecular weight is much lower than the polymer. In the cell was placed a solution of polymer/arsenate and these were washed with distilled water at constant volume and fixed pH.

Water-soluble cationic polyelectrolytes containing different exchanger counterions have been synthesized and studied recently (see fig. 9 of experimental part). They present different capacities of arsenate retention. Polymeric structures with quaternary ammonium salts with different counterions, such as methyl sulphate, chloride and bromide, show different interactions with arsenate in aqueous solution since the type of counterion influences the retention. However, all the polymers remove more efficiently arsenate ions at pH 9 than at pH 6 to 3.

#### **3.1.1.1 The effect of pH on the arsenate retention**

It is well established (see Chapter 1, table 2) that different inorganic As(V) species coexist in an aqueous medium according to the pH:  $\text{H}_2\text{AsO}_4^-$ ,  $\text{HAsO}_4^{2-}$  and  $\text{AsO}_4^{3-}$ ;  $\text{pK}_{a1}$ : 2.2;  $\text{pK}_{a2}$ : 7.0 y  $\text{pK}_{a3}$ : 11.5.

The effect of pH on the retention of arsenate was studied. The removal of As(V) in form of mono and divalent oxy-anions was determined using the LPR with different cationic polyelectrolytes through the washing method in a range from acidic to basic pH.

The results are expressed in retention profile (see fig. 24) that shows the rate of retention, R versus filtration factor Z of different water-soluble cationic polyelectrolytes, at different pH. In general, the As(V) is more easily retained at pH between 6 and 9 than at a lower pH. At pH 3

monovalent anionic species ( $\text{H}_2\text{AsO}_4^-$ ) are in equilibrium with the coupled salt. It is assumed that the polarity of the functional group of the polymer should be a parameter to control the selectivity of ion exchange. At pH 6 the monovalent ( $\text{H}_2\text{AsO}_4^-$ ) and divalent ( $\text{HAsO}_4^{2-}$ ) oxy-arsenic species exist in equilibrium. The retention capacity of the polymer is due to the presence of a positively charged quaternary ammonium group. These interactions are produced through the anion exchange between chloride counterion of quaternary ammonium salt and the arsenate anions. This can be corroborated by the higher retention capacity of the polymers at basic pH because divalent As(V) species are predominant. In this study we used the washing method in mole ratio polymer : As(V) of 20:1. The polymers removed between 80 - 100% of ion arsenates at pH between 6 and 9, where arsenate is in the form of oxy-anionic divalent species. However, at pH 3 the species of monovalent arsenate prevail and the clearance is below 60%.

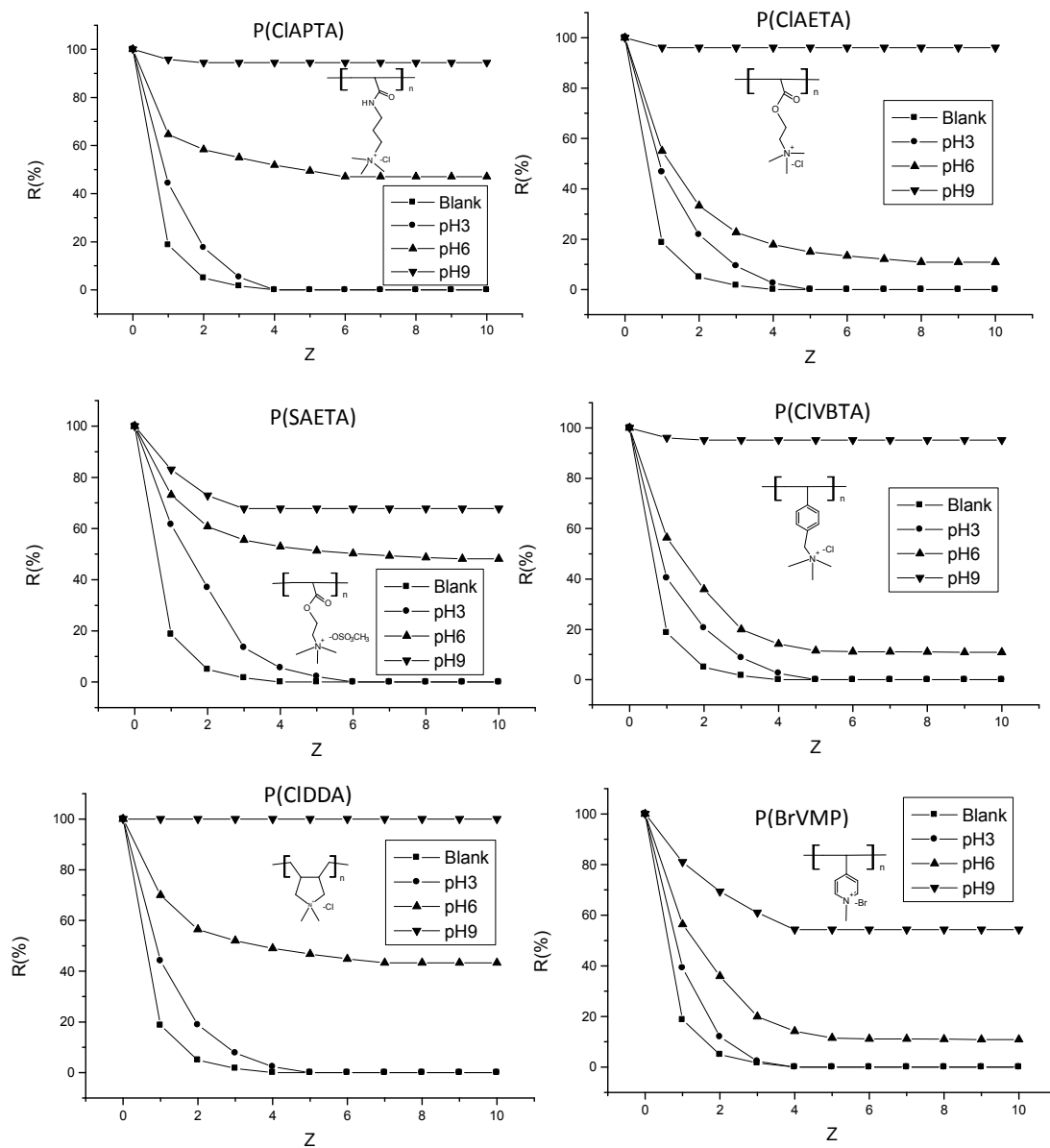


Figure 24. Retention profile of As(V) using diverse water-soluble polyelectrolytes, at different pH, with  $2 \times 10^{-4}$  mol absolute polymer and  $1 \times 10^{-5}$  mol absolute As(V) ion.

### 3.1.1.2 Effect of polymer : As(V) mol ratio on arsenate retention

The removal of arsenate was optimized by changing the polymer : arsenate ratio in moles. The influence of the concentration of polymers P(CIAETA) and P(CIVBTA) in the arsenate removal was studied using the washing method. Different of polymer : As(V) molar ratios such as 31:1, 20:1, 10:1, 6:1 and 3:1, were prepared at pH 8. The results of retention R (%) of As(V) with a filtration factor of  $Z = 10$  (see fig. 25), P(CIVBTA) and P(CIAETA) by the washing method are presented in table 11. The retention capacity was limited by the of polymer concentration when 10 – 84 mg L<sup>-1</sup> arsenic concentration range was used.

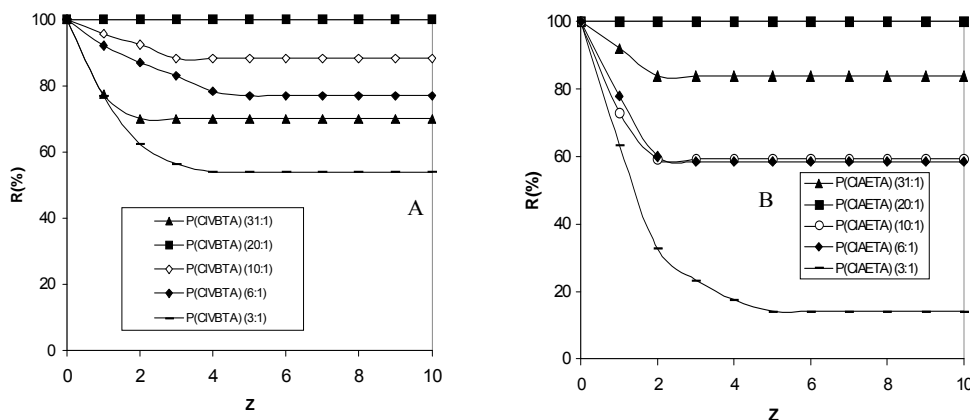


Figure 25. Retention profile of As(V) by (A) P(CIVBTA) and (B) P(CIAETA) at pH 8, using different molar ratio of polymer : As (V),  $\blacktriangle$  31:1,  $\blacksquare$  20:1,  $\blacklozenge$  10:1,  $\diamond$  6:1,  $\times$  3:1.

The results indicate an optimum of 20:1 (polymer : arsenate) molar ratio for the complete removal of arsenate. This happened even in two range orders of magnitude:  $2 \times 10^{-4}$  and  $7 \times 10^{-5}$  mol of polymer. This is important from the point of view of application due to the high efficiency of the polymer with respect to the recovery of the species of As(V), even at high concentrations.

Table 11. Behavior of different molar ratio polymer : As(V) in the removal of arsenate using P(CIVBTA) and P(CIAETA) at pH 9.

Molar ratio	Mole of polymer	Mole of As(V)	P(CIVBTA)	P(CIAETA)
Polymer : As(V)			R(%), pH 9	R(%), pH 9
(31:1)	$7 \times 10^{-5}$	$2.25 \times 10^{-4}$	70.0	84.0
(20:1)	$7 \times 10^{-5}$	$3.45 \times 10^{-6}$	100.0	100.0
(20:1)	$2 \times 10^{-4}$	$1.00 \times 10^{-5}$	100.0	100.0
(10:1)	$7 \times 10^{-5}$	$6.90 \times 10^{-6}$	88.0	59.0
(6:1)	$7 \times 10^{-5}$	$1.12 \times 10^{-5}$	77.0	60.0
(3:1)	$7 \times 10^{-5}$	$2.25 \times 10^{-5}$	54.0	14.0

### 3.1.1.3 Influence of the polymer anion exchanger groups on arsenate retention

Poly[2-(acryloyloxy)ethyl]trimethylammonium chloride, P(CIAETA), and poly[2-(acryloyloxy)ethyl]trimethylammonium methylsulphate, P(SAETA), have similar structures except the exchanger groups; chloride ( $\text{Cl}^-$ ) and methylsulphate ( $\text{CH}_3\text{OSO}_3^-$ ) respectively. All the retention experiments were done by the washing method and with a 20:1 polymer : arsenate mole ratio. Both polymers were capable of interacting and removing arsenate species at pH 9. These results are shown in Figure 26. This demonstrates that polyelectrolytes with chloride exchanger groups, such as P(CIAETA), showed a higher ability to remove arsenate than P(SAETA), which contains methyl sulphate as anion exchanger group at the same conditions. Polymers with chloride exchanger groups have the highest capacity to remove arsenate oxy-anions (100%) at basic pH.

These results can be attributed to the easier release of the chloride anion compared to the methyl sulphate one, which is associated with the quaternary ammonium groups. Monovalent ions, such as methylsulphate, are strongly retained by hydrophobic sites of quaternary

ammonium groups due to the difference in size, solvation and polarity, as compare to chloride. It has been reported in literature that larger and polarized ions produce a disruption in the local structure of water allowing an easy association with the quaternary ammonium group [6]. Specifically, monovalent ions can be polarized and retained better in comparison with chloride due to the high hydrophobicity of the anion exchanger site. The hydrophobic nature of the monovalent anion ( $\text{CH}_3\text{OSO}_3^-$ ), which contains a methyl group, may explain this efficiency in the removal of arsenate due to the difficulty of exchanging this large group.

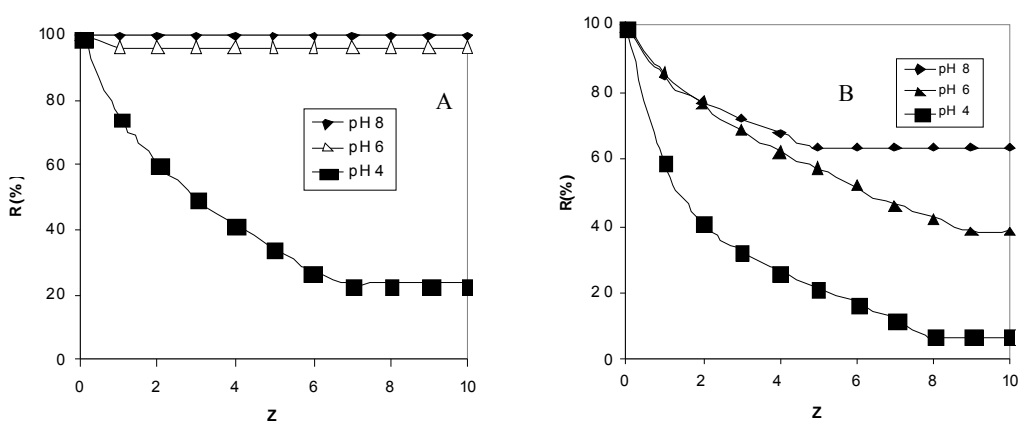


Figure 26. Retention profile of As(V) by (A) P(CIAETA) and (B) P(SAETA) at pH 4, 6 and 8, using  $30 \text{ mg L}^{-1}$  of As(V) and mole ratio of 20:1 polymer:As(V) ( $1.6 \times 10^{-4} \text{ mol} : 8 \times 10^{-6} \text{ mol}$ ).

On the other hand, it has been reported for halogens that when the electronegativity decreases in the order of  $\text{F} > \text{Cl} > \text{Br} > \text{I}$  the exchange capacity increases for the P(CIVBTA) resin [7]. The lower selectivity presented for P(BrVMP) at a basic pH could be attributed to the effect of aryl ammonium quaternary ion on the structure and the role of the bromide ion size (see Fig. 24). It is known that the alkyl ion is a stronger base than the pyridinium ion, and its conjugate, the quaternary ammonium ion, is a weaker acid [2].

The effect of the exchange of the methylsulphate counterion with sulphate anions was also studied. The P(SAETA) containing an equimolar amount of sulphate anions was stirred at room temperature for 24 hours. The retention properties of the resulting mixture towards arsenate species were studied using the LPR technique-washing method. The results show (see figure 27a) that the retention of arsenate decreased to 40 % at pH 8. The decrease on the retention ability of the cationic polymer is likely due to an increase in the ionic strength of the solution following the addition of  $\text{Na}_2\text{SO}_4$   $10^{-2}$  M, which induced a change in polarization. However, the exchange in the polymeric structure of the methylsulphate species by the sulphate anions was difficult. Divalent sulphate ions have a great affinity for water because they are well-hydrated anions. These ions presumably have less affinity for the more hydrophobic alkylammonium sites in the exchanger polymer. The high affinity of a divalent anion is attributed to electroselectivity [8]. On the other hand, it is known that adsorption diminishes as the ionic strength of media increases in certain cases of non-specific adsorption [9].

Another experiment was performed to study the exchange properties of a polymer solution that was contacted with chloride prior to the washing method. The solution of P(SAETA) containing a  $10^{-1}$  M of chloride anions was stirred for 24 hours at room temperature and then the retention properties of the resulting solution were studied using the LPR technique-washing method. Results are shown in figure 27 b. It is probable that some methyl sulphate groups were exchanged for chloride anions. In these experimental conditions the experiments showed different retention profiles in comparison to those obtained without chloride anions (see figure 26 b). The R value significantly increased at pH 8 and pH 6, in 90 and 60 % respectively, although R value does not show modification at pH 4 (see figure 27 b).

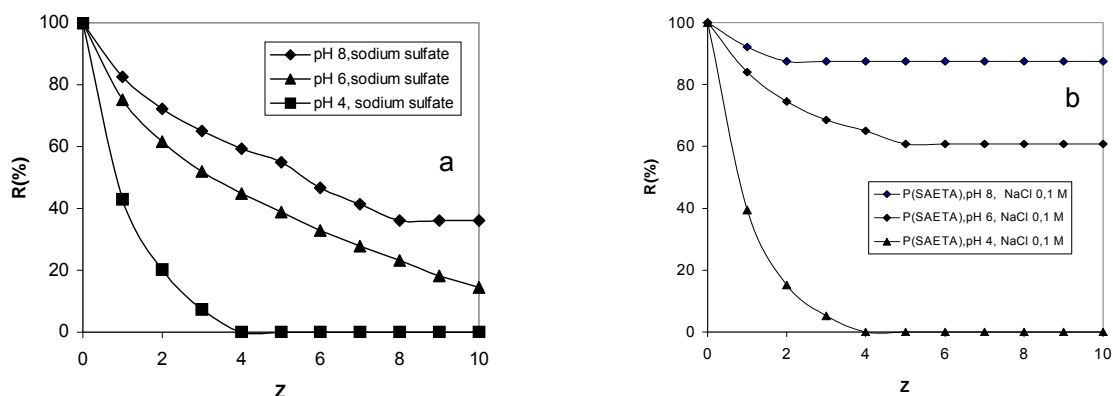


Figure 27. Retention profiles of As(V) using (a) P(SAETA), in  $10^{-2}$  M  $\text{Na}_2\text{SO}_4$  and (b) P(SAETA), in  $10^{-1}$  M NaCl. Polymer amount: 0.2 mmol. Absolute As(V) ion: 0.01 mmol.

### 3.1.1.4 Competitive effect of other monovalent and divalent anions on arsenate retention

The cationic polyelectrolytes maintain the highest retention of arsenate species but in absence of other anions in the solution. In order to determine the influence of ionic strength different experiments in presence of divalent and monovalent anions, such as a sulphate and chloride, at different concentrations were done at pH 8. In this study we used the washing method at constant ionic strength adding in both the reservoir and the ultrafiltration cell concentrations from  $1 \times 10^{-3}$  M to  $1 \times 10^{-1}$  M of NaCl and  $\text{Na}_2\text{SO}_4$  in separate experiments in conjunction with the 20 : 1 of polymer : As(V) mole ratio inside of ultrafiltration cell.

It was found that the arsenate retention decreased with the increasing salt concentration and the increased valence of the added anion. The decrease in the retention, due to the presence of the added salts, declining in the following order  $\text{Na}_2\text{SO}_4 > \text{NaCl}$ .

According to the literature [10] the order of interference in the arsenic retention is: trivalent ions  $>$  divalent ions  $>$  monovalent ions. The effect of added electrolytes on arsenic binding to

the polyelectrolyte can be understood as due to the competition between arsenate and other anions for binding sites on the polymer. The affinity of anions to bind onto the polymer has a similar behavior to that in the ion-exchange resin containing ammonium groups observed in arsenic removal by ion exchange process [10]. Another way of explaining the effect is that the electrical double layer is compressed around the polymer as the ionic strength increases thus reducing the electrical potential of the polymer. The divalent anions reduce arsenic retention more than the monovalent anions because the divalent anions bind more strongly to the charged sites on the polymer and also compress the electrical double layer around the polymer more effectively than the monovalent anions [11, 12].

It is reasonable that sulphate or chloride anions show different interference toward arsenate retention. The results prove the adsorption of the interfering ions to the same active sites on the polymer, especially in the case of sulphate that like arsenate has a tetrahedral structure. The results showed that just adding  $1 \times 10^{-3}$  M of sodium sulphate the retention of arsenic decreased from 96 % to 20% at  $Z = 10$ . Moreover the arsenate retention dropped down to zero when the concentration of sulphate ions increased up to  $5 \times 10^{-3}$  M (see fig. 28 b). On other hand, the competition between arsenate and monovalent chloride was lower than between sulphate and arsenate. When the minimum concentration of chloride was added, corresponding to  $1 \times 10^{-3}$  M, the retention capacity of arsenate decreased from 96% to 55% at  $Z = 10$  (see fig. 28 a). When the concentration of chloride increased, the retention of arsenate gradually decreased. These results prove that when the ionic strength increases the retention capacity of the polymer decreases due to the competition between ions in solution. This behavior depends directly of the type and charge of interfering ion. Even at a low concentration, interfering ions block and diminish the extracting capability of the water-soluble polymer.

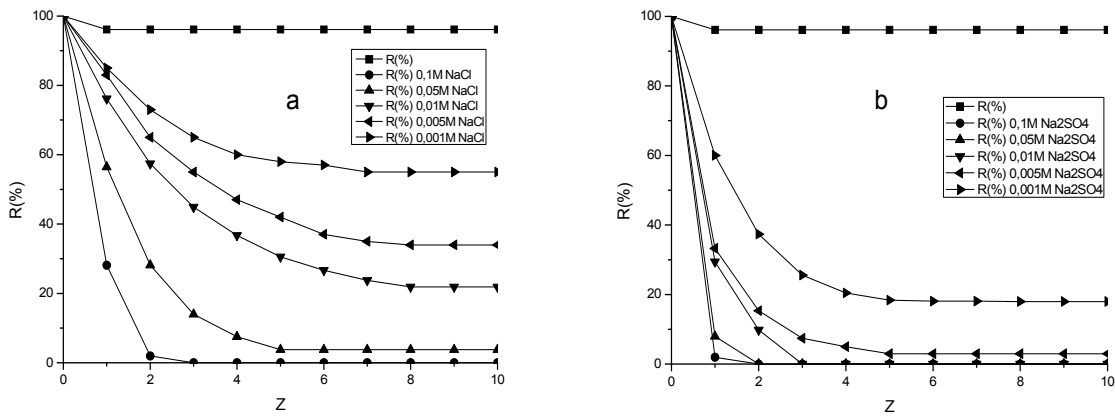


Figure 28. Retention profile of As(V) by P(CIAETA) in presence of different concentrations of (a) NaCl and (b) Na<sub>2</sub>SO<sub>4</sub> in both the reservoir and ultrafiltration cell at pH 8, using molar ratio (20:1) polymer : As (V) ( $1.6 \times 10^{-4}$  mol :  $8 \times 10^{-6}$  mol).

### 3.1.2 Maximum retention capacity of arsenate through the enrichment method

The maximum retention capacity (C) of arsenate by the polyelectrolyte was determined by the enrichment method. This method consists in adding to a solution of polyelectrolyte the maximum concentration of the arsenate anion that the polymer can bind in order to reach saturation. The maximum retention (enrichment method) is defined as:

$$C = (M V) / Pm \quad (9)$$

Where Pm is the amount of polymer (g), M is initial concentration of As(V) ( $\text{mg L}^{-1}$ ), V is the volume of filtrate (volume set) containing As(V) (mL) that passes through the membrane. The maximum retention capacity of arsenate C was calculated in the total volume of filtrate (300 mL). Assuming a quantitative retention of As(V), the enrichment factor E is a measure of the binding capacity of the polymer and it is determined as follows:

$$E = (P C) / M \quad (10)$$

where P is the concentration of polymer ( $\text{g L}^{-1}$ ). As the arsenate ion-polymer interactions are processes in equilibrium, a lower slope in the rate of increase of the arsenate concentration in the filtrate is normally observed. From the differences in the slopes the amounts of arsenate ions bound to the polymer and free in solution, the maximum retention capacity can be easily calculated [12].

The C and E values for arsenate anions are summarized in the table 12. The behavior observed in different cationic water-soluble polyelectrolytes using the enrichment method in aqueous solutions at pH 8 using  $8 \times 10^{-4}$  mol of polymer into the ultrafiltration cell and adding a solution of  $4 \times 10^{-3}$  mol of As(V) from the reservoir are shown in Figure 29. In similar polymeric structures but with different counterions, such as P(CIAETA) and P(SAETA), the results were different. The values of C were  $165 \text{ mg g}^{-1}$  for P(CIAETA) and  $79 \text{ mg g}^{-1}$  for P(SAETA) and the total volume of filtrate was 300 mL. Assuming quantitative retention of As(V), the enrichment factor was analyzed ( $E = 4$  for P(CIAETA) and  $E = 2.5$  for P(SAETA)). The type of anion exchanger was an important factor in the retention of arsenate.

Table 12. Maximum retention capacity of arsenate and enrichment factor of water-soluble polyelectrolytes

Polymer	Maximum retention capacity (C), mg As(V) /g polymer	Enrichment factor (E)
P(CIAETA)	165	4
P(CIAPTA)	369	9.4
P(SAETA)	79	2.5
P(CIVBTA)	311	8
P(BrVMP)	144	3.5
P(CIDDA)	380	7.5

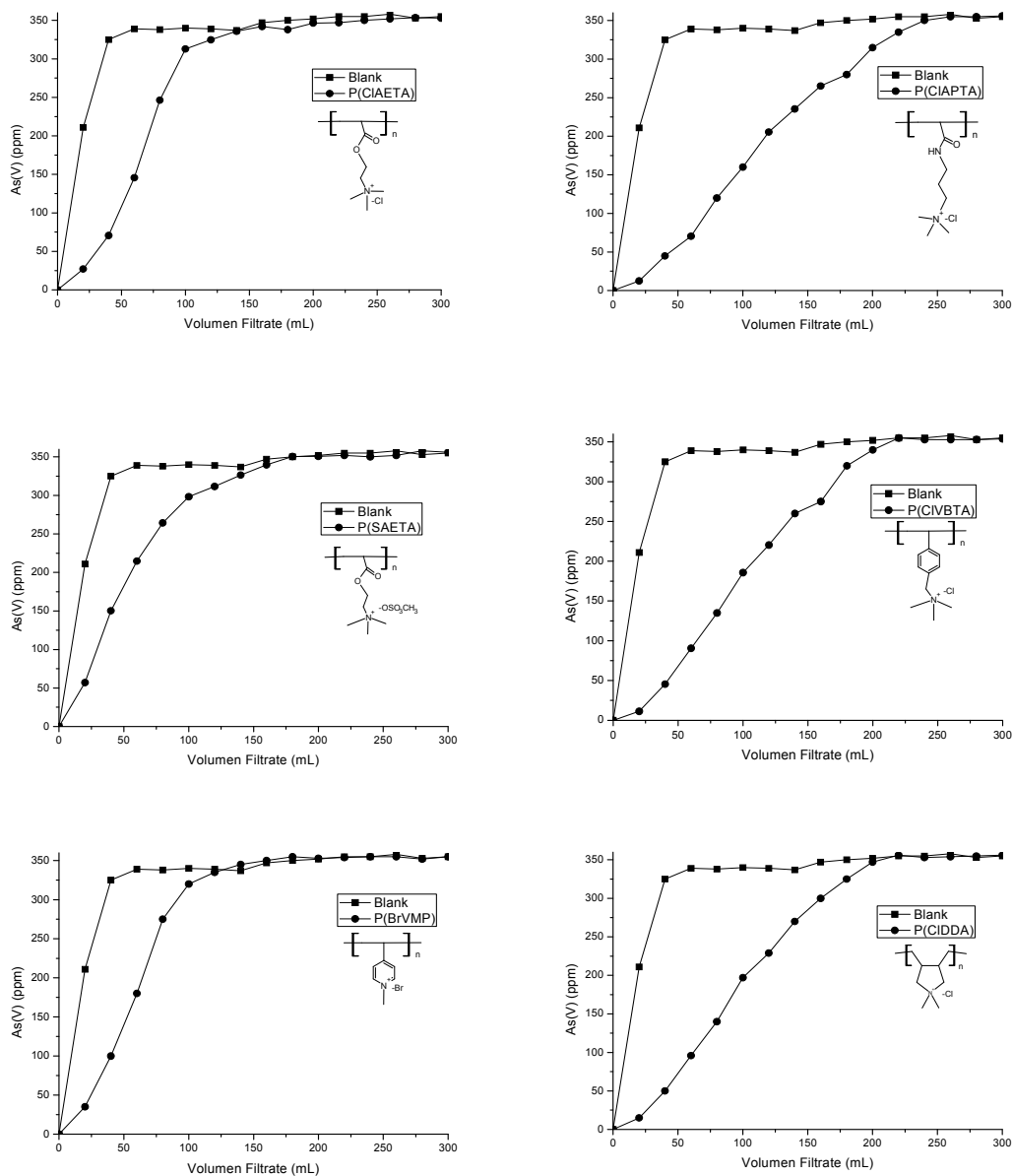


Figure 29. Maximum retention capacity (C) of arsenate using different polyelectrolytes at pH 8. Mole ratio of  $8 \times 10^{-4}$  mol of polymer and  $4 \times 10^{-3}$  mol of As(V).

The interaction between the polymer and arsenate was not obviously purely electrostatic, presumably because of the formation of a covalent bond between a partially movable functional group on the polymeric network and one on the oppositely charged arsenate anion.

This pairing may be explained by the water structure induced by ion pairing, where the larger and more polarizable ions disrupt the local water structure and associate more easily with a given quaternary ammonium ion [1, 6].

The FTIR spectra of P(ClAPTA) before and after the maximum retention capacity of the polymer with As(V) are shown in Figure 30. In the high region of the spectra only the vibrations of a functional group corresponding to P(ClAPTA) could be identified. Some modifications were observed in the spectra in the 1700 to 1300  $\text{cm}^{-1}$  range. The intensity of the band at 1649  $\text{cm}^{-1}$ , corresponding to the C=O stretching vibration was taken as a reference. Following the addition of arsenate at different pH, a marked decrease in the intensity of the bands at 1552  $\text{cm}^{-1}$  [coupling of  $\nu(\text{C-N})$  and  $\delta(\text{N-H})$ ] and 1482  $\text{cm}^{-1}$  by  $\delta(-\text{N}^+(\text{CH}_3))$  was observed, along with the appearance of a new band at 1380  $\text{cm}^{-1}$  from arsenate groups corresponding to  $\nu(\text{As=O})$  [13, 14].

The fact that the intensity of the band at 1380  $\text{cm}^{-1}$  depends on the pH clearly supports that there is an interaction between the polymer and the arsenate oxy-anions. The intensity of this band was lower at pH 4 than at pH 8, indicating a weaker interaction with arsenate anions at lower pH. The band at 845  $\text{cm}^{-1}$  was assigned to the  $\nu(\text{As-O})$  stretching vibration. At lower frequencies, the region of 200–500  $\text{cm}^{-1}$ , deformation modes showed one strong band at 369  $\text{cm}^{-1}$  by  $\delta(\text{As-O})$ .

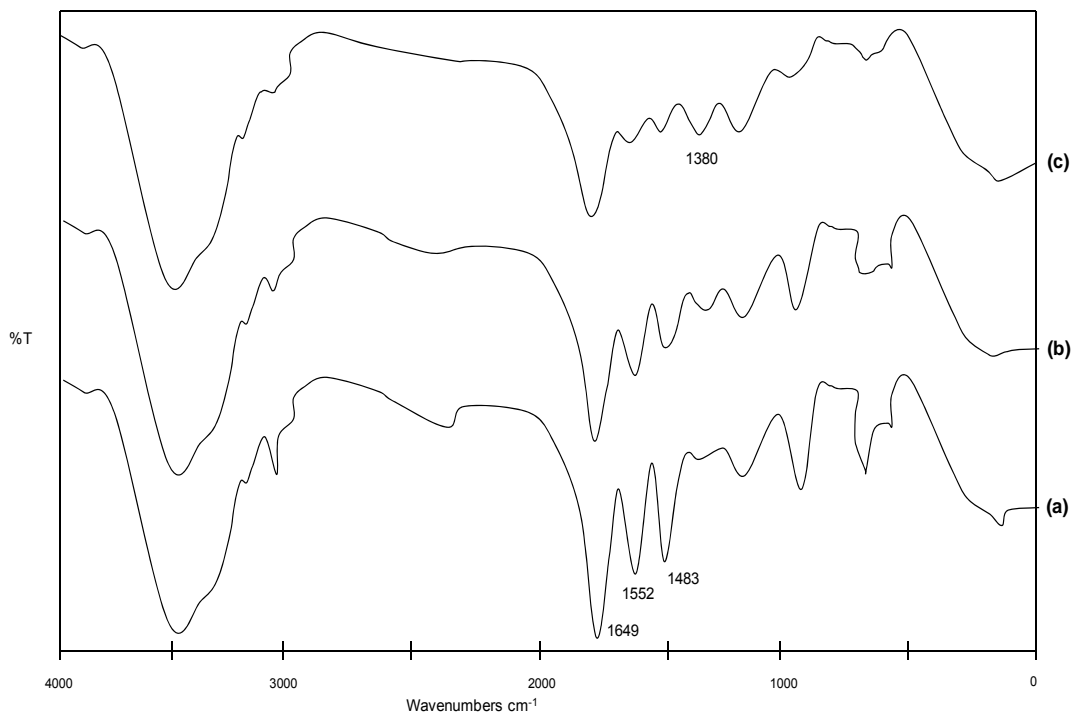


Figure 30. FTIR spectra (KBr) of (a) poly[(3-acryloylamino) propyl]trimethylammonium chloride (CIAPTA), (b) P(CIAPTA) with arsenate at pH 4, (c) P(CIAPTA), with arsenate at pH 8.

### 3.1.3 Desorbing of arsenate: the charge-discharge process

In order to study the process of charge-discharge the enrichment and washing methods were alternately used. In these experiments P(CIAETA) and P(SAETA), which differ only in their counterions, were studied. The first step of the experiment was the saturation of the polymers through the enrichment method using the conditions previously described; the enrichment method was performed at pH 8, using  $8 \times 10^{-4}$  mol of polymer into the ultrafiltration cell (20 mL) and adding a solution  $4 \times 10^{-3}$  M in As(V) from the reservoir. After reaching the saturation the polymer : As(V) solution retained in the cell was washed with water buffered at pH 3 from reservoir. This was done in the ultrafiltration cell in a similar way to the washing method. It was assumed that the activity of the polymers can be recovered in strongly acid

conditions of the media and that this did not affect significantly the active sites of the polymer because acid pH was used in the radical polymerization. The same process of charge-discharge was repeated two times for each polymer in order to determine the capacity of arsenate delivery and to regenerate the extracting ability of the water-soluble polyelectrolyte.

Figure 31 shows the behavior of charge-discharge for both polymers. In the figure 31(a) it is possible to see the enrichment process (charge) reaching the same maximum retention capacity (C) obtained previously in both polymers at pH 8 (see table 13). After the charge process the discharge process was done changing the pH from basic to acid using buffered solution of  $10^{-1}$  M HCl. In the figure 31(b) it is possible to observe the discharge process of the arsenate ions from both polymers when the polymer-arsenate is in contact with acid solution at pH 3 from the reservoir. The first discharge of arsenate was effective and was carried out almost entirely in the first 100 mL of solution when higher ion arsenate concentration is discharged rather from P(CIAETA) than P(SAETA) at the same volume. Both polymers discharge all the amount of arsenate at 300 mL of filtrate.

Figure 31(c) shows that the second charge process did not improve the maximum retention capacity of the polymers compared with the first charge process. P(CIAETA) lost the capacity to remove arsenate and this behavior is almost the same for P(SAETA) at the same conditions. This occurs probably because of the presence of more species in the solution when the pH was adjusted from basic to acid in the discharge process and from acid to basic in the second charge process. Finally, the second discharge process (see figure 31d) showed almost the same behavior in both polymers releasing most of the arsenates ions to the filtrate at the first 100 mL in similar manner.

It is necessary to repeat this experiment several times in the future in order to determine until what point it is possible to use the same polymer in charge-discharge process.

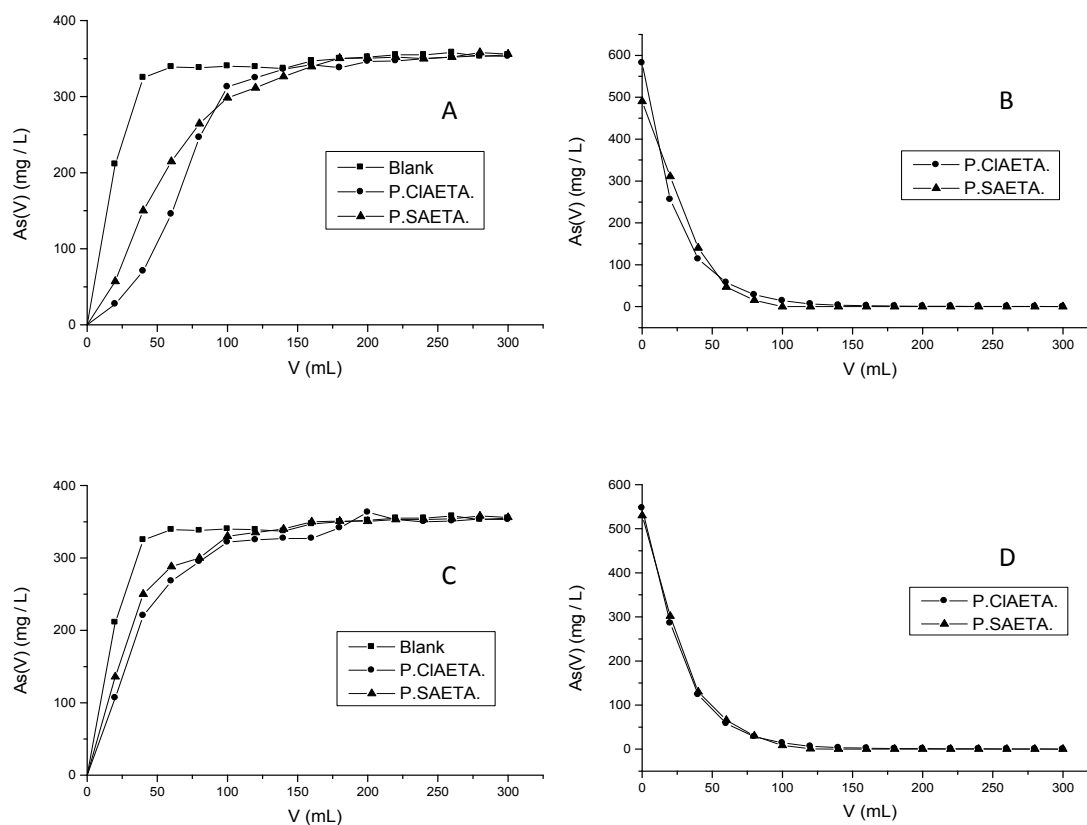


Figure 31. Charge-discharge process of arsenate ions using P(CIAETA) y P(SAETA). (A) first charge process of polymers through enrichment method at pH 8, (B) first discharge process of polymers using washing method at pH 3 with HCl  $10^{-1}$  M. (C) recharge of polymers through enrichment method at pH 8, (D) second discharge process of polymers using washing method at pH 3 with HCl  $10^{-1}$  M.

Table 13. Maximum retention capacity of the first and second charge ( $C_1$  and  $C_2$ ) process and enrichment factor ( $E_1$  and  $E_2$ ) using homopolymers P(CIAETA) and P(SAETA).

Polymer	$C_1$	$E_1$	$C_2$	$E_2$
	mg As(V) /g polymer		mg As(V) /g polymer	
P(CIAETA)	165	4	83	2
P(SAETA)	79	2.5	47	1.5

### 3.1.4 Conclusions

The liquid-phase polymer- based retention (LPR) has proved to be a convenient method to significantly retain arsenate anions in solution using a polymer with quaternary ammonium groups. The results shows the high affinity of the water-soluble cationic polymers to interact and remove As(V) species, and the non-retention of As(III) species between pH 3 to 9. The capacity of interaction and retention of the arsenate anions depend on the pH, the nature of the counterion of the quaternary ammonium group and the polymer concentration.

The retention capacity of the polymer is due to the presence of a positively charged quaternary ammonium group. The interactions are produced mainly through the anion exchange between counterion of quaternary ammonium salt and the arsenate anions at basic pH. This can be corroborated by the higher retention capacity of the polymers at basic pH because divalent As(V) species are predominant. All the polymers remove more efficiently arsenate ions at pH 9 than at pH 6 to 3.

The polymer P(SAETA) containing bulky counterions ( $\text{CH}_3\text{OSO}_3^-$ ) which are more hydrophobic than  $\text{Cl}^-$  ions - showed a lower retention capacity of arsenate ions. Thus, the nature of the anionic exchanger groups appears to be an important factor in the retention of arsenate through these water-soluble polymers because the electrostatic interactions are predominant in these systems.

The effect of the exchange of the methylsulphate counterion with sulphate anions show that the retention of arsenate decreased to 40 % at pH 8. This decrease is likely due to an increase in the ionic strength of the solution following the addition of  $\text{Na}_2\text{SO}_4$ , which induced a change in polarization. On the other hand, the polymer solution was contacted with chloride prior to the washing method. It is probable that some methylsulphate groups were exchanged for chloride anions. In these conditions the experiments showed different retention profiles in

comparison to those obtained without chloride anions.

The cationic polyelectrolytes maintain the highest retention of arsenate species but in absence of other anions in the solution. The arsenate retention is found to decrease with the increasing salt concentration and the increased charge of the added anion. The divalent anions reduce arsenic retention more than the monovalent anions because divalent anions bind more strongly to the charged sites on the polymer and also compress the electrical double layer around the polymer more effectively than the monovalent anions.

The retention capacity is limited by the concentration of polymers. The results indicate an optimum molar ratio of 20:1 polymer : arsenate mole ratio for the complete removal of arsenate.

The enrichment method shows the maximum capacity of retention  $C$  for arsenate anions in aqueous solutions at pH 8. The type of anion exchanger was an important factor in the maximum retention capacity of arsenate.

The interaction between the polymer and arsenate was not purely electrostatic, presumably because of the formation of a covalent bond between a partially movable functional group on the polymeric network and one on the oppositely charged arsenate anion. The FTIR spectra before and after the maximum retention capacity of the of P(CIAPTA) with As(V) shows some modifications were observed the spectra in the 1700 to 1300  $\text{cm}^{-1}$  range.

The charge-discharge process shows that is possible to do the discharge process of the arsenate ions from polymers when the polymer-arsenate was in contact with acid solution from the reservoir. The second charge process did not improve the maximum retention capacity of the polymers, compared with the first charge process. Finally, the second discharge process showed almost the same behavior in both polymers releasing most of the arsenates ions to the filtrate in similar manner.

### ***3.2 Electrocatalytic oxidation (EO) of arsenite at analytical and preparative scales***

The high toxicity and widespread occurrence of arsenic in groundwater have lately put forward a pressing need for efficient and selective analytic and remediation strategies. Electrochemical techniques have lot to offer in this field.

Numerous analytical methods for arsenic have been developed [15-17]. The use of electrochemical methodologies for the determination of arsenic is of growing interest, owing to the possibilities of trace detection, automation and real-time on-site analysis [16, 17]. A number of research works have been reported about arsenic detection using voltammetric techniques, mainly anodic and cathodic stripping voltammetry with various electrode materials, including mercury films, gold and platinum electrodes [16]. Direct oxidation of As(III) to As(V) species on platinum electrodes can also be used for the detection of As(III) [18-20], allowing to avoid interferences by various metals that could occur in stripping voltammetry. Moreover, it has been shown that using platinum nanoparticle modified carbon electrodes results in better sensitivity than platinum macroelectrodes for the determination of arsenic [20].

Firstly, this section summarizes the electroanalytical performances of platinum and palladium nanoparticles dispersed into alkylammonium-substituted polypyrrole films modified electrodes (C|poly1-metal and C|poly2-metal; see the the experimental part) towards As(III) oxidation and detection. The electrocatalytic behavior of the nanocomposites-film modified electrodes was evaluated by direct anodic sweep voltammetry (ASV) and cyclic voltammetry (CV). Finally, this section presents results about the exhaustive electrocatalytic oxidation of arsenite to arsenate at the preparative scale, using C|poly1-Pt<sup>0</sup> modified carbon felt

macroelectrodes, under different conditions. The advancement of the electrolysis of As(III) solution was monitored using C|poly1-Pt<sup>0</sup> analytical electrodes.

### 3.2.1 Oxidation of arsenite using massive platinum electrodes

The catalytic behaviour of noble metal (platinum and palladium) nanoparticles modified electrodes was compared to that of a platinum bulk electrode by studying currents and potentials for the oxidation of arsenic(III) with the different electrodes.

At first, the analytical detection or oxidation of As(III) was monitored by anodic sweep voltammetry (ASV), using a platinum massive electrode ( $d = 5\text{mm}$ ). The reference electrode was a Ag/AgCl electrode and the counter electrode a platinum wire. The oxidations were performed in  $10^{-1}\text{M}$  Na<sub>2</sub>SO<sub>4</sub>. Calibration curves were built using 8 concentrations of As(III), from  $2.5 \times 10^{-4}\text{ M}$  to  $2.8 \times 10^{-3}\text{ M}$ . The blank was subtracted in each measurement (see fig. 32).

With the addition of As(III), a peak was observed at about + 0.7 V (vs. Ag/AgCl) in the anodic scan. This peak corresponds to the oxidation of As(III) to As(V) and the peaks heights show a good linear relationship. According to the literature, the reaction is likely electrocatalyzed by the formation of PtOH on the electrode (equations 3 and 4 chapter 1, paragraph 1.6). Small anodic peaks between + 0.2 and + 0.3 V can be attributed to the oxidation of As(0) to As(III), formed by cathodic deposition at 0 V [20].

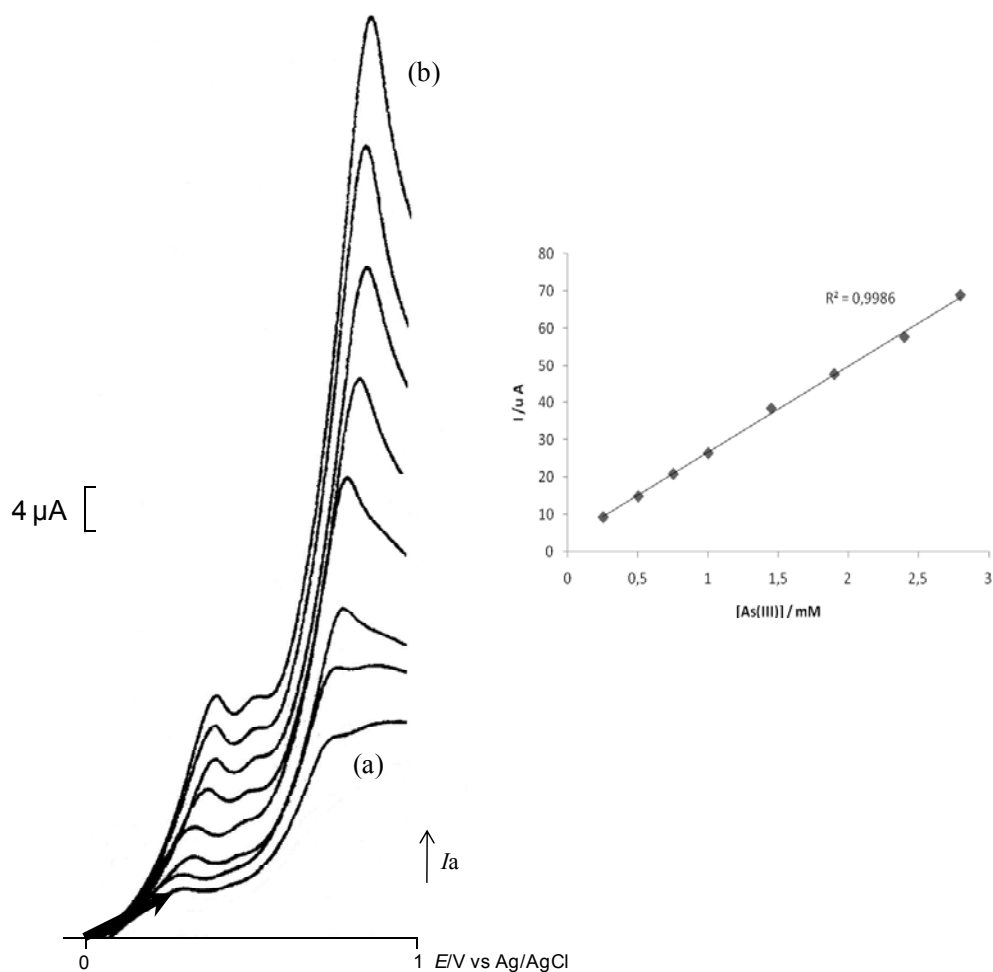


Figure 32. Direct anodic scan voltammograms recorded in  $10^{-1}$  M aqueous  $\text{Na}_2\text{SO}_4$  at analytic platinum disc electrodes (5 mm diameter) vs. Ag/AgCl, in the presence of increasing amounts of As(III), from  $2.5 \times 10^{-4}$  M (curve a) to  $2.8 \times 10^{-3}$  M (curve b); scan rate  $10 \text{ mV s}^{-1}$ . (B) Inset Plot of main peak currents vs. the concentration of As(III).

### 3.2.2 Electrocatalytic oxidation of As(III) to As(V) with different metal-polymer film modified electrodes

#### a) C|Poly1-Pt<sup>0</sup>, C|Poly1-Pd<sup>0</sup> and C|Poly1-Rh<sup>0</sup>

The behavior of As(III) with different platinum metal-polymer film modified electrodes was first examined in  $1 \times 10^{-1}$  M  $\text{Na}_2\text{SO}_4$  using anodic sweep voltammetry. The oxidation of arsenite is ineffective at naked glassy carbon electrode, giving very small anodic

peaks above + 1 V (Fig. 33A, curve e). Interestingly, the coating of the carbon surface by a metal- free poly1 film leads to the rise of a small, clear oxidation peak at about + 1 V (Fig. 33A, curves c and d).

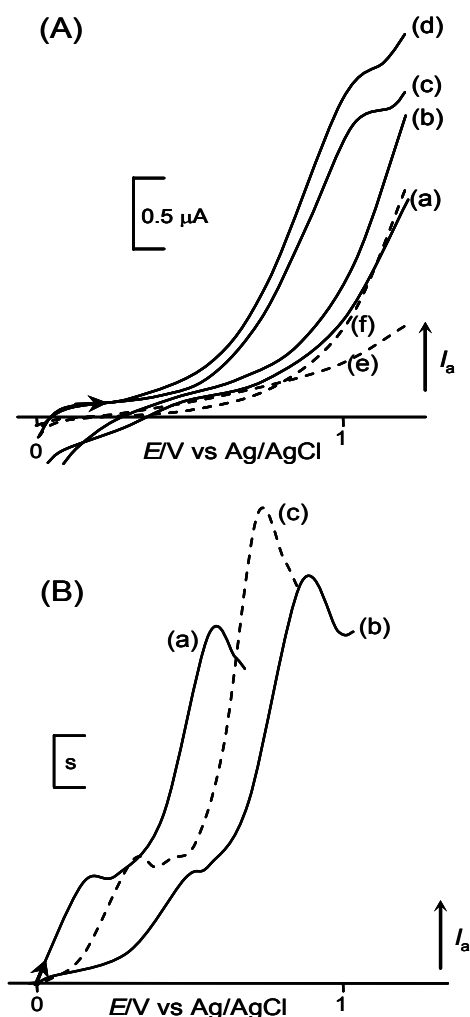


Figure 33. Anodic scan voltammograms (scan rate  $10 \text{ mV s}^{-1}$ ) recorded in  $10^{-1} \text{ M}$  aqueous  $\text{Na}_2\text{SO}_4$ . (A) C|poly1 glassy carbon modified electrodes (3 mm diameter; curves a, c:  $\Gamma_{\text{N}^+}^- = 1.8 \times 10^{-8} \text{ mol cm}^{-2}$ , curves b, d:  $\Gamma_{\text{N}^+}^- = 4.2 \times 10^{-8} \text{ mol cm}^{-2}$ ) and naked glassy carbon electrode (3 mm diameter; curves e, f) in the absence (curves a, b, e) and in the presence (curves c, d, f) of  $1 \times 10^{-3} \text{ M}$   $\text{NaAsO}_2$ . (B) Anodic scan voltammograms recorded in the presence of  $1 \times 10^{-3} \text{ M}$   $\text{NaAsO}_2$ : (a) C|poly1-Pt<sup>0</sup> (3 mm diameter,  $\Gamma_{\text{N}^+}^- = 2 \times 10^{-8} \text{ mol cm}^{-2}$ , 0.5 μg of Pt); (b) C|poly1-Pd<sup>0</sup> (3 mm diameter,  $\Gamma_{\text{N}^+}^- = 2 \times 10^{-8} \text{ mol cm}^{-2}$ , 0.27 μg of Pd); scale s = 1 μA. Curve c (dashed line) is recorded in the same conditions at a Pt disc (5 mm diameter) electrode; scale s = 3 μA.

Since the electroactivity of the polymer matrix was previously destroyed (see the experimental section) in order to obtain voltammograms free of the electrochemical response of the polypyrrole skeleton, this oxidation peak can be attributed to the oxidation of As(III) species. As compared to the very poor oxidation of arsenite with naked carbon, this large increase in the anodic current corresponding to the oxidation of As(III) species at C|poly1 glassy carbon modified electrodes could be explained by the concentration by ion exchange of anionic oxy-arsenic species in the polyammonium films coated onto the carbon surface. This assumption is corroborated by the fact that the oxidation current for As(III) is larger at the electrode modified by the thickest polyammonium film, as shown by the comparison between curves c and d in Figure 33A.

The figure 33B (curve a) illustrates the strong catalytic activity towards oxidation of As(III) to As(V) brought about by the inclusion of a small amount of platinum in C|poly1 films, leading to the rise to + 0.52 V of a large oxidation peak. This reaction is likely electrocatalyzed by surface oxides [19, 21]. The small anodic peak at + 0.2 V can be attributed to the oxidation of a small amount of As(0) formed by cathodic deposition at 0 V [20]. This behavior is similar to that observed in the platinum disc electrode in the same experimental conditions (see Fig. 33B, curve c). However, it should be emphasized that the oxidation of As(III) occurs at a less positive potential at the C|poly1-Pt<sup>0</sup> electrode ( $E_p = + 0.52$  V) than at a platinum macro electrode ( $E_p = + 0.7$  V). This observation indicates that the use of the platinum-polymer nanocomposite markedly decreases the overpotential for arsenite oxidation, in spite of the small amount of metal catalyst electroprecipitated in the polymer film (2.6 nmol, 0.5  $\mu$ g). It is now well recognized that dispersing metal nanoparticles can result in enhanced electrocatalytic properties compared to the reactivity of the bulk metal [22]. Moreover, in the case of the C|poly1-Pt<sup>0</sup> electrode material the concentration by ion exchange of anionic oxy-

arsenic species in the polymer film could also have a beneficial effect on the electrocatalytic properties of the nanocomposite. The beneficial effect of the dispersion of the metal catalyst in the polyammonium film was further confirmed by the rather poor catalytic activity of a modified electrode prepared by electrodeposition of the same amount of platinum (2.6 nmol, 0.5  $\mu\text{g}$ ) onto a naked carbon electrode (3 mm diameter). In our experimental condition the oxidation of As(III) occurs at a higher positive potential ( $E_p = + 0.65 \text{ V}$ ), and the oxidation current was only half that obtained at the C|poly1-Pt<sup>0</sup> electrode.

The oxidation of arsenite was also effective at C|poly1-Pd<sup>0</sup> electrode (2.6 nmol, 0.5  $\mu\text{g}$  of palladium; Fig. 33B, curve b), but this system displayed a lower catalytic activity ( $E_p = + 0.86 \text{ V}$ ) than the platinum-based composite. Finally, less active materials have been obtained with the C|poly1-Rh<sup>0</sup> composite. Although the intensity of the catalytic currents were similar to that obtained with Pt and Pd-based materials, the use of rhodium significantly increased the overpotential for a As(III) oxidation that was observed at + 1.15 V.

Current densities were used to further compare the results from the platinum metal nanocomposites and the platinum disc electrode. For the C|poly1-M<sup>0</sup> electrodes the current densities were calculated based on the surface area of the carbon support (0.07  $\text{cm}^2$ ). In our experimental conditions (1 mM arsenite in unbuffered aqueous Na<sub>2</sub>SO<sub>4</sub>, scan rate 10  $\text{mV s}^{-1}$ ), current densities of 102 and 124  $\mu\text{A cm}^{-2}$  were recorded at Pd and Pt-containing film modified electrodes, respectively. This compares well with the current density obtained (134  $\mu\text{A cm}^{-2}$ ) in the same experimental conditions at the platinum disc (0.2  $\text{cm}^2$ ) electrode, in spite of a very low loading of platinum metal (a few nmol) incorporated into the polymer matrix.

To maximize the electrocatalytic properties of the nanocomposites, C|poly1-Pt<sup>0</sup> electrodes have been synthesized in different experimental conditions, and their catalytic activity has been evaluated towards the oxidation of millimolar solutions of arsenite (see table 14).

Table 14. Experimental conditions of modified electrodes elaboration (C|poly1-Pt<sup>0</sup>) and their catalytic activity toward the As(III) oxidation in unbuffered aqueous Na<sub>2</sub>SO<sub>4</sub>, scan rate 10 mV s<sup>-1</sup>.

<b>Experimental conditions of C poly1-Pt<sup>0</sup></b>						
Polymerization charge, mC	1	1	1	0.25	0.5	1.5
Cathodic charge of Pt reduction, mC	0.25	0.5	1	0.5	0.5	0.5
<b>Electrocatalytic oxidation of As(III)</b>						
Concentration of As(III), mM	Current, $\mu$ A					
0.25	1.5	1.9	1.5	1	1.7	1.6
0.49	2.9	3.6	2.3	1.7	3.2	2.7
0.98	4.8	6.8	5.6	3.1	6.6	5.6
1.92	9.2	13.5	11.2	5.6	12	10.8

At first, we found that best catalytic systems were obtained using a polymerization charge of 1 mC, which gave films of  $\Gamma_{N^+}$  around  $2 \times 10^{-8}$  mol cm<sup>-2</sup>, and a cathodic charge of 0.5 mC (2.6 nmol, 0.5  $\mu$ g) for the inclusion of platinum in the polymer film. Thicker films gave lower catalytic currents, which could be due to a slower diffusion of the substrate through the polymeric film to the catalytic sites. Moreover, using higher metal loadings by passing a higher charge for the electroreduction of the metal salt did not markedly improve the catalytic efficiency of the electrodes. It seems that full utilization of the catalyst was not obtained, with could be due to the increase of the particle size or to their coalescence.

Figure 34 (A) shows the typical voltammetric response (scan rate 10 mV s<sup>-1</sup>) of a C|poly1-Pt<sup>0</sup> modified electrode when adding increasing amounts of arsenic (III) to 10<sup>-1</sup> M of Na<sub>2</sub>SO<sub>4</sub> solution. Depending on the arsenite concentration the pH ranged between 9 and 10.

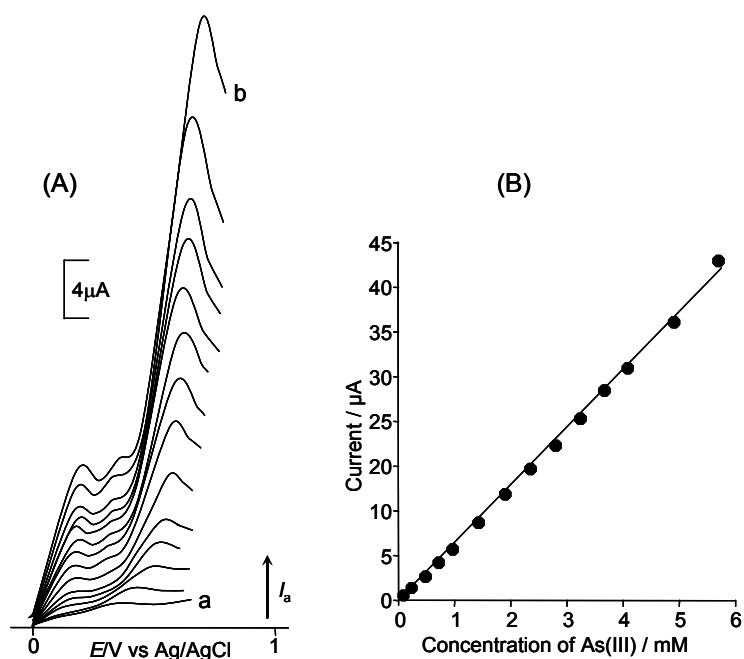


Figure 34. (A) Direct anodic scan voltammograms recorded in  $10^{-1}$  M aqueous  $\text{Na}_2\text{SO}_4$  at a C|poly1-Pt<sup>0</sup> electrode (3 mm diameter;  $\Gamma_{\text{N}^+} = 2.1 \times 10^{-8}$  mol  $\text{cm}^{-2}$ ; 0.5  $\mu\text{g}$  of Pt) in the presence of increasing amounts of As(III), from  $1 \times 10^{-4}$  M (curve a) to  $5.75 \times 10^{-3}$  M (curve b); scan rate  $10 \text{ mV s}^{-1}$ . (B) Plot of main peak currents vs. the concentration of As(III).

The plot of the peak current vs. the concentration of As(III) is presented in figure 34 (B). The peak height increased linearly with the addition of arsenic species. The linear range is from  $1 \times 10^{-4}$  M to  $5.75 \times 10^{-3}$  M ( $r^2 = 0.999$ ). The calibration slope was  $0.012 \text{ A M}^{-1}$  and the limit of detection (LOD [23]) was calculated to be  $2.4 \mu\text{M}$  (0.17 ppm). In the same experimental conditions, with Pt disc (5 mm diameter) electrode the calibration slope was  $0.014 \text{ A M}^{-1}$  and the LOD was more than 10 times higher ( $33.6 \mu\text{M}$ , 2.41 ppm), showing again the good catalytic activity of the polymer-Pt nanocomposite towards As(III) oxidation.

Stability of the C|poly1-Pt<sup>0</sup> modified electrodes was investigated only to a limited extent, and showed marginal loss of activity (less than 10%) after a series of at least 10 experiments as described above.

Similar voltammetric responses to increasing amounts of As(III) were obtained using C|poly1-Pd<sup>0</sup> modified electrodes. The best results were obtained with polymer films synthesized using polymerization charge of 1 mC ( $\Gamma_{N^+} = 2 \times 10^{-8} \text{ mol cm}^{-2}$ ) and containing 0.3  $\mu\text{g}$  of palladium. In these experimental conditions, the linear range of the calibration curve was also from  $1 \times 10^{-4} \text{ M}$  to  $5.75 \times 10^{-3} \text{ M}$  ( $r^2 = 0.999$ ).

#### **b) C|Poly2-Pt<sup>0</sup> and C|Poly2-Pd<sup>0</sup>**

It is very well recognized that redox-active polymers could offer useful application for the development of new electrochemical sensors devices [24, 25]. The aim of these systems is to convert the interactions at molecular levels into measurable electrochemical signals. In this context, we have performed preliminary investigations on the sensing properties of materials of the type C|Poly2-M<sup>0</sup>, synthesized by the incorporation of Pt and Pd particles into (ferrocenylmethyl)trialkylammonium films, synthesized by the oxidative polymerization of the pyrrole-substituted monomer **2** (see chapter 2, experimental part).

In order to compare the behavior of the C|poly2, C|poly2-Pt<sup>0</sup> and C|poly2-Pd<sup>0</sup> towards arsenite oxidation and sensing, different experiments using these systems have been carried out.

First, a C|Poly2 modified electrode was transferred to aqueous  $1 \times 10^{-1} \text{ M}$  LiClO<sub>4</sub> and its electrochemical behavior was examined using cyclic voltammetry (CV). In figure 35A (curve a) it is possible to see the stable electrochemical response of the ferrocene center (Fc) at + 0.48 V vs Ag/AgCl. This peak was found at + 0.26 V vs. Ag<sup>+</sup>/10<sup>-2</sup> M Ag<sup>+</sup> in CH<sub>3</sub>CN electrolyte solution [26].

No clear redox systems due to electroactivity of pyrrole matrix could be detected on the CV curves.

When transferred to a  $1 \times 10^{-1}$  M aqueous  $\text{LiClO}_4$  in the presence of  $\text{H}_2\text{AsO}_3^-$  anions, the CV curves for poly2 is deeply modified, showing a strong decrease in the electroactivity of the film (see fig. 35A curve b). When transferred again into clean ( $\text{H}_2\text{AsO}_3^-$ -free) aqueous solution, the original electroactivity of the film was not fully restored. It can be thus concluded that cationic poly2 film present affinity toward  $\text{H}_2\text{AsO}_3^-$ . The loss of electroactivity in presence of  $\text{H}_2\text{AsO}_3^-$  can be explained by the irreversible doping of poly2 film by  $\text{H}_2\text{AsO}_3^-$  anions, which is responsible for a restricted transport of counterion, and, thus, to a decrease in the rate of charge propagation in the films. As already noticed for the other redox polymer film, the charge propagation in poly2 appears dominated by the counterion diffusivity in the film and ion trapping effects [27]. As in homogeneous solution strong ion pairs are formed between alkylammonium group and  $\text{H}_2\text{AsO}_3^-$  in the reduced state of the film, and the ion-pairing is strongly reinforced in the oxidized ferrocenium form film. It is possible that the increase in the electron density around the Fc centers stabilizes the  $\text{Fc}^+$  form. The behavior of poly2 in presence of  $\text{H}_2\text{AsO}_3^-$  is thus similar to the previous reports about poly(ferrocenylalkylammonium)-film modified electrodes in the presence of  $\text{H}_2\text{PO}_4^-$  [26, 27].

The analysis of the electrochemical response of a C|poly2 electrode ( $\Gamma = 9.2 \times 10^{-10}$  mol  $\text{cm}^{-2}$ ) towards  $\text{H}_2\text{AsO}_3^-$  oxidation was achieved from cyclic voltammetry experiments (see fig. 36). Well defined curves are obtained in presence or in absence of  $\text{H}_2\text{AsO}_3^-$ . In  $\text{H}_2\text{AsO}_3^-$ -free aqueous solution, the signal corresponding to  $\text{Fc}/\text{Fc}^+$  redox couple observed at + 0.46 V (see fig. 36 curve a) progressively decreases in the presence of increasing amount of  $\text{H}_2\text{AsO}_3^-$ , from  $1 \times 10^{-4}$  M to  $1 \times 10^{-3}$  M, (see fig. 36 curve b, c, d, e) by the ion pairs formed between alkylammonium group and  $\text{H}_2\text{AsO}_3^-$  anions.

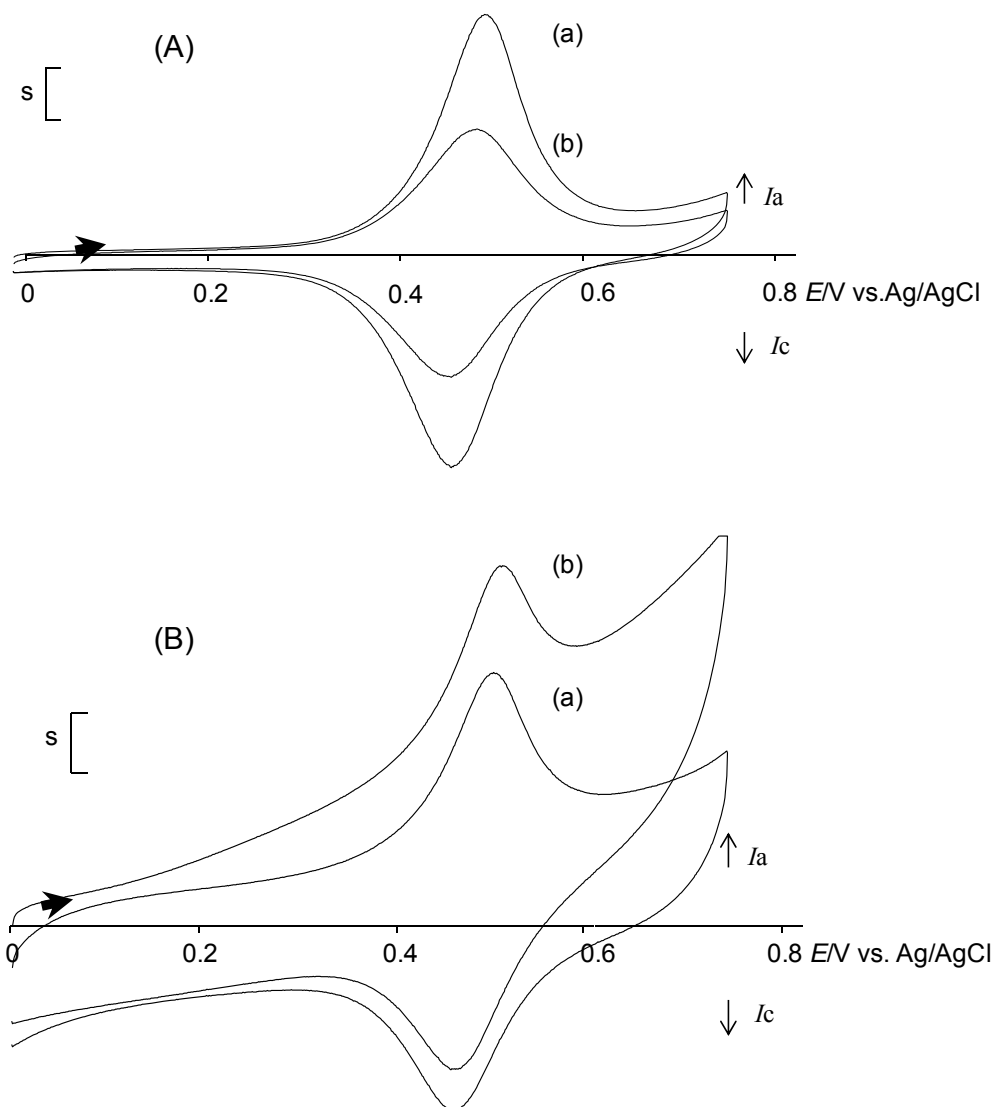


Figure 35. Cyclic voltammograms (scan rate  $50 \text{ mV s}^{-1}$ ) recorded in  $10^{-1} \text{ M}$  aqueous  $\text{LiClO}_4$ . (A) C|poly2 glassy carbon modified electrodes (3 mm diameter); curve (a):  $\Gamma = 9.2 \times 10^{-10} \text{ mol cm}^{-2}$  in the absence and curve (b) in the presence of  $10^{-3} \text{ M H}_2\text{AsO}_3^-$ ; scale  $s = 1 \mu\text{A}$ . (B) Cyclic voltammograms of C|poly2-Pt<sup>0</sup> glassy carbon modified electrodes (3 mm diameter); curve (a):  $\Gamma = 9.2 \times 10^{-10} \text{ mol cm}^{-2}$ , in the absence and curve (b) in the presence of  $10^{-3} \text{ M H}_2\text{AsO}_3^-$ ; scale  $s = 2 \mu\text{A}$

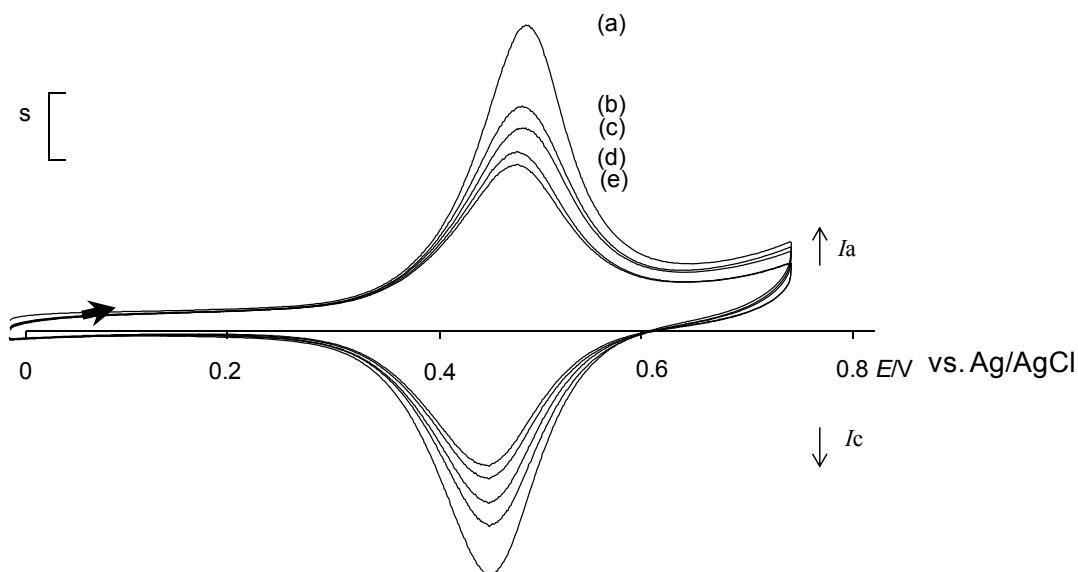


Figure 36. Cyclic voltammograms recorded in  $10^{-1}$  M aqueous  $\text{LiClO}_4$  at a C|poly2 electrode (3 mm diameter;  $\Gamma = 9.2 \times 10^{-10}$  mol  $\text{cm}^{-2}$ ) in absence of  $\text{H}_2\text{AsO}_3^-$  (curve a) and in the presence of increasing amounts of  $\text{H}_2\text{AsO}_3^-$  =  $10^{-4}$  M (curve b),  $2.5 \times 10^{-4}$  M (curve c),  $5 \times 10^{-4}$  M (curve d) and  $10^{-3}$  M (curve e); scan rate  $50 \text{ mV s}^{-1}$ . Scale  $s = 1 \mu\text{A}$ .

In contrast, after the incorporation of platinum particles into poly2 films, the resulting C|poly2-Pt<sup>0</sup> nanocomposite-film modified electrodes displayed a clear catalytic activity towards the oxidation of As(III) to As(V), as shown in figure 35 B (curve b). The CV curves were characterized by the rise at + 0.48 V of a large oxidation peak corresponding to the oxidation of arsenite. In the system C|poly2-Pt<sup>0</sup> the oxidation of arsenite occurs at the same potential than the Fc/Fc<sup>+</sup> oxidation peak. This behavior is different to that observed with the metal-free poly2 modified electrode. Due to the presence of metal particles into the polymer film, it could be assumed that the arsenite ions diffusing into the polymer are catalytically oxidized, and the redox activity of the film is no more blocked by its irreversible doping with arsenite ions, like in the case of the metal-free film.

Figure 37 (A) shows the cyclic voltammetric response (scan rate  $50 \text{ mV s}^{-1}$ ) of a C|poly2-Pt<sup>0</sup> modified electrode when adding increasing amounts of  $\text{H}_2\text{AsO}_3^-$ , from  $10^{-4} \text{ M}$  to  $3 \times 10^{-3} \text{ M}$ , in  $10^{-1} \text{ M}$   $\text{LiClO}_4$  aqueous solution. The CV curves show a progressive increase in the oxidation peak for the ferrocene moieties ( $E_p = +0.48 \text{ V}$ ). This behaviour is probably due to the catalytic oxidation of arsenite by the metal particles incorporated into the polymer film. Moreover it could be assumed that the ferrocene groups attached to the polymer play the role of an electron relay able to shuttle electrons to the catalytic sites. The concentration of arsenite can be thus monitored at  $+0.48 \text{ V}$ , i.e. at a lower potential than with a redox inactive polymer film modified electrode like C|poly1-Pt<sup>0</sup> ( $+0.52 \text{ V}$ ).

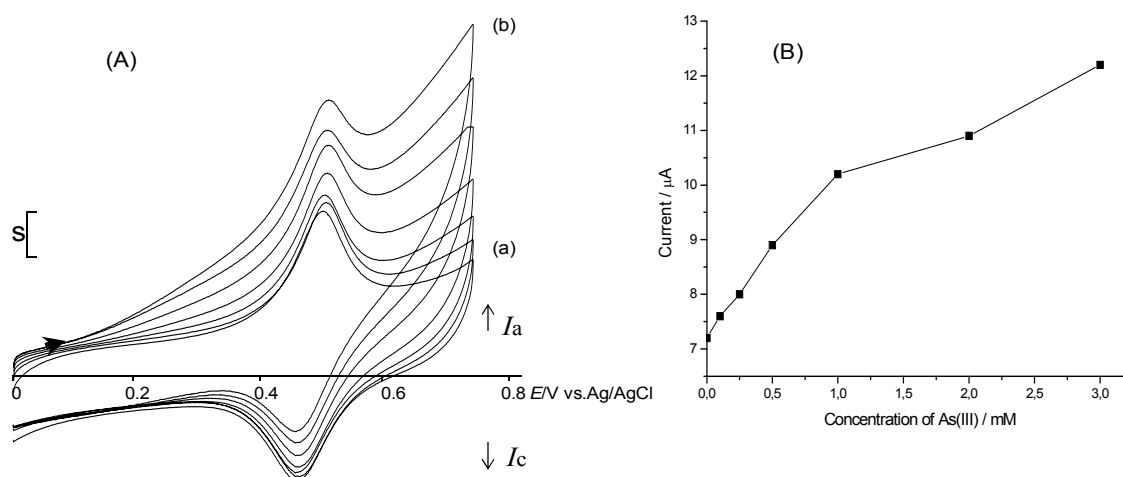


Figure 37. (A) Cyclic voltammograms recorded in  $10^{-1} \text{ M}$  aqueous  $\text{LiClO}_4$  at a C|poly2-Pt<sup>0</sup> electrode (3 mm diameter;  $\Gamma = 9.2 \times 10^{-10} \text{ mol cm}^{-2}$ ) in the presence of increasing amounts of  $\text{As(III)}$ , from  $10^{-4} \text{ M}$  (curve a) to  $3 \times 10^{-3} \text{ M}$  (curve b); scan rate  $50 \text{ mV s}^{-1}$ ; Scale  $s = 2 \mu\text{A}$ . (B) Plot of main peak currents vs. the concentration of  $\text{As(III)}$ .

The plot of the peak current vs. the concentration of  $\text{As(III)}$  is presented in figure 37 B. The peak height increased linearly with the addition of arsenite until  $1 \times 10^{-3} \text{ M}$  of arsenic species. Above of this concentration the current did not reach the linearity and loss the detection

properties. The range is from  $1 \times 10^{-4}$  M to  $3 \times 10^{-3}$  M ( $r^2 = 0.933$ ). The calibration slope was  $0.004 \text{ A M}^{-1}$  and the limit of detection (LOD [23]) was calculated to be  $1.45 \times 10^{-4}$  M (10.4 ppm), higher than LOD of C|poly1-Pt<sup>0</sup> modified electrodes.

Stability of the C|poly2-Pt<sup>0</sup> modified electrodes was investigated only to a limited extent and showed marginal loss of activity (less than 10%) after a series of at least 10 experiments.

Similar voltammetric responses to increasing amounts of As(III) were obtained using C|poly2-Pd<sup>0</sup> modified electrodes (see fig. 38 A). This results were obtained with polymer films synthesized using polymerization charge of 1 mC ( $\Gamma = 8.4 \times 10^{-10} \text{ mol cm}^{-2}$ ). In these experimental conditions, the oxidation potential for arsenite detection was increasing constantly from + 0.48 V to + 0.7 V. The linear range of the calibration curve was also from  $2.5 \times 10^{-4}$  M to  $3.75 \times 10^{-3}$  M ( $r^2 = 0.999$ ) (see fig. 38 B).

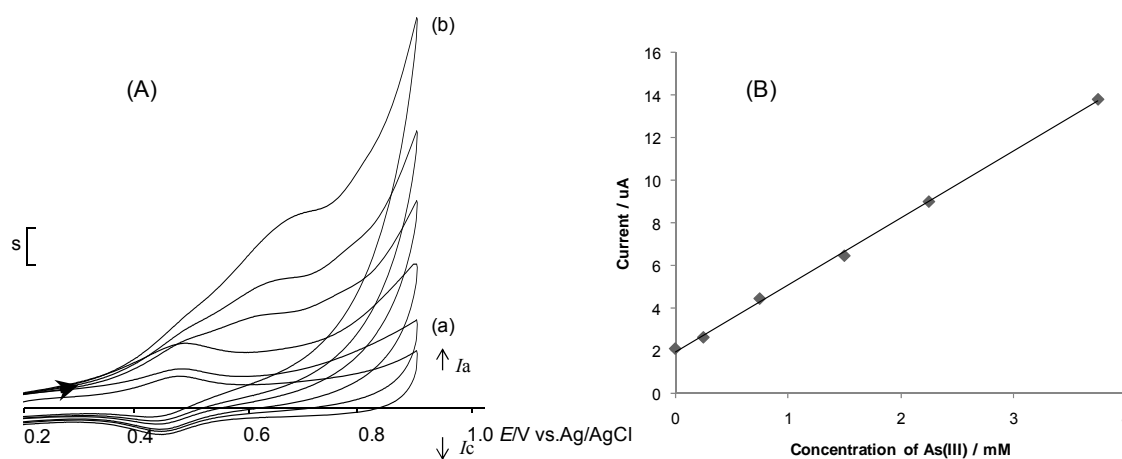


Figure 38. (A) Cyclic voltammograms recorded in  $10^{-1}$  M aqueous  $\text{LiClO}_4$  at a C|poly2-Pd<sup>0</sup> electrode (3 mm diameter;  $\Gamma = 8.4 \times 10^{-10} \text{ mol cm}^{-2}$ ) in the presence of increasing amounts of As(III), from  $2.5 \times 10^{-4}$  M (curve a) to  $3.75 \times 10^{-3}$  M (curve b); scan rate  $50 \text{ mV s}^{-1}$ . (B) Plot of main peak currents vs. the concentration of As(III); scale  $s = 2.5 \mu\text{A}$ .

The calibration slope was  $0.002 \text{ A M}^{-1}$  and the limit of detection (LOD [23]) was calculated to be  $2.44 \times 10^{-4} \text{ M}$  (17.5 ppm). The C|poly2-Pd<sup>0</sup> presented lowest sensibility toward arsenite detection showing the highest LOD of all the modified electrodes studied in this work.

### 3.2.3 Electrocatalytic oxidation of arsenite to arsenate at the preparative scale using C|poly1- Pt<sup>0</sup> under different conditions

The efficiency of the C|poly1-Pt<sup>0</sup> modified electrodes in the macroscopic electro-oxidation of As(III) to As(V) was evaluated under different experimental conditions, using  $20 \times 20 \times 4 \text{ mm}$  carbon felt modified electrodes (see the experimental section).

#### (a) Electrocatalytic oxidation of arsenite in phosphate buffer

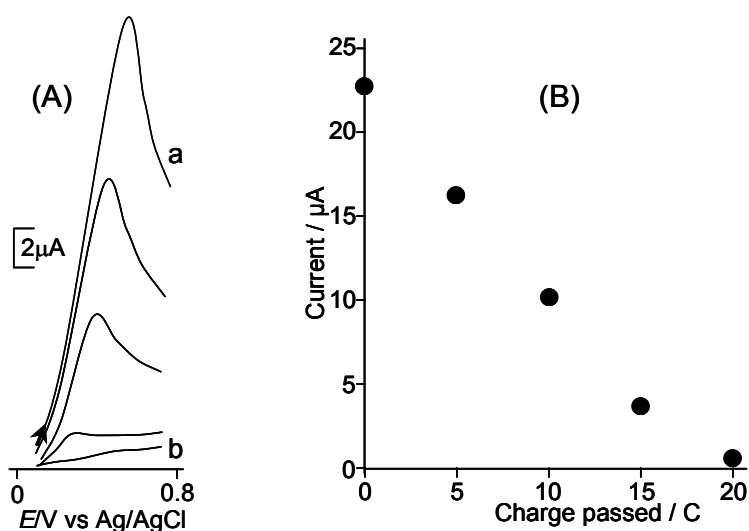


Figure 39. (A) Direct anodic scan voltammograms recorded at a C|poly1-Pt<sup>0</sup> electrode (3 mm diameter;  $\Gamma_{\text{N}^+} = 2 \times 10^{-8} \text{ mol cm}^{-2}$ ; 0.5  $\mu\text{g}$  of Pt), during the course of the electrolysis at a poly1-Pt<sup>0</sup> (9  $\mu\text{mol}$  of ammonium groups, 25  $\mu\text{mol}$  of platinum) carbon felt modified electrode ( $E_{\text{app}} = +0.6 \text{ V}$ ) of a solution of 35 mL of phosphate buffer (pH 8) containing  $3 \times 10^{-3} \text{ M}$  of NaAsO<sub>2</sub>; (a) initial curve, (b) curve recorded after a charge of 20 C has been passed; scan rate  $10 \text{ mV s}^{-1}$ . (B) Plot of the As(III) oxidation current recorded at the microelectrode vs. charge consumed.

In a typical experiment, the oxidation of a 35 mL solution  $3 \times 10^{-3}$  M NaAsO<sub>2</sub> in phosphate buffer (pH 8) onto a C|poly1-Pt<sup>0</sup> (25 μmol of platinum) modified electrode was conducted into in a H-shaped three-compartment cell (the working electrode was separated from the carbon felt auxiliary electrode by a glass frit), at a constant applied potential of + 0.6 V until the theoretical charge (20 C) required for the two-electron oxidation of As(III) to As(V) has been consumed (see fig. 39 B). The electrolysis progress was followed *in situ* from the height of the As(III) oxidation peak recorded at a C|poly1-Pt<sup>0</sup> analytical modified electrode (see fig. 39 A). The exhaustive oxidation of the As(III) solution was completed in 3 hours. This experiment confirmed the good activity of the poly1-Pt<sup>0</sup> nanocomposite electrode material towards the electrocatalytic oxidation of As(III) to As(V), as well for analytical purpose as for preparative scale oxidation of arsenite to arsenate.

**(b) Electrocatalytic oxidation of arsenite in the presence of poly(diallyldimethyl ammonium) chloride as supporting electrolyte**

The electrocatalytic oxidation of As(III) at carbon felt modified macroelectrodes was also tested in solutions containing as supporting electrolyte a cationic water-soluble polymer able to complex As(V) oxy-anionic species. Several electrolyses were carried out in different experimental conditions, in the presence of P(CIDDA), at a 20:1 polymer:As(III) molar ratio (solutions  $88 \times 10^{-3}$  M in polymer and  $4.4 \times 10^{-3}$  M in As(III)). In these experimental conditions the initial pH of the solution was around 9. The theoretical charge required for the exhaustive two-electron oxidation of 35 mL solutions of As(III) was 30 C. The advancement of the electrocatalytic oxidations was monitored *in situ* from the height of the As(III) oxidation peak recorded at a Pt disc (5 mm diameter) microelectrode (see fig. 40).

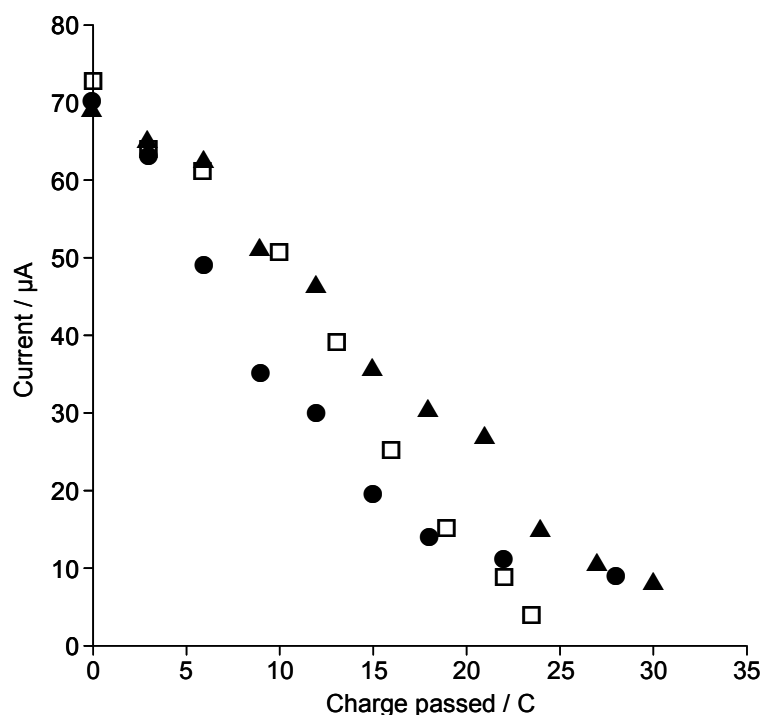


Figure 40. As(III) oxidation currents recorded at Pt disc (5 mm diameter) electrode (scan rate  $10 \text{ mV s}^{-1}$ ) during the electrolyses at a poly1-Pt<sup>0</sup> (9  $\mu\text{mol}$  of ammonium groups, 25  $\mu\text{mol}$  of platinum) carbon felt modified electrode of solutions (35 mL) containing  $4.4 \times 10^{-3} \text{ M NaAsO}_2$  and  $88 \times 10^{-3} \text{ M P(CIDDA)}$ : (□) electrolysis carried out in a three-compartment cell, the working electrode being separated from the carbon auxiliary electrode by a glass frit; (●) electrolysis carried out in a one-compartment cell, without separator, using carbon felt as auxiliary electrode; (▲) electrolysis carried out in a one-compartment cell without separator, using a platinum basket as auxiliary electrode.

In a first experiment, the poly1-Pt working electrode was separated from the carbon felt auxiliary electrode by a glass frit. In these experimental conditions the pH of the solution dramatically decreases during the course of the electrolysis (see table 14) due to the release of protons associated with the conversion from trivalent to pentavalent arsenic-oxy species [21, 28]. The pH changed from 9.0 to 3.5 after the consumption of 10 C, to reach a value of about 2

when 20 C has been passed. This resulted in a large positive shift in the oxidation potential of As(III) species [29], which required to increase the applied oxidation potential up + 1.1 V to try to complete the electrolysis. After all, the oxidation was incomplete; only 23.5 C could be passed in 3 hours (see fig. 40, open squares).

Better results were obtained when working in a one-compartment cell, without separator between the working and auxiliary electrodes. When a piece of carbon felt was used as counter electrode, the change in pH was less important than in the previous experiment. It decreased from 9.5 to 6 after the consumption of 10 C, to reach 3 at the end of the electrolysis. This can be explained by the reduction at the auxiliary electrode of some protons released during the electrocatalytic oxidation of arsenite. The amount of charge that could be passed (28 C) was close from the theoretical value (see fig. 40, solid circles), but it was necessary to move the oxidation potential up to + 0.9 V to maintain a reasonable oxidation current and to complete the electrolysis in less than three hours.

As expected, the use of a Pt counter electrode i.e., a Pt basket set around the working electrode, improved the system due to the good catalytic activity of platinum for proton reduction. In these last experimental conditions the exhaustive oxidation of the As(III) solution was rather efficient at the poly1-Pt<sup>0</sup> carbon felt modified electrode (see fig. 40, solid triangles). The pH changed only from 9.5 to 5.1 after the consumption of 30 C. In these experimental conditions the oxidation potential could be kept below + 0.8 V, and the exhaustive oxidation of the As(III) solution was completed in less than 2 hours (see table 15).

Table 15. pH recorded during each point of the electrolysis at different passed charge.

<b>Charge passed in electrolysis (□)</b>	<b>pH</b>	<b>Charge passed in electrolysis (●)</b>	<b>pH</b>	<b>Charge passed in electrolysis (▲)</b>	<b>pH</b>
0	9.0	0	9.5	0	9.5
3	8.7	3	8.2	3	9.4
6	6.6	6	6.5	6	9.2
10	3.5	9	6.0	9	8.8
13	2.8	12	5.8	12	7.7
16	2.5	15	5.1	15	6.7
19	2.0	18	4.5	18	6.3
22	2.0	22	4.0	21	6.1
23.5	2.0	28	3.0	24	5.7
--	--	--	--	27	5.4
--	--	--	--	30	5.1

### 3.2.4 Conclusions

This study demonstrates that platinum and palladium metal-polyammonium nanocomposites film modified electrodes (C|poly1-Pt<sup>0</sup>, C|poly1-Pd<sup>0</sup>) present strong electrocatalytic properties towards the oxidation of arsenite to arsenate, in spite of the small amount of metal catalyst electroprecipitated in the polymer films. Moreover, as compared to massive platinum electrodes, the use of the platinum-polymer nanocomposite markedly decreases the overpotential for arsenite oxidation. The oxidation of As(III) occurs at a less positive potential in the C|poly1-Pt<sup>0</sup> electrode ( $E_p = + 0.52$  V) than a platinum electrode ( $E_p = + 0.7$  V). It is now well recognized that dispersing metal nanoparticles can result in enhanced electrocatalytic properties compared to the reactivity of the bulk metal.

The oxidation of arsenite was also effective at a C|poly1-Pd<sup>0</sup> electrode but this system displayed a lower catalytic activity ( $E_p = + 0.86$  V) than the platinum-based composite.

The nanocomposite films modified electrodes can be use as well for analytical purpose, as well as for the exhaustive transformation of As(III) solutions to As(V). The progress of macroscale oxidations of As(III) to As(V) could be readily followed using C|poly1-Pt<sup>0</sup> modified glassy carbon analytical electrodes, thanks to the rather low limit (2.4  $\mu$ M) of detection for As(III) reached with these catalytic electrodes. Similar voltammetric responses to increasing amounts of As(III) were obtained using C| poly1-Pd<sup>0</sup> modified electrodes.

In the case of C|Poly2, it is possible to see the stable electrochemical response of the ferrocene center (Fc) at + 0.48 V in aqueous solution, higher potential than the peak recorded in CH<sub>3</sub>CN electrolyte solution + 0.26 V. When transferred to aqueous solution in presence of H<sub>2</sub>AsO<sub>3</sub><sup>-</sup> anions, the CV curves for poly2 was deeply modified by strong decrease in the electroactivity of the film. It can be thus concluded that cationic poly2 film presents affinity toward H<sub>2</sub>AsO<sub>3</sub><sup>-</sup>. This loss of electroactivity in presence of H<sub>2</sub>AsO<sub>3</sub><sup>-</sup> can be explained by the irreversible doping

of poly2 film by  $\text{H}_2\text{AsO}_3^-$  anions, which is responsible for a restricted transport of counterion, and thus to a decrease in the rate of charge propagation in the films.

The use of C|poly2-Pt<sup>0</sup> for the arsenite detection showed catalytic activity towards oxidation of As(III) to As(V) brought about by the inclusion of a small amount of platinum. The electrocatalytic activity of the anodic increased peaks was due to the presence of metal particles into the polymer film, similar to the C|poly1-Pt<sup>0</sup>, but at + 0.46 V. The limit of detection of C|poly2-Pt<sup>0</sup> was calculated being 145  $\mu\text{M}$ , higher than LOD of C|poly1-Pt<sup>0</sup> modified electrodes.

Similar voltammetric responses to increasing amounts of As(III) were obtained using C|poly2-Pd<sup>0</sup> modified electrodes. The limit of detection was calculated to be 244  $\mu\text{M}$ . The C|poly2-Pd<sup>0</sup> presented lowest sensibility toward arsenite detection showing the highest LOD of all the modified electrodes studied in this thesis.

### ***3.3 Off-line coupled (EO - LPR) techniques to remove arsenic from aqueous solutions***

Here it is described the work about the combination of electrochemical and membrane ultrafiltration methods (electro-oxidation, EO, and liquid phase polymer based retention technique, LPR, respectively) to remove inorganic arsenic species from aqueous solutions. Since the main oxidation states of arsenic species present in water are V (arsenate) and III (arsenite), an efficient extraction of arsenic species can be performed by associating the liquid-phase polymer based retention (LPR) procedure, based on the As(V) adsorption properties of cationic water-soluble polymers, with the electrocatalytic oxidation (EO) process of As(III) into its more easily removable analogue As(V).

Previous studies have demonstrated the efficient removal of As(V) species using various water soluble polyquaternary ammonium salts as extracting agents using the LPR technique [1-5]. Moreover, it has recently been shown in our laboratories that the treatment by the LPR technique of arsenite solutions previously submitted to oxidation at bulk platinum [5] or iridium oxide film modified electrodes [30], in order to convert quantitatively arsenic (III) to arsenic (V) species, allowed removing hazardous arsenic with a process cationic in which polyquaternary ammonium salts were used both as supporting electrolyte and As(V) extracting agents.

#### **a) Electrolysis of arsenite solution at a massive platinum electrode, followed by LPR**

In a previous study in our Lab, the electrocatalytic oxidation of As(III) to As(V) at a bulk platinum electrode was performed in the presence of different water-soluble poly(quaternary ammonium) salts acting also as supporting electrolyte (*i.e.*, P(CIAPTA), P(CIVBTA) or P(BrVMP)), was also combined with the extraction of arsenic using the LPR [5]. In these

experiments, the macroscopic electro-oxidation of As(III) to As(V) using a large surface platinum gauze electrode was conducted in unbuffered aqueous solutions at a constantly applied potential between + 0.8 to + 0.9 V vs. Ag/AgCl until the theoretical charge required for the two-electron oxidation of As(III) to As(V) was consumed. Similar results were obtained by oxidation at + 0.8 or + 0.9 V, but the electrolysis time was greatly reduced at an applied voltage of + 0.9 V. The initial solutions were basic (pH 9 - 10), but the pH decreased continuously as the consumed charge increased, reaching a value of 3 - 4 at the end of the electrolysis. The progress of the macro-scale oxidation of As(III) to As(V) could be readily judged from the height of the As(III) oxidation peak recorded at a platinum disc analytical electrode.

Before carrying out the ultrafiltration process to remove As(V) species from the electrolyzed solution, the pH was adjusted to 8 with NaOH, and stirring was maintained for about 1 - 4 h. After that the mixtures were introduced into LPR cell, the washing method at different polymer and arsenic concentrations and molar ratios were carried out in order to remove the As(V)-polymer adducts.

Ultrafiltration runs were performed under a total pressure of 3.5 bar using a ultrafiltration membrane of polyethersulfone with an exclusion rating of 10000 Da. The total volume in the cell was maintained constant during the process. Fractions of 20 mL were collected up to a total volume of 200 mL. The complete arsenic retention was achieved (see fig. 41). Moreover, the As(V) retention efficiency turned out to be directly related to the charge consumed during the electrochemical conversion of As(III) to As(V) [5].

A blank assay was also performed with a solution of polymer and As(III) (20:1 mole ratio), which had not been previously electrochemically oxidized. This ratio was selected to ensure an excess of the repeat polymer unit. The results of the As(V) uptake are systematically

presented as the percentage of retention  $R(\%)$  vs. the filtration factor  $Z$  (volume of the filtrate/volume of the cell).

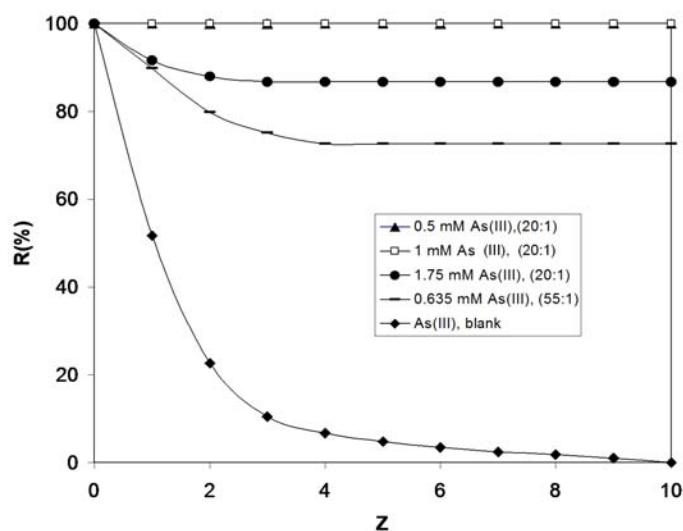


Figure 41. Arsenic retention profile using P(CIVBTA) as supporting electrolyte and polychelator at pH 8, at different concentrations of As(III); (▲)  $5 \times 10^{-4}\text{M}$ , (○)  $6.35 \times 10^{-4}\text{M}$ , (□)  $10^{-3}\text{M}$ , (●)  $1.75 \times 10^{-3}\text{M}$  and (◆) blank, in the electrolysis cell; polymer:As(III) molar ratio 20:1; solutions were previously electrolyzed onto a Pt-gauze electrode (potential applied + 0.9 V vs Ag/AgCl) up to the consumption of the theoretical charge for the complete oxidation of As(III) to As(V).

It should be emphasized that this combined electro-oxidation EO-LPR method allows to avoid the use of chemical oxidants. Moreover, an important point is that the whole process can be performed in the same reactor without any additives other than the extracting polycationic polymer, which also serves as supporting electrolyte. In the conventional oxidation processes with chemical dosing, effective oxidants are free chlorine, hypochlorite, permanganate and hydrogen peroxide /  $\text{Fe}^{2+}$  (so called Fenton's reagent). Chlorine has the disadvantage that it leads to chlorinated byproducts, namely trihalogenmethanes, from reactions with natural organic matter. Ozone is quite effective but it is not feasible for a specific application to As(III) oxidation because it is a strong oxidant that would partly oxidize the natural organic

matter. The most reasonable oxidants are  $\text{KMnO}_4$  and Fenton reagent ( $\text{H}_2\text{O}_2 / \text{Fe}^{+2}$ ) with which the As(V) is removed by precipitation–coagulation. Oxidation using  $\text{H}_2\text{O}_2$  is applicable when the water contains some ferrous ions, but only for certain  $\text{H}_2\text{O}_2 / \text{Fe}^{+2}$  mass ratio and the residual  $\text{H}_2\text{O}_2$  may not exceed  $0.1 \text{ mg L}^{-1}$ . The most adequate oxidant would be  $\text{KMnO}_4$  for cases with a subsequent precipitation and filtration step. In the precipitation – coagulation process, the use of aluminum or ferric salts is common. Indeed, the removal of As(III) by precipitate of  $\text{Fe}^{+2}$  salts was found to be only 50 – 60% lower than that of As(V) using the same coagulant.

A series of experiments were performed to estimate the effect of the oxidation of As(III) to As(V) species on arsenic removal efficiency with LPR. In all these experiments, P(CIVBTA) was used as capturing and supporting polyelectrolyte. Several solutions of As(III) were oxidized at an applied potential of + 0.8 V or + 0.9 V. Electrolysis was stopped after the consumption of 0.5, 1, 1.5, 1.75, and 2 electrons per As(III) species. Then, the arsenic retention by the LPR technique was determined for each electrolyzed solution (see fig. 42), and the retention factor (R) was calculated for the electrolyzed (+ 0.9 V) arsenic solutions ( $5 \times 10^{-4} \text{ M}$  and  $10^{-3} \text{ M}$ ) containing P(CIVBTA) as polyelectrolyte as a function of the consumed charge during electrolysis. In all these experiments, the polymer: As(III) mol ratio was 20:1. After electrolysis, the pH of solutions was adjusted to 8 and arsenic was removed by ultrafiltration.

Similar results were obtained using a lower oxidation potential (+ 0.8 V). The linear increase of arsenic retention as a function of the electrolysis charge (regression linear factor  $r^2 = 0.998$ ), reaching 100% after the consumption of 2 electrons per As(III) species, clearly demonstrates that the arsenic removal efficiency is directly related to the oxidation of As(III) to As(V). These experiments also demonstrate that the combination of LPR with an electrocatalytic

oxidation process is an efficient, straightforward procedure to remove arsenic from contaminated aqueous solutions.

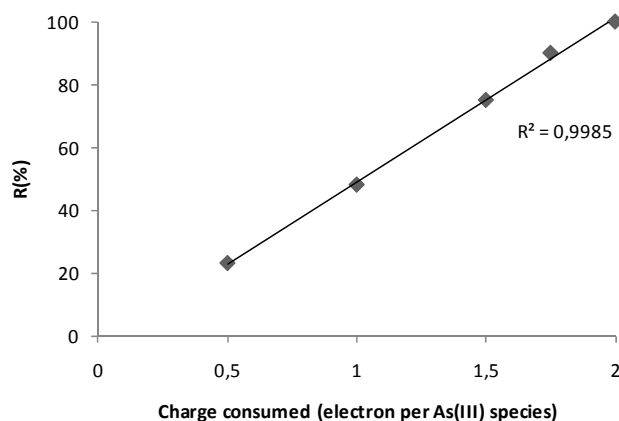


Figure 42. Arsenic retention as a function of the charge passed during the electrolysis (massive Pt electrode, Potential applied + 0.9 V of  $10^{-3}$  M As(III) solutions containing P(CIVBTA) as polyelectrolyte; P(CIVBTA) : As(III) mol ratio 20:1).

#### **b) Removal of arsenic by oxidation at C|poly1-Pt<sup>0</sup> modified carbon felt electrodes followed by LPR**

Our preliminary studies indicate that the electrocatalytic oxidation of arsenite can be efficiently performed at the preparative scale (see section 3.4.3), using electrodes modified with catalytically active materials based on nano particles of noble metals (Pt and Pd) dispersed in polymer films coated onto carbon electrodes.

Using a carbon felt macroelectrode modified with a poly1-Pt<sup>0</sup> composite film previously described (see experimental part), a solution of As (III) was electrolyzed at + 0.7 V vs. Ag/AgCl until the complete conversion of As(III) to As(V) was achieved.

In these experiments the polyelectrolyte was used as supporting electrolyte and as extracting polymer. In a typical experiment, a solution of arsenite and cationic polymer at a 20:1

polymer:As(III) molar ratio of (As(III)  $7.5 \times 10^{-4}\text{M}$ , polyelectrolyte  $15 \times 10^{-3}\text{M}$ ) was submitted to electrocatalytic oxidation. The electrolysis was conducted in a one-compartment cell, without separator between the working electrode (a C|poly1-Pt<sup>0</sup> modified carbon felt) and the auxiliary electrode (a platinum basket). During the electrolysis the solution was stirred at 1000 rpm. The pH was measured at each point of electrolysis. The theoretical charge for the complete oxidation was calculated according to Coulomb law ( $Q = \text{number electrons} \times 96500 \times \text{As(III) concentration}$ ).

The pH of the solution, which was around 9 before the oxidation, did not decrease below 5 in the course of the electrolysis because the protons generated were subsequently reduced to hydrogen at the Pt basket counter electrode. The progress of the oxidation of As(III) to As(V) was monitored *in-situ* using an analytical modified electrode (C|poly-Pt<sup>0</sup>, 1mC of polymerization charge and 0.5mC charge of metal incorporation), used as an amperometric sensor to determine the remaining arsenite (see fig. 43 A, B, C). The results showed a complete conversion of As(III) to As(V), reaching the theoretical charge calculated for the process under these conditions.

After consumption of the charge required for the exhaustive oxidation of As(III) to As(V), the pH of the electrolyzed solution was adjusted to 8 with NaOH. Then the resulting solution was assayed by LPR-technique by the washing method, and the arsenic concentration in the filtrate was determined by atomic absorption spectrometry (see experimental). In these experimental conditions, arsenic retention reached between 27% to 98%, being it maximum for polyelectrolytes with chloride as a counterion as a P(CIDDA) [31], P(CIVBTA) and P(CIAPTA) and minimum for P(SAETA) (see fig. 43 D, E, F). This behavior is similar to the previous results obtained in the study of the influence of the counterion in the arsenate retention, but the use of P(SAETA) as a support in the electrochemical process increases the

response in current of arsenite measurements at +0.8 V (see fig. 43 C). The time required for electrolysis process was 1 to 2 hours.

Finally, we checked that the recovery of arsenic was 0% for a solution containing polyelectrolyte and As(III) in a 20:1 mol ratio that has not been submitted to electrolysis (see fig. 43 D, E, F curve (▲)).

The main informations on these off line (EO- LPR) coupled experiments are given in Table 16, where are summarized the following data: charge consumed during the electrolyses, peak current for the oxidation of As(III) remaining in the electrolyzed solutions (measured with an analytical modified electrode), pH and time measured during the advancement of the electrolysis; the retention percentage (R%) at  $Z = 10$  of As(V) previously electro-oxidized was informed after to complete electrolysis.

These results confirm that the combination of the LPR with the electrocatalytic oxidation of arsenic at a polymer-platinum nanocomposite film modified electrode might be an useful technique for arsenic removal from contaminated solutions.

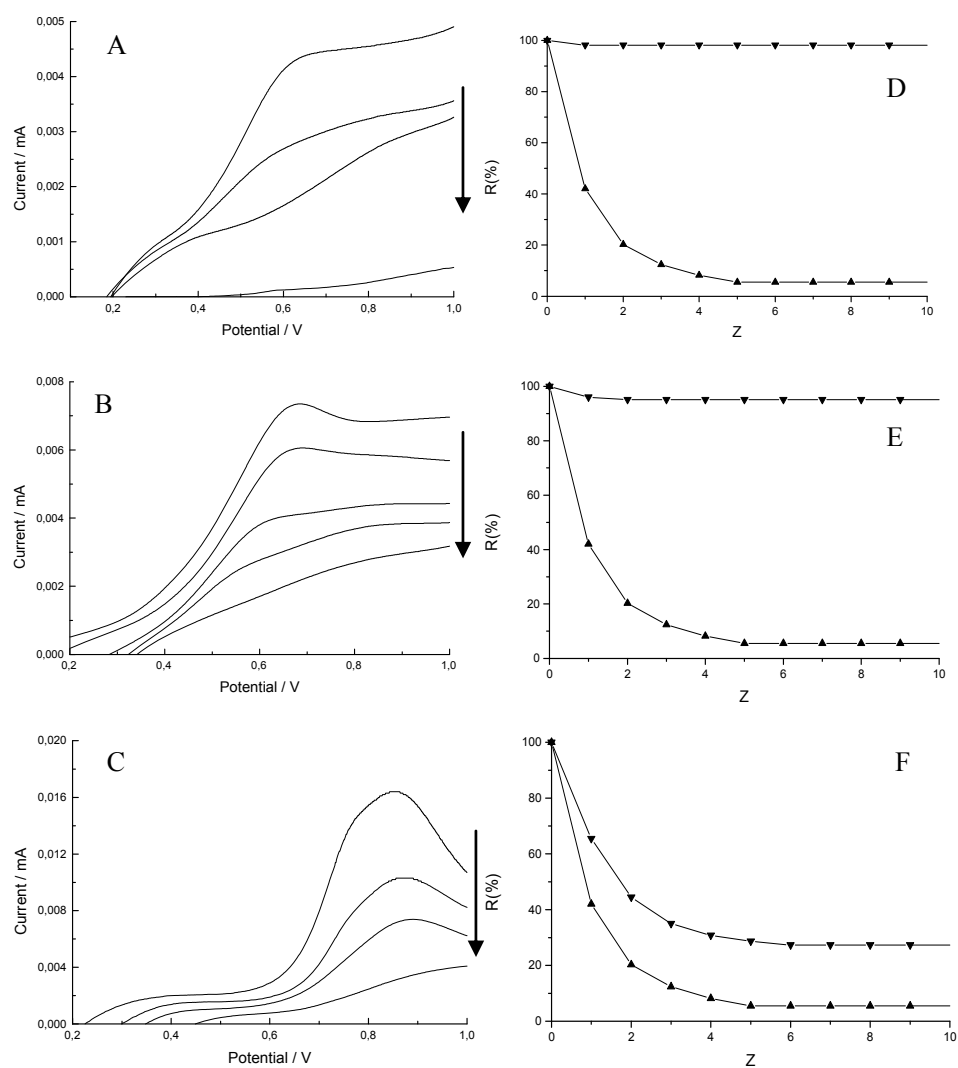


Figure 43. Off- line coupled EO - LPR experiments of  $7.5 \times 10^{-4}$  M of As(III) at a poly1-Pt<sup>0</sup> carbon felt modified macroelectrode, using (A, D) P(CIDDA), (B, E) P(CIVBTA) and (C, F) P(SAETA) as supporting polyelectrolyte and extracting agent. Figures A, B, C shows the advancement of electrolyses (carried out at  $E = +0.7$  V vs. Ag / AgCl), monitored *in-situ* by recording at a C|poly1-Pt<sup>0</sup> analytical modified electrode the decrease of the anodic CV peak corresponding to the remnant As(III) species. Figures D, E, F shows the retention profile of As(III) after exhaustive oxidation of the solution (▼) and without oxidation (blank; ▲), extraction by LPR was performed at pH 8. The mol ratio polymer: As (III) was 20:1 in both processes.

Table 16. Charge applied, peak current of As(III) remnant, pH and time measured during the advancement of the electrolysis of  $7.5 \times 10^{-4}$  M of As(III) to As(V) at the preparative scale using C|poly1-Pt<sup>0</sup> carbon felt modified working macroelectrode ( $E = + 0.7$  V vs. Ag/AgCl). Retention percentage (R%) of As(V) previously electro-oxidized.

Water-soluble polymer	Total charge applied / C	Peak current / $\mu$ A	pH	Total time of electrolysis / min	R (%)
P(CIDDA)					
	0	4.2	9.8	0	--
	1.6	2.68	7	20	--
	2.6	1.65	5.8	40	--
	4.3	0.12	5.6	60	98
P(CIVBTA)					
	0	7.19	8.7	0	--
	1	5.9	5.6	20	--
	2.34	4	4	40	--
	3.34	3.02	3.7	60	--
	4.34	1.98	3.4	90	96
P(CIAPTA)					
	0	7.04	9.2	0	--
	1	5.66	6.1	20	--
	2	4.02	4.9	40	--
	3	2.62	4.2	60	--
	4.3	1.37	3.9	120	94
P(SAETA)					
	0	16.2	3.3	0	--
	2.2	10.1	3.2	20	--
	3.2	7.12	3.1	42	--
	4.3	3.25	3	52	27

### 3.3.1 Conclusions

This study shows that the combination of the liquid phase polymer based technique with the electrocatalytic oxidation of arsenic (III) to arsenic (V) is an effective process to remove the hazardous As(III) species from aqueous solution. It is noteworthy that the efficiency of arsenic removal is directly linked to the oxidation of As(III) to As(V).

We have also shown the capability of these nanocomposite electrode materials (C|poly1-Pt<sup>0</sup>) to carry out bulk electrocatalytic oxidation of arsenite solutions in the presence of a water-soluble poly(quaternary ammonium) salts acting as supporting electrolyte and also as agent to remove As(V) species, allowing to combine the electrocatalytic oxidation (EO) of As(III) with a liquid phase polymer based retention (LPR) process to efficiently remove arsenic. These are a decisive advantages in their application as does not require the addition of other reagents such as salts medium in homogeneous electrocatalytic processes.

Compared to our previous work carried out in bulk platinum electrodes, the use of C|poly1-Pt<sup>0</sup> modified electrode allows to perform catalytic oxidation of arsenic (III) at a lower potential.

Future work will focus on the development of a on line LPR-electrocatalysis process, where electrolysis is carried out directly inside the LPR cell, or in a separated cell inserted in the fluid circuit and connected to the reservoir of the LPR equipment. In this context, the use a flow cell equipped with a porous carbon felt modified electrode with a nanocomposite material is as an attractive approach.

### **3.4 Final remarks**

The versatility of polymer chemistry has been shown throughout this thesis. This versatility makes it possible to combine different areas such as environmental, analytical, electrochemical, catalysis, organometallic and engineering science among others, and offers new alternatives in different fields of technology.

The ability that the conducting functional polymers have in the formation of nanocomposite catalytic materials with metal particles has also been shown in this work. These conducting functional polymers have shown benefits as to their metallic counterparts in bulk as the polymers present electrocatalytic activity towards the oxidation of oxy-anions arsenite. It was then possible to develop stable electrochemical sensors of low cost that work in aqueous media in a wide range of oxidation potential and pH.

Not only has it been possible to use these materials for analytical purposes but also as a convenient tool for the complete removal of arsenic species from water. This is because it is possible to use this material in the quantitative conversion of As(III) species to As(V) in aqueous solution. This step is required in most existing technologies for arsenic removal, because the As(V) is more easily removed than As(III) from aqueous solution over a wide pH range. One of the benefits of this process is the use of water-soluble cationic polyelectrolytes, which are used as supporting electrolytes in the electrochemical cell. This was the key to achieve the next goal, which was the removal of species of As(V).

Previously to this was studied the removal capacity of As(V) by water-soluble cationic polyelectrolytes that have quaternary ammonium salt groups with different ion exchangers. These polymers were synthesized and characterized in our laboratory, showing an acceptable yield of synthesis, water solubility, high thermal resistance, electrical conductivity and molecular weights suitable to use as an extracting agent of As(V) through the technique of

liquid phase polymer based retention, LPR. This technique is promising for the study of functional polymer interactions with ions in solution and for the separation of polluting species, which is carried out in homogeneous medium, it is simple and inexpensive.

These water-soluble cationic polymers showed excellent properties for the removal of arsenate ions from aqueous solution. The quaternary ammonium groups of the polymer interact with the arsenate ions and these can be separated from the aqueous solution through an ultrafiltration membrane. The study was optimized by analyzing variables such as pH, polymer: arsenate molar ratio, influence of the polymer counterion and influence of other ions in solution to remove arsenate. On the other hand, the maximum removal capacity and recovery of the polymer through charge-discharge cycles were also determined.

After proving the possibility to use these water-soluble polymers as the supporting electrolyte in the electrolysis and as the extracting agent in ultrafiltration, the next challenge was to couple off line electrocatalytic oxidation with ultrafiltration. The results showed an almost complete removal of species of As(III), which were previously electro-oxidized on the electrode modified with polymer films containing metal nanoparticles. The dual use of water-soluble polyelectrolyte was the key to couple both processes because it avoids the use of external agents as support or oxidants. It was also possible to follow the oxidation process *in situ* by monitoring the residual concentration of As(III) using the modified electrodes in analytical scale.

Finally, it is necessary to set new challenges and improve the use of these electrocatalytic processes and ultrafiltration together. It would be ideal to perform the electrolysis directly in the ultrafiltration cell, or to explore the possibility of realizing the two processes circuit connected. Another important point is to be able to conduct monitoring of As(III) as well as

the total removal of arsenic species in real water samples, either in naturally contaminated water or industrial waste water, to permissible levels.

Each aqueous system is different and requires a previous optimization in order to use analytical technologies for monitoring and for the removal of contaminant arsenic species. For this, much remains to be done in this area.

### 3.5 References

- 1) Rivas, B.L.; Aguirre, M.C. and Pereira, E. Retention properties of arsenate anions of water-soluble polymers by a liquid-phase polymer-based retention technique. *J. Appl. Polym. Sci.* 2006;102:p.2677-2684.
- 2) Rivas, B.L.; Aguirre, M.C. and Pereira, E. Cationic water-soluble polymers with the ability to remove arsenate through ultrafiltration technique. *J. Appl. Polym. Sci.* 2007;106:p.89-94.
- 3) Rivas, B.L.; Aguirre, M.C.; Pereira, E.; Moutet, J-C. and Saint-Aman, E. Capability of cationic water-soluble polymers in conjunction with ultrafiltration membranes to remove arsenate ions. *Polym. Eng. Sci.* 2007;47:p.1256-1261.
- 4) Rivas, B.L. and Aguirre, M.C. Arsenite retention properties of water-soluble metal-polymers. *J. Appl. Polym. Sci.* 2007;106:p.1889-1894.
- 5) Rivas, B.L.; Aguirre, M.C., Pereira, E.; Bucher, C.; Royal, G.; Limosin, D.; Saint-Aman, E. and Moutet, J-C. Off-line coupled electrocatalytic oxidation and liquid phase polymer based retention (EO-LPR) techniques to remove arsenic from aqueous solutions. *Water Res.* 2009;43:p.515-521.
- 6) Barron, R. and Fritz, J. Effect of functional groups structure on the selectivity of low-capacity anions-exchangers for monovalent anions. *J. Chromatogr.* 1984;284:p.13-25.
- 7) Bard, A.J. *Chemical Equilibrium*; Harper's Chemistry Series; Harper and Row. New York, 1966.
- 8) Barron, R. and Fritz, J. Effect of functional group structure and exchange capacity on the selectivity of anion exchangers for divalent anions. *J. Chromatogr.* 1984;316:p.201-210.
- 9) Pearson, P. and Lovgren L. Potentiometric and spectroscopic studies of sulphate complexation at the Goethite-water interface. *Geochim. Cosmochim. Acta.* 1996;60:p.2789-2799.
- 10) Berdal, A.; Verrie, D. and Zaganaris, E. Removal of arsenic from potable water by ion exchange resins. In *Ion Exchange at the Millennium, Proceedings of IEX 2000*; Greig, J.A., Ed.; Imperial College Press: London, 2000;p.101-108.
- 11) William, R.A. *Colloid and Surface Engineering: Applications in the Process Industries*; Butterworth-Heinemann: Oxford, 1992; p.11-18.

- 12) Rivas, B.L.; Pereira, E.D. and Moreno-Villoslada, I. Water-soluble polymer–metal ion interactions. *Progr Polym Sci.* 2003;28:p.173-208.
- 13) Bentley, F.; Smith, L. and Rozek, A. Infrared spectra and characteristic frequencies, 700-300  $\text{cm}^{-1}$ . A collection spectra. Interpretation and bibliography. John Wiley and Sons: New York, 1968.
- 14) Tables of spectral data for structure determinate of organic compounds  $^{13}\text{C}$ -NMR,  $^1\text{H}$ -NMR, IR-MS, UV–vis. Chemical lab. Practice. Pretsch-Clerc-Seibl-Simons. Springer-Verlag: Berlin, Heidelberg, 1983.
- 15) Gong, Z.; Lu, X.; Ma, M.; Watt, C. and Le, X.C. Arsenic speciation analysis. *Talanta* 2002;58:p.77-96.
- 16) Cavicchioli, A.; La-Scaela, M.A. and Gutz, I.G.R. Analysis and speciation of traces of arsenic in environmental, food and industrial samples by voltammetry: a Review. *Electroanalysis* 2004;16:p.697-711.
- 17) Hung, D.Q.; Nekrassova, O. and Compton, R.G. Analytical methods for inorganic arsenic in water: a review. *Talanta* 2004;64:p.269-277.
- 18) Lown, J.A. and Johnson, D.C. Anodic detection of arsenic(III) in a flow-through platinum electrode for flow-injection analysis. *Anal Chim. Acta.* 1980;116:p.41-51.
- 19) Williams, D.G. and Johnson, D.C. Pulsed voltammetric detection of arsenic(III) at platinum electrodes in acidic media. *Anal Chem.* 1992;64:p.1785-1789.
- 20) Dai, X. and Compton, R.G. Detection of As(III) via oxidation to As(V) using platinum nanoparticle modified glassy carbon electrodes: arsenic detection without interference from copper. *Analyst.* 2006;131:p.516-521.
- 21) Cabelka, T.D.; Austin, D.S. and Johnson, D.C. Electrocatalytic oxidation of As(III). Part I. Voltammetric studies at Pt electrodes in 0.5 M  $\text{HClO}_4$ . *J. Electrochem. Soc.* 1984;131:p.1595-1602.
- 22) Malinauskas, A. Electrocatalysis at conducting polymers. *Synth. Met.* 1999;107:p.75-83.
- 23) Skoog, D.A. in *Principles of Instrumental Analysis*, Ed. F. J Holler, T. A. Nieman, Saunders College Publishing, Philadelphia, 1998.
- 24) McQuade, D.T.; Pullen, A.E. and Swager, T.M. Conjugated polymer-based chemical sensors. *Chem. Rev.* 2000;100:p.2537-2574.

- 25) Ion, A.; Ion, I.; Popescu, A.; Ungureanu, M.; Moutet, J-C. and Saint-Aman, E. A ferrocene crown ether-functionalized polypyrrole film electrode for the electrochemical recognition of barium and calcium cations. *Adv. Mater.* 1997;9:p.711-713.
- 26) Reynes, O.; Royal, G.; Chaînet, E.; Moutet, J-C. and Saint-Aman, E. Poly(ferrocenylalkylammonium): a molecular electrode material for dihydrogenphosphate sensing. *Electroanalysis.* 2003;15:p.65-69.
- 27) Reynes, O.; Moutet, J-C. Royal, G. and Saint-Aman, E. Electrochemical sensing of anions by (ferrocenylmethyl)trialkylammonium cations in homogeneous solution and polymer films. *Electrochim. Acta.* 2004;49:p.3727-3735.
- 28) Kao, W.-H. and Kuwana, T. Electrochemical oxidation of arsenious acid at a platinum electrode. *J. Electroanal. Chem.* 1984;169:p.167-179.
- 29) Kedzierzawski, P. and Szklarska-Smialowska, Z. Oxidation of As(3+) to As(5+) on a Gold Electrode in Aqueous Solutions *J. Electroanal. Chem.* 1981;122:p.269-278.
- 30) Rivas, B.L.; Aguirre, M.C.; Pereira, E.; Bucher, C.; Moutet, J.-C.; Royal, G.; Saint-Aman, E. and Royal, G. Efficient polymers in conjunction with membranes to remove As(V) generated *in situ* by electrocatalytic oxidation, *Polym. Adv. Technol.* In press.
- 31) Sánchez, J.; Rivas, B.L.; Pooley, A.; Basaez, L.; Pereira, E.; Pignot-Paintrand, I.; Bucher, C.; Royal, G.; Saint-Aman, E. and Moutet, J-C. Electrocatalytic oxidation of As(III) to As(V) using noble metal-polymer nanocomposites. *Electrochim. Acta.* 2010, 55: p. 4876-4882.

## ABBREVIATIONS AND SYMBOLS

$Mz^c$	Absolute amount of ions that are in the feed phase
$Mz^{INIT}$	Absolute amount of ions at the start of the experiment
$T$	Absolute temperature
ATP	Adenosine-5-triphosphate
C poly1	Alkylammonium N-substituted polypyrrole films
Pm	Amount of polymer
A	Ampere
ASV	Anodic sweep voltammetry
$\Gamma_{N^+}$	Apparent surface coverage in ammonium units, mol cm <sup>-2</sup>
H <sub>3</sub> AsO <sub>4</sub>	Arsenic acid
H <sub>3</sub> AsO <sub>3</sub>	Arsenous acid
As(V)	Arsenate (oxidation state V)
As(III)	Arsenite ions (oxidation state III)
AAS	Atomic absorption spectroscopy
AFM	Atomic force microscopy
$b$	Average distance
$k$	Boltzmann constant
BDD	Boron doped diamond
$\epsilon$	Bulk dielectric constant of medium
<sup>13</sup> C-NMR	Carbon nuclear magnetic resonance
$ z_c $	Charge
$\xi$	Charge density parameter
$\kappa$	Conductivity
C	Coulomb

I	Current
CV	Cyclic voltammetry
Da	Dalton
DSC	Differential scanning calorimetry
DEPT	Distorsionless enhancement by polarization transfer
EO	Electrocatalytic oxidation
E	Enrichment factor
$\Lambda$	Equivalent molar conductivity
$F$	Faraday number
Fc	Ferrocene
C poly2	Ferrocenylalkylammonium N-substituted polypyrrole films
FT-IR	Fourier transform-infrared spectroscopy
$f$	Fraction of the free counterions
ICP	Inductively coupled plasma
ICP-AES	Inductively coupled plasma /atomic emission spectroscopy
ICP-MS	Inductively coupled plasma /mass spectrometry
$\lambda^{\circ}$	Infinite dilution
$z$	Ion valence
LOD	Limit of Detection
LPR	Liquid-phase polymer-based retention technique
C	Maximum retention capacity
MMCO	Molar mass cut-offs
M	Molar, mol L <sup>-1</sup>
$n$	Number of electrons exchanged by pyrrole unit during the oxidation
$Q_a$	Oxidation charge
ppb	Parts per billion, $\mu\text{g L}^{-1}$

ppm	Parts per million, mg L <sup>-1</sup>
P(CIAPTA)	Poly[3-(methacryloylamino)-propyl]trimethylammonium chloride
P(CIAETA)	Poly[2-(acryloyloxy)ethyl]trimethylammonium chloride
P(CIVBTA)	Poly(ar-vinylbenzyl)trimethylammonium chloride
P(SAETA)	Poly[2-(acryloyloxy)ethyl]trimethylammonium methyl sulfate
P(BrVMP)	Poly(4-vinyl-1-methyl pyridinium)bromide
P(CIDDA)	Poly(diallyl dimethyl ammonium) chloride
$\lambda_p$	Polyion residue
<sup>1</sup> H-NMR	Proton nuclear magnetic resonance
<i>e</i>	Proton charge
E	Potential
N	Pyrrole sites
(R) <sub>4</sub> N <sup>+</sup> X <sup>-</sup>	Quaternary ammonium group
Z	Ratios between the total volume of permeate and the volume of retentate
<i>R<sub>z</sub></i>	Retention factor
SEM	Scanning electron microscopy
SERS	Surface enhanced raman spectroscopy
TGA	Termogravimetry
TBAP	Tetra-n-butylammonium perchlorate
V <sub>f</sub>	Total volume of permeate
TEM	Transmission electron microscopy
UNICEF	United Nations International Children's Emergency Fund
V <sub>o</sub>	Volume of retentate
V	Volume of filtrate
V	Volt
WHO	World Health Organization

## RESUME

L'arsenic, existe dans l'environnement sous une grande variété de formes et à divers degrés d'oxydation. Aux pH naturels, l'arsenic libre se rencontre essentiellement sous forme inorganique aux degrés d'oxydation +III (arsénite) et +V (arséniate). Il est reconnu que l'efficacité des processus d'élimination de l'arsenic dépend fortement de la possibilité de convertir les espèces de l'arsenic (III) en celle de l'arsenic (V), plus faciles à extraire.

La recherche développée au cours de cette thèse démontre d'abord qu'il est possible d'éliminer l'arséniate de solutions aqueuses par extraction par des polymères solubles (LPR : liquid-phase polymer-based retention). La technique LPR utilise l'ultrafiltration sur membrane pour la séparation, basée sur des effets de taille, d'espèces ioniques suite à leur complexation par des polyélectrolytes solubles. Les espèces oxo-anioniques de l'arsenic(V), associés à des polyélectrolytes du type polyalkylammonium, ne passent pas à travers la membrane et peuvent être ainsi séparés des espèces non-complexées de plus petite taille.

Nous avons aussi montré la grande activité catalytique des matériaux composites du type nanoparticules de Pt<sup>0</sup> et Pd<sup>0</sup> dispersées dans des matrices de poly(pyrrole-alkylammonium), pour l'oxydation électrochimique de l'arsénite en arséniate. En particulier, des microélectrodes de carbone modifiées par des films de ces nanocomposites ont été appliquées à l'analyse de l'arsenic(III).

Enfin, l'oxydation exhaustive de solutions d'arsénite a été réalisée sur des électrodes de carbone modifiées de grande surface. L'utilisation de sels poly(alkyl-ammonium) jouant le rôle à la d'électrolyte support et d'agent d'extraction des espèces de l'arsenic(V) a permis de combiner les processus d'électrocatalyse et d'extraction par LPR, permettant ainsi d'extraire efficacement des traces d'arsenic de solutions aqueuses.

**Mots clés** : électrocatalyse ; nanocomposites polymère-metal ; LPR ; polyelectrolytes solubles en milieu aqueux ; élimination de l'arsenic.

## ABSTRACT

Arsenic occurs in a variety of forms and oxidation states and is a very toxic element. The main arsenic species present in natural waters are arsenate (oxidation state V) and arsenite ions (oxidation state III). The efficiency of arsenic extraction depends strongly on the ability to convert As(III) into more easily extractable As(V) species.

This research proves that it was possible to remove arsenate from aqueous solutions by the liquid-phase polymer-based retention (LPR). The LPR technique using an ultrafiltration membrane enables the separation of ionic species, which are retained by the (R)<sub>4</sub>N<sup>+</sup>X<sup>-</sup> functional groups of water-soluble polyelectrolytes. The ions do not pass through the membrane and are separated from the aqueous solution.

On the other hand, this research shows that nanocomposite electrode materials synthesized by incorporation of Pt<sup>0</sup> and Pd<sup>0</sup> nanoparticles dispersed in poly(pyrrole-alkylammonium) matrix present strong electrocatalytic properties towards the oxidation of arsenite to arsenate. The nanocomposite films modified electrodes can be use for As(III) analysis. The capability of these nanocomposite electrode materials deposited onto carbon felt macroelectrodes for exhaustive electrocatalytic oxidation of arsenite solutions was also demonstrated.

The use of water-soluble poly(quaternary ammonium) salt acting both as supporting electrolyte and as agent to remove As(V) species allowed to combine the electrocatalytic oxidation (EO) of As(III) with a LPR process to efficiently remove arsenic. The results show almost the complete retention of As(V) previously electro oxidized.

**Keywords**: Electrocatalysis; Polymer-metal nanocomposite; Liquid-phase polymer-based retention; Water-soluble polyelectrolyte; Arsenic removal.